uOttawa

L'Université canadienne
Canada's university

FACULTÉ DES ÉTUDES SUPÉRIEURES ET POSTOCTORALES

uOttawa

L'Université canadienne
Canada's university

FACULTY OF GRADUATE AND POSDOCTORAL STUDIES

Jie Yuan
AUTEUR DE LA THÈSE / AUTHOR OF THESIS

M.A.Sc. (Chemical Engineering)
GRADE / DEGREE

Department of Chemical and Biological Engineering
FACULTÉ, ÉCOLE, DÉPARTEMENT / FACULTY, SCHOOL, DEPARTMENT

Exergy Minimization in Ethanol Dehydration Using Hybrid Distillation/Membrane Systems
TITRE DE LA THÈSE / TITLE OF THESIS

Jules Thibault
DIRECTEUR (DIRECTRICE) DE LA THÈSE / THESIS SUPERVISOR

Andre Tremblay
CO-DIRECTEUR (CO-DIRECTRICE) DE LA THÈSE / THESIS CO-SUPERVISOR

Sidney Omelon

Artura Macchi

Gary W. Slater
Le Doyen de la Faculté des études supérieures et postdoctorales / Dean of the Faculty of Graduate and Postdoctoral Studies

Exergy Minimization in Ethanol Dehydration using Hybrid Distillation/Membrane Systems

By

Jie Yuan

A thesis submitted to the Faculty of Graduate and Postdoctoral Studies in Partial fulfillment of the requirements for the degree of

Master of Applied Science

in the

Department of Chemical and Biological Engineering

University of Ottawa

© Jie Yan, Ottawa, Canada, 2011

Library and Archives Canada

Published Heritage Branch

395 Wellington Street
Ottawa ON K1A 0N4
Canada

Bibliothèque et Archives Canada

Direction du Patrimoine de l'édition

395, rue Wellington
Ottawa ON K1A 0N4
Canada

Your file Votre référence
ISBN: 978-0-494-74186-3
Our file Notre référence
ISBN: 978-0-494-74186-3

NOTICE:

The author has granted a non-exclusive license allowing Library and Archives Canada to reproduce, publish, archive, preserve, conserve, communicate to the public by telecommunication or on the Internet, loan, distribute and sell theses worldwide, for commercial or non-commercial purposes, in microform, paper, electronic and/or any other formats.

The author retains copyright ownership and moral rights in this thesis. Neither the thesis nor substantial extracts from it may be printed or otherwise reproduced without the author's permission.

AVIS:

L'auteur a accordé une licence non exclusive permettant à la Bibliothèque et Archives Canada de reproduire, publier, archiver, sauvegarder, conserver, transmettre au public par télécommunication ou par l'Internet, prêter, distribuer et vendre des thèses partout dans le monde, à des fins commerciales ou autres, sur support microforme, papier, électronique et/ou autres formats.

L'auteur conserve la propriété du droit d'auteur et des droits moraux qui protège cette thèse. Ni la thèse ni des extraits substantiels de celle-ci ne doivent être imprimés ou autrement reproduits sans son autorisation.

In compliance with the Canadian Privacy Act some supporting forms may have been removed from this thesis.

While these forms may be included in the document page count, their removal does not represent any loss of content from the thesis.

Conformément à la loi canadienne sur la protection de la vie privée, quelques formulaires secondaires ont été enlevés de cette thèse.

Bien que ces formulaires aient inclus dans la pagination, il n'y aura aucun contenu manquant.

Canada

Statement of Contributions of Collaborators

I hereby declare that this thesis was performed under the supervision of Professors Jules Thibault and Andre Y. Tremblay of the Department of Chemical and Biological Engineering at the University of Ottawa. The material in this thesis has been the outcome of two years of research efforts by the author and her two supervisors. I personally wrote the first version of the thesis under the guidance of my supervisors. They made editorial corrections.

Signature: _____ Date: _____.

Abstract

As a renewable energy source, bioethanol is widely used for blending in gasoline in an attempt to partly alleviate the energy crisis and reduce the greenhouse gas emissions. To produce fuel grade ethanol, the dehydration process of bioethanol is a critical step for the economic viability of the whole process. With a single distillation column it is not possible to overcome the azeotropic point of the ethanol/water mixture. In addition, the distillation process is a very energy intensive and costly process.

In this thesis, two major topics concerning the dehydration process of bioethanol are discussed. First, the multiple objective optimization of the fuel grade bioethanol dehydration is performed along with a parametric analysis of A-type zeolite membrane pervaporation. Three cases were investigated using the ranked Pareto domain that was obtained in each case. The optimal results were identified as attractive compromised solutions considering the four objectives: the total number of stages, the total area, the energy consumed, and the exergy loss. The temperature drop per stage was found to be the dominating factor. The second theme is the exergy loss minimization of the pervaporation/distillation hybrid system at the tangent pinch on the vapor-liquid equilibrium curve. Results show that both the exergy loss and the reflux ratio of the hybrid system are reduced compared to a single distillation column. In addition, the exergy loss of the hybrid system is correlated with the variation of the reflux ratio.

Résumé

Comme source renouvelable d'énergie, le bioéthanol est largement utilisé dans les mélanges d'essence dans un effort pour partiellement alléger la crise énergétique et réduire les émissions de gaz à effet de serre. Pour produire de l'éthanol destiné pour son mélange au carburant, le procédé de déshydratation de bioéthanol est une étape critique pour la viabilité économique du procédé de fabrication. Une colonne de distillation ne peut être utilisée par elle-même pour briser l'azéotrope du mélange éthanol/eau. Par ailleurs, le procédé de distillation est un procédé très énergivore et coûteux.

Dans cette thèse, deux aspects importants du procédé de déshydratation du bioethanol sont discutés. Premièrement, l'optimisation multicritère de la déshydratation de bioéthanol est effectuée suivant une analyse paramétrique de la pervaporation par membrane de zéolite de type A. Trois études de cas ont été examinées à l'aide d'un domaine de Pareto obtenu pour chaque cas. Les résultats montrent que les solutions optimales obtenues dans chaque cas représentent des compromis attrayants selon les quatre objectifs suivants : le nombre total modules, la superficie totale de la membrane, l'énergie consommée et la perte d'exergie. La baisse de température par module est le facteur dominant. Le deuxième thème traite de la minimisation de la perte d'exergie du système hybride pervaporation/distillation au point d'étranglement de la tangente sur la courbe d'équilibre de vapeur-liquide. Les résultats montrent que la perte d'exergie et le reflux du système hybride sont plus faibles en comparaison à une seule colonne de distillation. Par ailleurs, la perte d'exergie du système hybride est reliée à la variation du reflux.

Table of Contents

List of Tables

List of Figures

Acknowledgements

I would like to thank my supervisors, Dr. Jules Thibault and Dr. André Y. Tremblay, for giving me the opportunity to carry out this interesting research topic under their enthusiastic guidance and support. I also wish to express my gratitude to them for helping me improving the language of the thesis. This thesis would not have been possible without their fruitful instruction and comments throughout this work.

CHAPTER 1
Introduction

Recently, the bioethanol industry is undergoing a fast expansion driven by policy and market, including environmental protection, potential economic profit, energy security, and the need of a domestic fuel supply. In order to reduce oil dependence and improve the nation's security, governments have been seeking renewable energy technologies for the past three decades. Transforming biomass into biofuel is one of them. Up to 36 states and provinces are mandated by law to blend 10-15% ethanol with gasoline (UNET, 2009). Also, many governments are making major investments to build bioethanol plants. The demand for fuel ethanol has grown rapidly in the U.S. and Brazil. According to the reports of Renewable Fuel Association (RFA), the U.S. fuel ethanol demand has increased from 350 to 695 barrels per day from 2006 to 2009. The average monthly demand of fuel ethanol was approximately 900 million gallons in the US in 2009 (RFA, 2010). Similarly, the world production of fuel ethanol jumped from 4.3 to more than 12 million gallons per year from 2000 to 2007 (UNET, 2009). There exists a considerable global market for fuel ethanol production.

Another reason to use bioethanol is its contribution in the reduction of green house gases (GHG). According to the reports of United Nations Environment Programme (UNEP) in 2009, more than 70% GHG reduction was estimated for bioethanol produced from sugar cane; for bioethanol from corn, the saving was estimated to be approximately 60% compared to fossil fuel (UNEP, 2009). If the feedstock comes from residues or wastes, bioethanol production can not only contribute significantly to CO_2 mitigation based on its life cycle, but can also reduce the demand of land comparing to the first generation bioethanol; furthermore, it prevents the food versus fuel conflict (UNEP, 2009). Conducting a life cycle assessment on bioethanol production, the energy life cycle makes it sustainable (Fu et al., 2003). The life cycle energy from different feedstocks were evaluated by the National Renewable Energy Laboratory (NREL), they are as follows: up

to 94% energy reduction in fossil and 72% in petroleum are obtained when ethanol is produced from forest residues; 75% energy input reduction in fossil and 77% in petroleum are reported for rice straw ethanol; 43.4% energy input reduction in fossil and 88% in petroleum were achieved for corn ethanol (NREL, 2001).

The first generation fuel ethanol is produced from three major resources: the US produce ethanol mainly from corn, Brazil from sugar cane, and the EU mostly from rapeseed (IEA, 2010). The feedstock of first generation bioethanol is a variety of seeds, grains or whole plants, which are primarily food sources. With the rapid expansion of bioethanol production, the second and third generation bioethanol are now starting to be implemented industrially. The second generation bioethanol is produced from non-food sources, such as waste biomass, farm residues, home wastes or forest wastes. The third generation bioethanol is produced from algae and bacteria (Tanner, 2009; Brittaine and Lutaladio, 2010; UNEP, 2009).

The basic technologies for the production of bioethanol are fermentation and hydrolysis for both the first and second generation bioethanol. Figure 1.1 illustrates the second generation bioethanol production process (Iogen, 2006). After pretreatment, the feedstock undergoes enzymatic hydrolysis, and the resulting fermentable sugars are sent to a fermentation vessel to produce the bioethanol. The ethanol concentration at the end of the fermentation process varies from 1 to 15 wt%, depending on the sugar composition and microorganism used. Finally, the fermentation broth is normally sent to one or more distillation columns to remove most water from the ethanol product.

The separation of ethanol and water by distillation becomes very inefficient and costly when the mixture composition approaches the azeotropic point. At the azeotropic concentration (95.6% ethanol in weight), both water and ethanol have identical composition in both the liquid and vapor phases (as shown in Figure 1.2). It is impossible to separate these two components based on volatility difference under normal conditions. In order to break the azeotropic equilibrium, changing either the operation conditions, such as the pressure (as shown in Figure 1.3), or adding another species to serve as an entrainer, such as ethylene glycol (Gil et al., 2008), are possible options. However, both approaches will increase the cost of the distillation process.

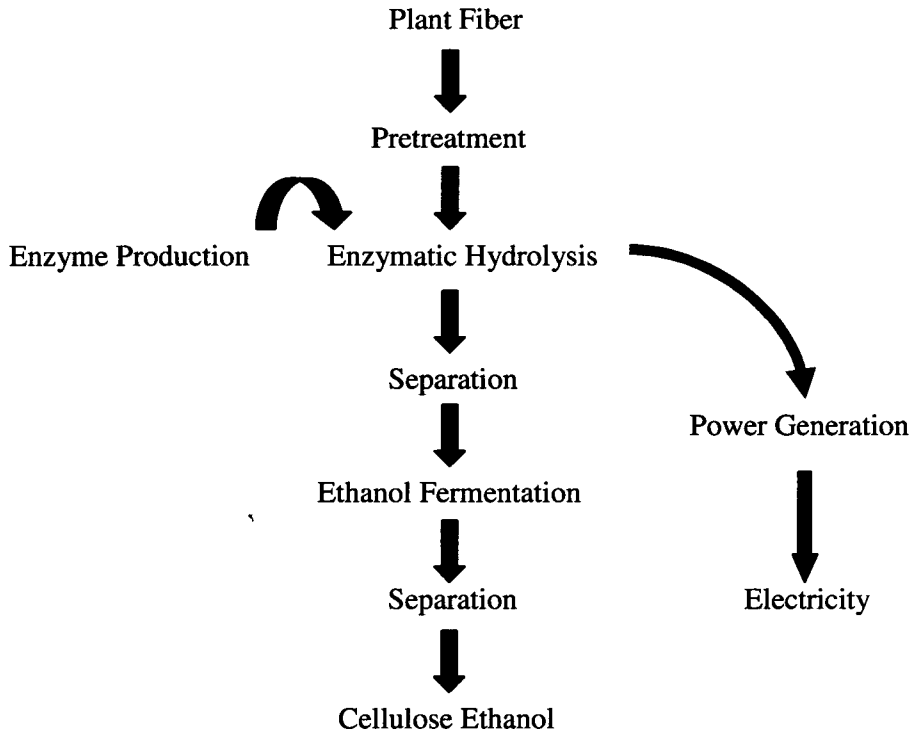

Figure 1.1 Second generation bioethanol process (IOGEN, 2006).

Figure 1.3 shows the variation of the azeotropic point for water/ethanol system under different pressures. It can be noticed that the azeotropic ethanol concentration increases with an increase in pressure (curves without symbols are boiling curves and curves with symbols are the dew lines). From 66 mbar to 986 mbar, the concentration increases less than 4%. Hence, changing the operating pressure to achieve high purity ethanol is very inefficient.

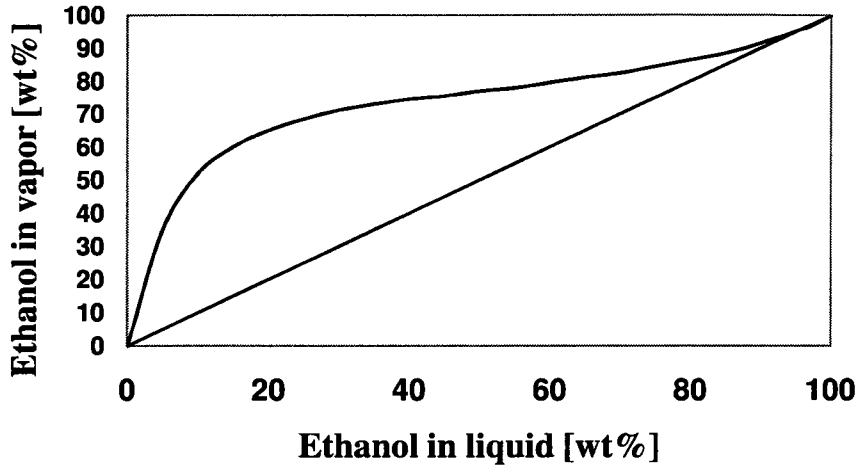

Figure 1.2 VLE equilibrium diagram of ethanol/water mixture under normal conditions (Brandenberger, 2002).

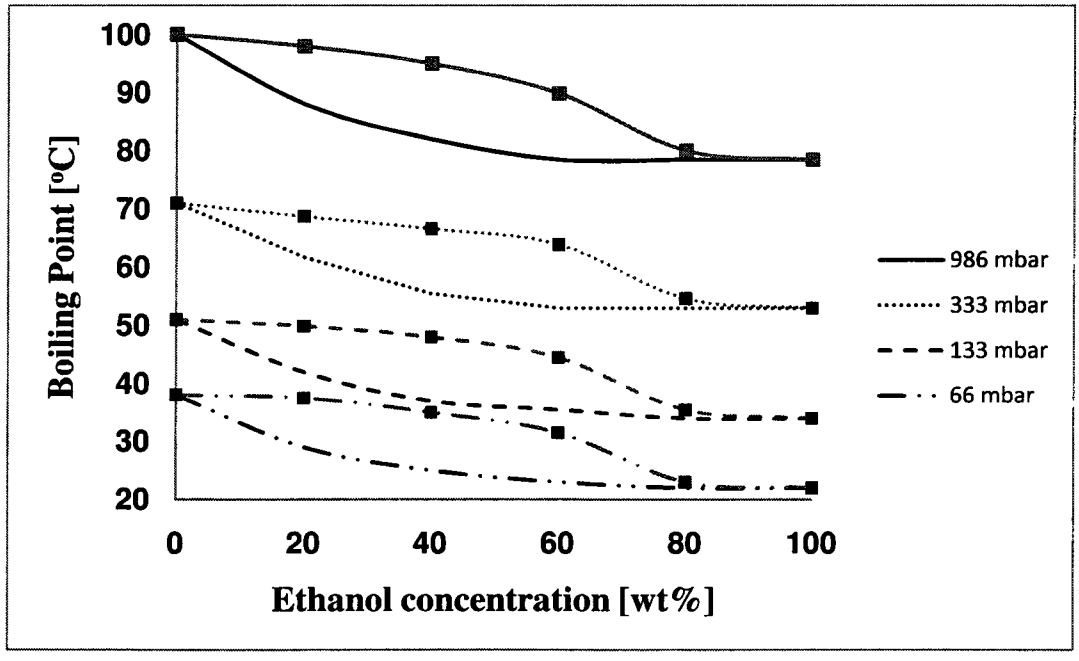

Figure 1.3 Boiling curve and condensation curve for a mixture ethanol and water at different pressures (Brandenberger, 2002).

Besides distillation, there exist other options for ethanol dehydration for overcoming the azeotropic point: liquid extraction, adsorption, and pervaporation. According to a study

performed at the University of Regina, compared to traditional packed adsorption column, the smaller volume of a pervaporation module can provide a larger contact surface area. In addition, membrane pervaporation can be easily implemented into current industrial plants. It can work with both pure gases and pure liquids. (University of Regina, 2005)

Many researchers have proposed and investigated various membranes and their operating parameters (Will and Lichtenthaler, 1992; Kita et al., 1995; Bruschke, 1995). Many membrane hybrid systems for ethanol recovery processes have been optimised (Sommer and Melin, 2005; Bausa and Marquardt, 2000).

The prime objective of this thesis is to model the application of the pervaporation process for the ethanol dehydration of existing ethanol production plants to study the separation process with a special emphasis on energy consumed and exergy loss. The distillation column, the membrane process and the combined hybrid system are evaluated respectively and compared to each other. Especially, the energy consumed and the exergy loss of a membrane process implemented in the vicinity of the tangent pinch are compared to other options, such as traditional distillation. Based on a simplified design, these evaluations and comparisons are to identify the weaknesses and strengths of the different combinations of the hybrid distillation and pervaporation system and to look for potential improvements.

The thesis is mainly comprised of two papers. Chapter 2 presents an optimization study of a membrane system for the ethanol dehydration by considering four objective criteria. Chapter 3 presents the simulation of a hybrid distillation column/membrane system in view of examining the benefit of adding a membrane to a distillation to reduce cost and enhance separation efficiency.

References

Aksoy, A., Karaosmanoglu, F., and Isüıgıgur, A., Effects of a New Blending Agent on Ethanol-Gasoline Fuels, Energy & Fuels, 10 (1996) 816-820.

Bausa, J., and Marquardt, W., Shortcut Design Methods for Hybrid Membrane/ Distillation Processes for the Separation of Nonideal Multicomponent Mixtures, Ind. Eng. Chem. Res., 39 (2000) 1658-1672

Brandenberger, H., Rectification of a two component mixture of solvents using a rotary evaporator, Evaporation & life science, 15 (2002)

Brittaine, R. and Lutaladio, N., Jatropha: a smallholder bioenergy crop: The potential for pro-poor development, Integrated crop management, 8 (2010)

Bruschke, H., Industrial application of membrane separation processes, Pure &Appl. Chem., Vol. 67, No. 6, (1995) 993-1002.

Davis, K. S., Quality Issues for Ethanol as a Fuel, Hawkeye Gold, LLC, 2009

Enertech Lab, Inc., http://www.enertechlabs.com/fuel_phase_separation_in_ethanol.htm, 2009.

Fu , G. Z., Chan, A. W. and Minns, D. E., Life Cycle assessment of bio-ethanol derived from cellulose, The Int. J. Life Cycle Ass., Volume 8, Number 3, 2003

Gil, I. D., Uyazán, A. M., Aguilar , J. L., Rodríguez , G., and Caicedo , L. A., Separation of ethanol and water by Extractive distillation with salt and Solvent as entrainer: process Simulation, Braz. J. Chem. Eng., Vol. 25, No. 01, pp. 207 - 215, January - March, 2008

International Energy Agency (IEA), Sustainable production of second-generation biofuels: potential and perspectives in major economies and developing countries, 2010

Iogen, Cellulose ethanol is ready to go, Iogen company information brochure, 2006

Kita , H., Horii, K., Ohtoshi, Y., Tanaka, K., Okamoto, K., Synthesis Of A Zeolite Naa Membrane For Pervaporation Of Water/Organic Liquid Mixtures, J. Mater. Sci. Lett., 14 (1995) 206-208

National Renewable Energy Laboratory (NREL), Is bioethanol sustainable?, 2001, http://www-erd.llnl.gov/ethanol/proceed/etohsus.pdf , accesed Dec. 2010.

Renewable Fuel Association (RFA), Fuel ethanol Industrial guidelines, specifications, and procedures, 2003

Renewable Fuel Association (RFA), http://www.ethanolrfa.org/industry/statistics/#A, accessed June 2010.

Sommer, S., Melin, T., Influence Of Operation Parameters On The Separation Of Mixtures By Pervaporation And Vapor Permeation With Inorganic Membranes. Part 1: Dehydration Of Solvents, Chem. Eng. Sci., 60 (2005) 4509-45

Szitkai., Z., lelkes., Z., Rev., E., Fonyo. Z, Optimization of hybrid ethanol dehydration systems, Chem. Eng. Proc. 41 (2002) 631-646

United Nations Environment Programme (UNEP), Towards sustainable production and use of resources: ASSESSING BIOFUELS, 2009

University of Regina, http://www.co2-research.ca/index.php?id=51, 2005, accessed June 2010.

U.S Department of Energy, A Win-Win Strategy; U.S. Department of Energy Biofuels Systems Division: Washington, DC, 1994; pp 6-8.

CHAPTER 2

Multicriteria Optimization of Bioethanol Dehydration using Membrane Pervaporation

J. Yuan[1], J. Thibault[1], A. Tremblay[1] and Mikhael Sorin[2]

[1]Department of Chemical and Biological Engineering, University of Ottawa

Ottawa, Ontario, Canada K1N 6N5

[2]Canmet ENERGY, Natural Resources Canada Varennes, Quebec, Canada J3X 1S6

Abstract

Pervaporation is a competitive technique for the fuel grade bioethanol dehydration. In this investigation, a parametric analysis of A-type zeolite membrane pervaporation is first performed followed the multiple objective optimization of the fuel grade bioethanol dehydration. In the parametric analysis, a series of membrane pervaporation stages were simulated for a fixed water removal fraction from an ethanol/water mixture. Three parametric relationships are examined in view of suggesting in each case the optimal working conditions. To achieve multiple-objective optimization, a network-structure pervaporation system was simulated. Three cases are investigated and for each case the Pareto domain is circumscribed and ranked with the Net Flow Method (NFM). The optimization results show that it was possible to identify attractive compromised solutions considering four objectives: the total number of stages, the total area, the energy consumed, and the exergy loss. The temperature drop per stage was found to be the dominating factor in the pervaporation process.

2.1 Introduction

The foreseen energy shortage crisis and global warming cannot be ignored and, despite the economic resistance expressed by many countries, are beginning to affect the lives of the inhabitants at the level of the planet. One way to partly mitigate these problems, in addition to a drastic reduction in the level of consumption, is to develop new technologies that are more efficient and that use renewable resources. For transportation, many governments are targeting in using a larger proportion of biofuels to replace petroleum products. Biodiesel, bioethanol and biobutanol produced from biomass are the subject of numerous investigations and are starting to partly replace non renewable fuels (UNEP, 2009). Since the first oil crisis in the 1970s, ethanol has attracted significant attention for transportation fuel and has been mostly used up to now for gasoline blending in the proportion of 10 to 15% (RFA, 2003; UNEP, 2009). In the 1980s, ethanol was recognized as an environmental octane enhancer and began to replace lead in gasoline (RFA, 2003). From 1990, oxygenated fuel was mandatory in some regions of the United States as mandated by the Clean Air Act Amendments. Over 35 states and provinces have adopted mandatory oxygenated fuel programs and these programs affect a large portion of all gasoline sold (RFA, 2003). Ethanol is the most widely used oxygenate and both its demand and supply have drastically increased in North America. During the period between 2006 and 2009, the bioethanol production has almost doubled (RFA, 2010). There is still a large potential market for bioethanol.

Most bioethanol produced is currently used in fuel blending such as E10 and E15 (UNEP, 2009). It is required that the water content of the final bioethanol be less than 1 wt% even though research effort is now performed to allow using azeotropic ethanol for fuel applications (Karaosmanoglu et al., 1996). Hence, the dehydration of bioethanol is a very important step in the bioethanol production process. Furthermore, ethanol-water mixtures are non-ideal under standard conditions. The existence of an azeotrope at 95.6 wt% and the very low relative volatility in the vicinity of the azeotrope are major hurdles that need to be overcome to achieve an efficient recovery of ethanol using traditional separation processes. In addition, the high energy consumption is recognized as one of the main disadvantages of the distillation process (Eldridge and Seibert, 2005). In recent decades,

many investigators have worked at finding more efficient alternatives to either improve the energy efficiency of the distillation process or to replace it with other separation methods. Haelssig et al. (2008) simulated six distillation-hybrid alternatives for the dehydration of ethanol below the azeotropic point and evaluated their economic and technical perspectives. The six processes included basic steam stripping distillation, flash fermentation distillation, single column distillation, two-column distillation with different pressure, distillation with heat pump, and flash-vacuum distillation. They found that the two-distillation column process and the distillation process with heat pump were better alternatives than the others based on the separation efficiency consideration; otherwise, the flash fermentation distillation was better in terms of energy consumption.

When energy consumption is the prime consideration, membrane separation may be the best choice. Fontalvo et al. (2005) compared both the pervaporation (pure liquid inlet) and vapour permeation (pure vapor inlet) to the distillation-based separation for dewatering acetonitril and concluded that up to 60% in total annual cost was saved. Since the membrane capital cost is usually much higher, the significant saving is mainly due to the reduction of operating costs. In 2001, the first large-scale pervaporation plant was introduced by Morigami et al. (2001). Membrane separation is characterized by lower energy consumption. Membrane separation is also independent of the vapour/liquid equilibrium relationship such that the azeotropic point can be easily overcome. However, many disadvantages have prevented a wide penetration of membranes in industrial applications. The two most important disadvantages are: (1) their low capacity (permeation flux) such that large membrane areas are required and (2) the high capital cost. The physical performance of membranes depends on the type of membrane and species to be separated such that membranes must be manufactured with the end use in mind for best separation efficiency. Membrnaes are currently available for many industrial processes.

A-type zeolite membrane is one of the commercially available membranes that can be used for organic solvent dehydration. The thermal resistance and mechanical strength have been widely studied. Mitsui Engineering and Shipbuilding has shown that the hydrophilic zeolite membranes on tubular ceramic support can operate up to 300℃ and

100 bars (Sommer and Melin, 2005). Kita et al. (1995) measured the selectivity and the permeate flux of tubular NaA-zeolite membrane at 75℃ for ethanol dehydration of water-ethanol solutions containing 5.1 and 10.3 wt% water. The selectivity (the ratio of water and ethanol on the permeate side over the ratio of water and ethanol on the retentate side) and the permeate flux were 10000 and 2.15 kg/m^2h and 16000 and 1.1 kg/m^2h, respectively. Kondo et al. (2003) and Richter et al. (2006) studied the performance of membranes under different operating conditions and ethanol concentration. They found that both the permeate flux and the separation factor increased as the feed temperature increased. Their studies revealed that hydrophilic zeolite membranes represented the best choice for ethanol dehydration at higher ethanol concentration because the selectivity and the permeate flux were higher than those observed for the other types of membranes, for example, polymer membranes.

In a preliminary study, Bausa and Marquardt (2000) used Mixed Integer Nonlinear Programming (MINLP) to determine the minimum number of stages and the minimum membrane area in a pervaporation process for the separation of non-ideal mixtures. They suggested that the temperature drop of each membrane module should not exceed 10℃, otherwise the pervaporation efficiency decreases dramatically. However, it is difficult to deduce from their study the best operating conditions because of the numerous conflicting objectives that are involved. Cojocaru et al. (2009) used multi-response equations obtained through experimental factorial design to draw contour plots to identify the desirable working zone and the optimal pervaporation operating conditions to separate ethanol and acetonitrile from wastewater. The optimal operating conditions for the ethanol/water system were found to be a feed temperature of 55°C, a feed concentration of 4.53% ethanol, and a permeate pressure of 9.57 kPa based on two criteria: the maximation of the permeate flux and the maximation of the selectivity. Nemmani et al. (2009) optimized the pervaporation operation conditions to minimize wastewater treatment cost and to maximize the toluene removal fraction. These authors emphasised the existence of a compromise between the two objectives. Furthermore, they circumscribed the two-objective Pareto domain of their process by considering numerous decision variables: volumetric flow rate, membrane thickness, permeate pressure,

Reynold's number, fiber diameter, and feed concentration. However, to our knowledge, past studies did not consider energy consumed and exergy loss as objective criteria.

The objective of the present investigation is to study the multi-objective optimization of the bioethanol dehydration using the Net Flow Method (NFM). The NFM consists of first obtaining the Pareto domain and then ranking this Pareto domain using information from an experienced person. The work is presented in two sections. A parametric analysis is first performed to elucidate the relationships that exist between the main operating variables. Then, the multi-objective optimization is performed based on four conflicting objectives: the total number of stages, the total area, the energy consumed, and the exergy loss. Three different combinations of decision variables are investigated.

2.2 Shortcut Design of Membrane Pervaporation

The pervaporation system for ethanol dehydration consists of a series of membrane modules with inter-module heat exchangers, a liquid ring vacuum pump to lower the pressure on the permeate side, and a condenser to remove a large proportion of the condensable upstream to the vacuum pump. The operating conditions of the pervaporation system needs to be optimized to satisfy performance criteria. Some of these objective criteria are: (1) the number of membrane modules in series, (2) the total membrane area, (3) the total energy consumed, and (4) the total exergy loss. In this investigation, these four performance criteria will be used.

The schematic diagram of the membrane pervaporation system considered in this investigation is presented in Figure 1. The ethanol/water liquid mixture is fed to the first membrane section and flows through the membrane module where water selectively permeates through the membrane due to the low pressure on the permeate side. As water is removed, the temperature of the retentate solution decreases because of evaporation of the permeate such that it is necessary to increase the retentate temperature prior to entering the next membrane section. A number of membrane modules are used until the desired ethanol concentration of the retentate is achieved. Water and the small amount of ethanol permeating through the membrane are collected as the permeate flow.

The model proposed by Sommer and Melin (2005) was used to estimate the component permeate flux through the membrane:

$$J_{j,PV} = Q_{j,ref} \exp\left[\frac{E_j}{R_{gas}}\left(\frac{1}{T_{ref}} - \frac{1}{T_F}\right)\right] \times \left(x_{jF}\gamma_j p_{jF}^{sat} - x_{jP} p_P\right) \tag{2.1}$$

Where $J_{j,PV}$ is the pervaporation integral transport of component j [kg/m^2 h]; $Q_{j,ref}$ is the permeance of component j at the reference temperature [kg/m^2 h bar]; E_j is the activation energy [J/mol]; R_{gas} is the ideal gas constant [J/molK]; T_{ref} is the reference temperature [K]; T_F is the feed temperature [K]; x_{jF} is the feed concentration of component j [wt%]; γ_j is the activity coefficient of component j; p^{sat}_{jF} is the saturate pressure of component j in the feed [bar]; x_{jp} is the permeate concentration of component j [wt%]; p_p is the permeate pressure [bar] and j is the subscript for ethanol or water. The mixture of the permeate, which is predominantly water vapor, is considered ideal (γ=1). More detailed information on the modeling of the membrane system can be found in Appendix A. The validation of the membrane system modeling is contained in Appendix B.

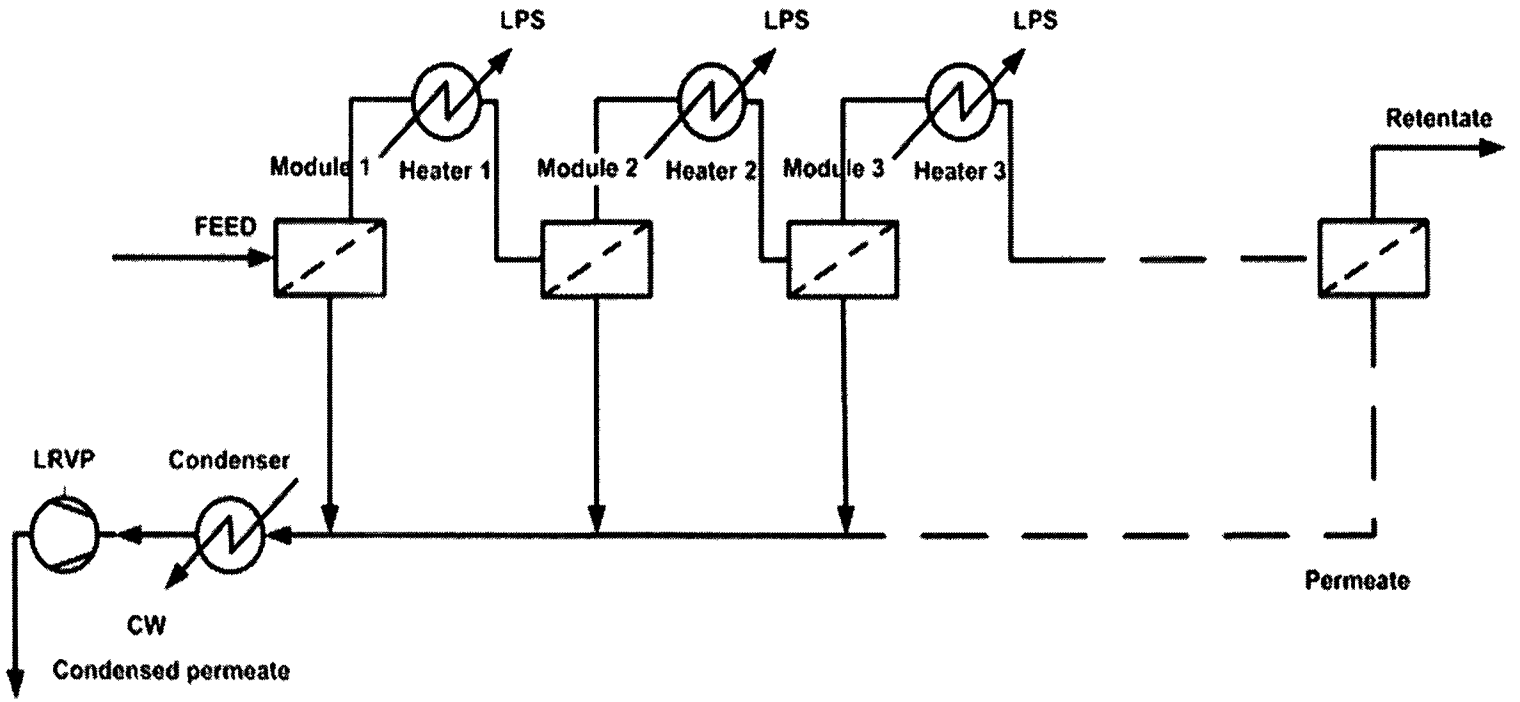

Figure 2.1 Schematic diagram of the membrane pervaporation process.

2.3 Parametric Analysis

Prior to performing the multi-objective optimization of the pervaporation membrane system, a parametric study was conducted to better comprehend the influence of some key operating variables. The membrane pervaporation process is both temperature and pressure dependent. In addition, other parameters such as the membrane module area and the concentration of feed also affect the membrane separation efficiency. In this section, the interrelationship between some important process variables is explored as a preliminary optimization step.

2.3.1 Laboratory-scale study for A-type zeolite membrane in a series arrangement

For the first preliminary analysis, the influence of the membrane area per stage was examined for a pervaporation process where 100 kg/h of a 80 wt% ethanol-water mixture entering at 101.3 kPa and 78°C is concentrated to a 99 wt% when the permeate pressure is fixed at 2 kPa. These conditions, summarized in Table 2.1 and used by Bausa and Marquardt (2000), were used for validating the simulation model.

Table 2.1 Operating conditions for a membrane pervaporation system in series

Variables	Value	Unit
Feed flow rate	100	kg/h
Feed ethanol concentration	80	wt%
Retentate ethanol concentration	99	wt%
Feed pressure	101.3	kPa
Permeate pressure	2	kPa
Feed temperature	78	℃

(Bausa and Marquardt, 2000)

The relationship between the total membrane area and the number of stages required to achieve the desired separation, when the membrane area per stage was varied between 5 to 100 m^2, is presented in Figure 2.2. As expected, when the membrane area per stage decreases, the number of stages required increases whereas the total membrane area decreases. In other words, if the objective were to solely minimize the total membrane area, a large number of

stages with small area per stage would be used. Indeed, the temperature drop across a single stage would be small which would then maintain a high operating temperature for each stage and, as a result, a higher efficiency would be achieved. These results are close to those obtained by Bausa and Marquardt (2000). It is obvious that a compromise must be made as both a minimum membrane total area and a minimum number of stages are desirable. It is important to stress that a heat exchanger is required between each stage such that the number stages must be kept to a minimum. In this case study, the optimal area per stage was selected to be 27 m^2 which corresponds to approximately 100 stages.

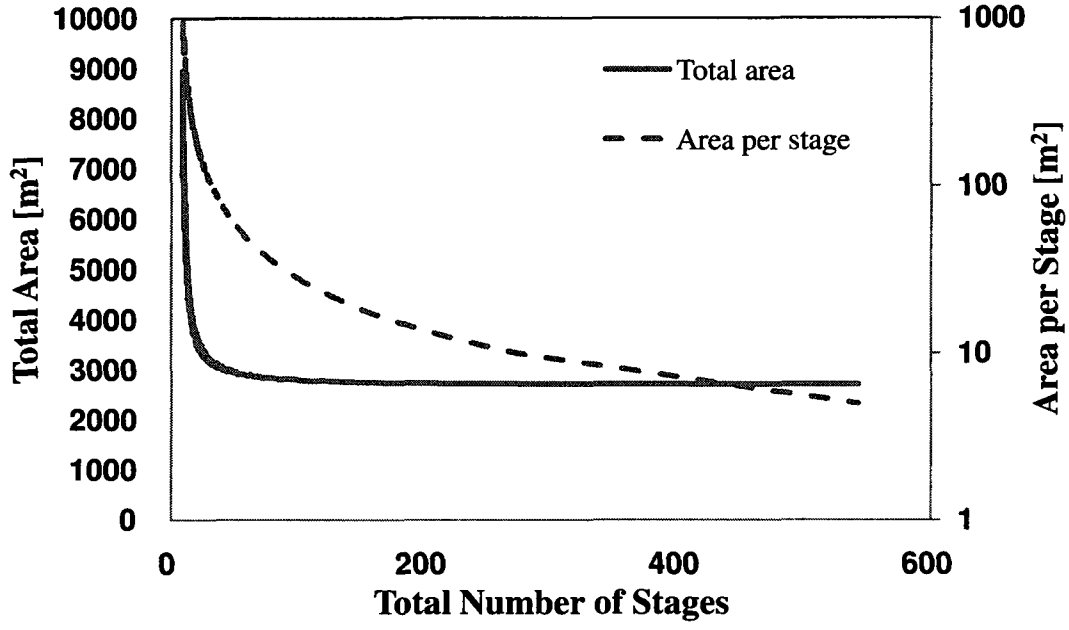

Figure 2.2 Relationship between the number of stages required with the total membrane area and the area per stage for a pervaporation system operating under the conditions given in Table 2.1.

2.3.2 Industrial-scale study for A-type zeolite membrane operating in a series arrangement

In North America, the capacity of the bioethanol industries varies from less than 3 million liters to over 400 million liters per year (Fagen INC., 2010; RFA, 2010). In this study, the Johnstown plant of Greenfield Canada was chosen as the base case. This plant has a fuel grade ethanol production capacity of 200 million liters per year (approximately 50 million

gallons per year). A summary of the operating conditions of the pervaporation membrane process used to simulate this bioethanol industrial scale production facility is presented in Table 2.2. In Table 2.2, the permeate pressure was increased to 13.3 kPa as compared to 2 kPa used in Table 2.1 because of the limitation of water ring vacuum compressors that needs to operate at higher pressure.

Table 2.2 Base case conditions for an industrial-scale membrane pervaporation process in a series arrangement.

Variables	Value	Unit
Feed flow rate	23225	kg/h
Feed ethanol concentration	80	wt%
Retentate ethanol concentration	92	wt%
Permeate pressure	13.3	kPa

As discussed above, the membrane area per stage was fixed to 27 m^2. It is now desired to examine the effect of the feed temperature on the number of stages for the operating conditions of Table 2.2. Figure 2.3 shows the evaporation energy per stage as a function of the number of stages required when the feed temperature varies between 78°C and 98°C. At each stage, the temperature entering the membrane module is at the same temperature as the feed temperature of the first stage. The pressure of each stage is set to a higher pressure than the atmospheric pressure if the feed temperature is above the saturation temperature. Figure 2.3 shows that an increase in the feed temperature leads to a decrease in the number of stages and an increase in the average evaporation energy per stage. When the temperature of the feed is increased, the vapor pressure of the ethanol-water mixture is higher and, as a result, both the driving force for pervaporation and the permeate flux increase. Since the separation efficiency is better at higher feed temperature, a lower number of stages are required to achieve the desired separation. On the other hand, Figure 2.3 shows that the total evaporation energy is nearly independent of the feed temperature. The small difference of the total evaporation energy is due to the small decrease in the latent heat of evaporation with temperature. Figure 2.4 provides more details on the variation of the evaporation energy used per stage as a function of the stage number for four different feed temperatures. For a higher

feed temperature, the permeate flux is larger initially and, as a result, the evaporation energy per stage is higher and the water concentration of the retentate decreases more rapidly. A decrease in the water vapor pressure leads to a decrease in the permeate flux. Therefore, the evaporation energy per stage decreases rapidly as a function to the stage number. For a lower feed temperature, the rate of pervaporation is much lower such that for a fixed membrane area per stage, the evaporation energy is significantly lower and a larger number of stages are required.

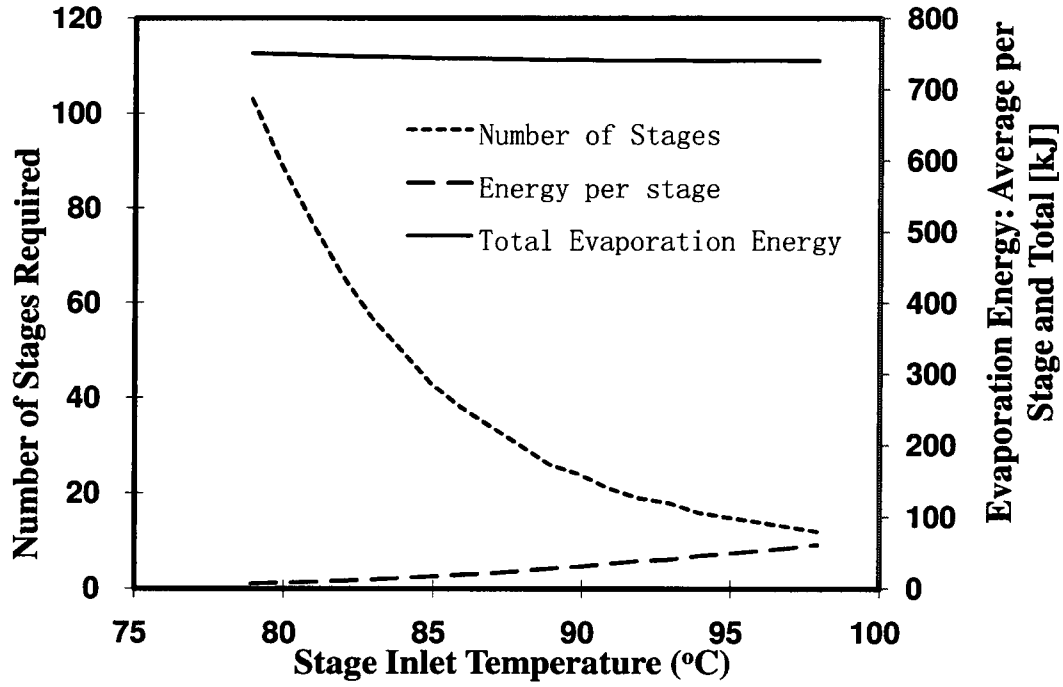

Figure 2.3 Number of stages required and evaporation energy (average per stage and total) as a function of the feed temperature with a fixed membrane area of 27 m^2 per stage for the operating conditions defined in Table 2.2.

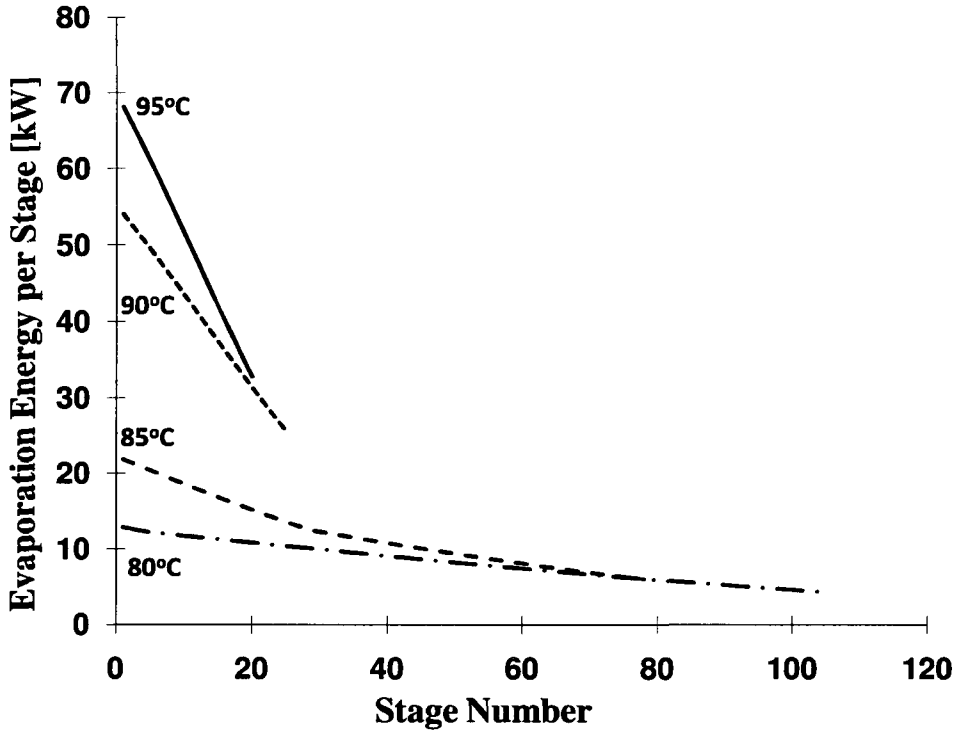

Figure 2.4 Evaporation energy per stage as a function of the stage number for four different feed temperatures with a fixed membrane area of 27 m^2 per stage for the operating conditions defined in Table 2.2

The results of Figures 2.3 and 2.4 were obtained for a fixed membrane of 27 m^2 per stage such that the temperature drop per stage varied. Another strategy is to use a varying membrane area per stage and maintain a fixed temperature drop per stage. Figure 2.5 presents the membrane area for the first stage as a function of the feed ethanol concentration and the feed temperature. The temperature drop per stage was fixed at 10°C. The curves in Figure 2.5 for higher feed temperatures are nearly parallel to each other prior to joining the plot that corresponds to the saturated temperature. The membrane area for the first stage is the smallest area of all the stages because the water concentration is higher and the minimum membrane module area increases as the feed ethanol concentration increases. The permeation flux relies on the vapor partial pressure difference between the retentate and the permeate. The water concentration progressively decreases through the module due to the selective permeation of water and the permeation flux decreases such that a higher membrane surface

area is required to achieve a temperature drop of 10°C. The membrane area required for the saturated feed temperature is smaller than the membrane area required for a fixed feed temperature such that it is recommended to use a saturated feed at each stage.

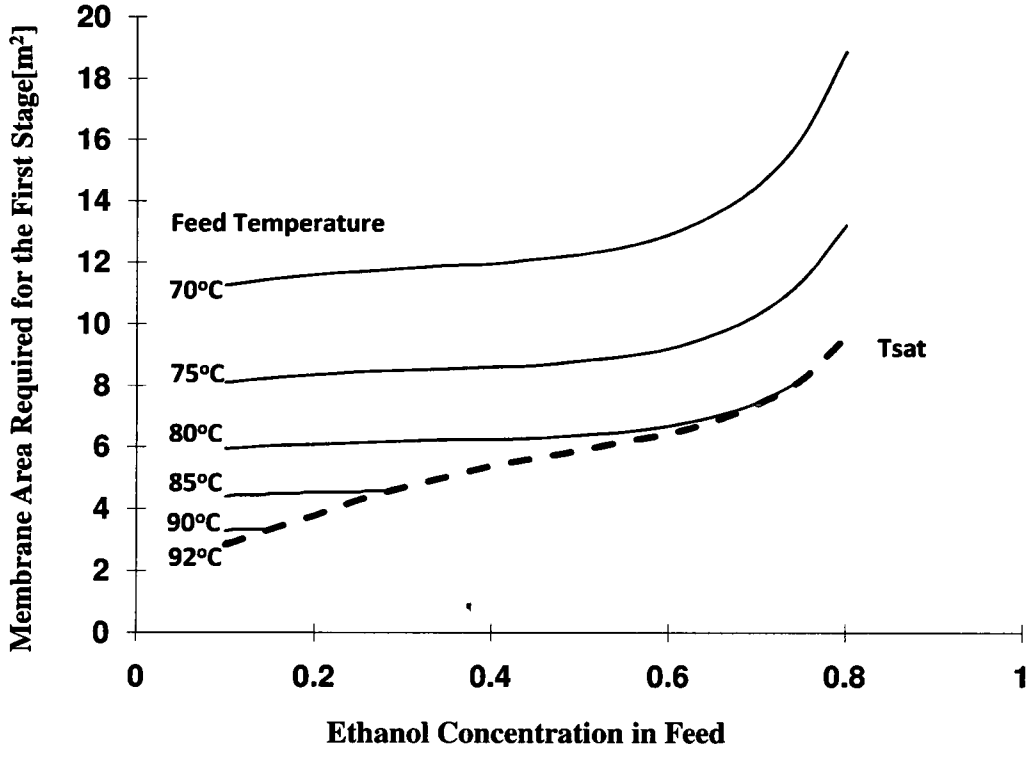

Figure 2.5 Membrane area required for the first stage to reach a 10°C temperature drop at the end of the stage as a function of inlet concentration for different feed temperatures for the operating conditions defined in Table 2.2

2.4 Multi-Objective Optimization

The parametric study performed in section 2.3 has highlighted the impact of the operating variables on the membrane area per stage and total area required to achieve a given separation. It is important to minimize the total membrane area and the number of stages simultaneously but results of the previous section have clearly demonstrated that these two objectives are conflicting (see Figure 2.2). In addition to the total membrane area and the number of stages, it is also important to minimize the energy consumed and the exergy loss to achieve a given separation. Multi-objective optimization is the process of simultaneously optimizing two or more conflicting objectives subject to some constraints. In this section, a multi-objective optimization method will used to determine the operating conditions that best satisfy the following four objectives: total number of stages, total membrane area, energy consumed and exergy loss. All four objectives need to be minimized. To make the analysis tractable, only two operating variables will be used in each case for the optimization. In the first case study, the membrane area per stage and the permeate pressure were changed. Table 2.3 summarizes the input and output variables of the optimization problem. All the other operating variables will be maintained constant. However, the variation of the latter will be the subject of different case studies. The values of all the other operating variables are listed in Table 2.4.

In this investigation, the Net Flow Method (NFM) will be used as the multi-objective optimization method (Thibault, 2009). This method consists of two steps. First, the domain of non-dominated solutions, i.e. the Pareto domain, is circumscribed. Then, the knowledge of an expert is used to rank all solutions of the Pareto domain in order to determine the best compromised solution. This method will be briefly described in the next sections and used for the optimization of the membrane pervaporation ethanol dehydration process.

2.4.1 Pareto Domain

The Pareto domain is the set of all non-dominated points. Pareto-optimal solutions are those for which an improvement in one objective can only occur with the worsening of at least one other objective. All solutions in the Pareto domain are at least better for one criterion when compared to all the other solutions of the Pareto domain. Thus, instead of a unique solution to the problem, the solution to a multi-objective problem is a set of Pareto-optimal solutions.

Many methods exist to determine the Pareto domain. In this investigation a diploid genetic algorithm is used and the main procedure to approximate the Pareto domain is as follow (Thibault et al., 2003; Thibault, 2009):

- The acceptable operating range of each input variable and the process constraints are specified.
- Values of all input variables are randomly generated within the allowable range. A large number of input variables are selected in order to have a good approximation of the Pareto domain.
- The process model uses each set of selected input variables to calculate the values of the output criteria or objective functions.
- All generated solutions are subjected to a pair-wise comparison to determine the number of times a point is dominated. A solution is dominated when it is worse for all criteria than any other solution within the Pareto domain. All solutions are then ranked with respect to the number of time they were dominated. All non-dominated solutions and a small fraction of the dominated solutions are kept. This population of solutions is used via a genetic algorithm to generate new solutions.
- The process is repeated until the desired number of non-dominated solutions is generated. This final population is an approximation of the Pareto domain. Only potential optimal solutions are retained.

Table 2.3 Input variables and objective criteria for determining the Pareto domain

Variables	Criteria	Optimized target
Area per stage	Total number of stages	Minimum
	Total area	Minimum
Permeate pressure	Total energy loss	Minimum
	Total exergy loss	Minimum

Table 2.4 Operating conditions for the membrane pervaporation process of an industrial-scale production facility with fixed temperature drop per stage.

Variables	Value	Unit
Feed flow rate	23225	kg/h
Feed ethanol concentration	80	wt%
Retentate ethanol concentration	92	wt%

2.4.2 Net Flow Method (NFM)

The Net Flow Method (NFM) is a multi-objective optimization method that is used to rank all solutions approximating the Pareto domain. NFM has been successfully used in the field of chemical engineering (Couroux et al., 1995; Halsall-Whitney et al., 2003; Perrin et al., 1997; Renaud et al., 2007; Thibault et al., 2001). NFM is used to rank all solutions of the Pareto domain based on the preferences of the decision-maker. In NFM, a priori knowledge of the process expressed by the decision-maker is incorporated into the optimization routine using four sets of ranking parameters: (1) the relative importance of each objective function, expressed as a relative weight, (2) the indifference threshold which defines the range of variation of each criterion for which it is not possible for the decision-maker to favour the criterion of one solution over the corresponding criterion of another solution, (3) the preference threshold whereby a preference is given to the better criterion if the difference between two values for a given criterion exceeds this threshold, and (4) the veto threshold which serves to ban a solution relative to another solution if the difference between the values of a criterion is too high to be tolerated. These four parameters are used to calculate the individual concordance index, the global concordance index and the discordance index, and finally the outranking matrix from which all solutions of the Pareto domain are ranked. The mathematical formulation of this calculation is found in Thibault (2009).

2.4.3 Optimization of an industrial-scale ethanol dehydration pervaporation process when the two input variables are the area per stage and the permeate pressure

In this section, the feed flow rate, the feed concentration, and the feed pressure are constant. The feed flow rate and the feed concentration are defined in Table 2.4 whereas the feed pressure was set to 3 atm. The feed temperature to each stage was fixed at the saturated temperature of the liquid mixture at the operating pressure. The membrane area per stage and the permeate pressure were used as input variables in the optimization procedure. Fixing the membrane surface area per stage implies that the temperature drop per stage will vary. A 50x50 grid of these two input variables was generated and, for each set of values, simulations were performed to calculate the four objective criteria (total number of stages, total membrane area required, total energy consumption, and total exergy loss) and to draw contour plots of these four objective criteria. The grid of solutions contains both dominated and non-dominated solutions. Then, for the same operating conditions, the Pareto domain

was determined using the diploid genetic algorithm and ranked with NFM. The four NFM parameters for each objective used to rank all points in the Pareto domain are given in Table 2.5.

Table 2.5 NFM parameters used to rank the Pareto domain.

Variable	Relative weight	Indifference threshold	Preference threshold	Veto threshold
Total number of stages	0.10	5	10	20
Total membrane area [m^2]	0.10	200	400	1000
Energy consumed [kW]	0.40	50	100	200
Exergy loss [kW]	0.40	5	10	20

Figure 2.6 presents the contour plot of the total number of stages as a function of the area per stage and the permeate pressure. As expected, the total number of stages decreases with an increase in the area per stage and with a decrease in the permeate pressure. Superimposed to the contour plot is the ranked Pareto domain using NFM. To minimize the total number of stages, the area per stage should be maximized and the permeate pressure should be minimized. The best solution is obtained for a low permeate pressure but with a relatively low area per stage. However, it is important to point out that the ranked Pareto domain considered the minimization of the four objective criteria simultaneously and the results must be viewed as compromised solutions. The best 10% of all solutions of the Pareto domain are located in two distinct regions: (1) low permeate pressure and small area per stage and (2) high permeate pressure and small area per stage. The right portion of the best 10% is dominated by the minimum energy consumption and minimum exergy loss, which will be seen in Figures 2.8 and 2.9. The best 10 to 50% of the Pareto-optimal solutions are located at small to medium area per stage and relatively high permeate pressure (15-20 kPa). Any solution on the graph not located in the Pareto domain is a dominated solution which implies that this solution is worse on all objective criteria than any solution contained in the Pareto domain.

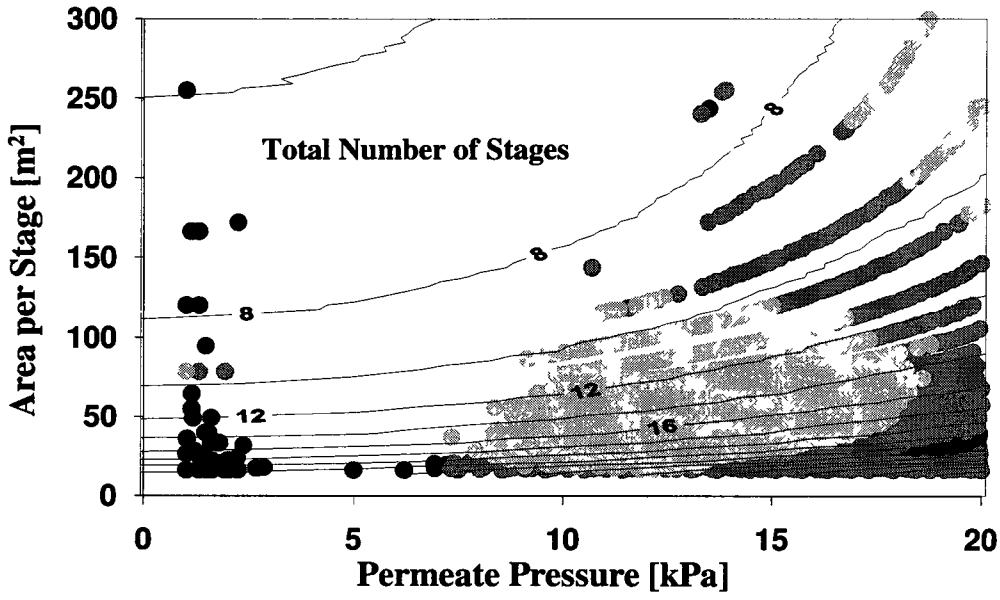

Figure 2.6 Pareto domain and contour plot of the total number of stages as a function of area per stage and permeate pressure for 3 atm feed pressure and operating variables defined in Table 2.4. (● – best solution; ● – best 10% solutions; ● - best 10% to 50% solutions; ● - remaining 50%).

Figure 2.7 presents the contour plot of the total membrane area as a function of the area per stage and the permeate pressure. The total membrane area is minimized when both the area per stage and the permeate pressure are minimum. The best compromised solution identified using the NFM does minimize the total membrane surface area. Figures 2.8 and 2.9 present the contour plots of the total energy consumed and the exergy loss as a function of the area per stage and the permeate pressure. Figures 2.8 and 2.9 show that the highest total energy consumed and the highest exergy loss are located in the vicinity of 5 kPa permeate pressure and 150 to 300 m^2 area per stage. Both of these criteria need to be minimized such that a high permeate pressure and a small area per stage are required. A high permeate pressure requires less energy consumed for the liquid ring vacuum compressor which is one of the major contributors to the energy consumption. Another contributor is the energy consumed by the heaters between two membrane modules. This energy contribution is determined by the retentate flow rate and the number of stages. For the combined effect of all variables, there is

a weak minimum occurring for the energy consumed and the exergy loss for low permeate pressure and high area per stage (low number of stages).

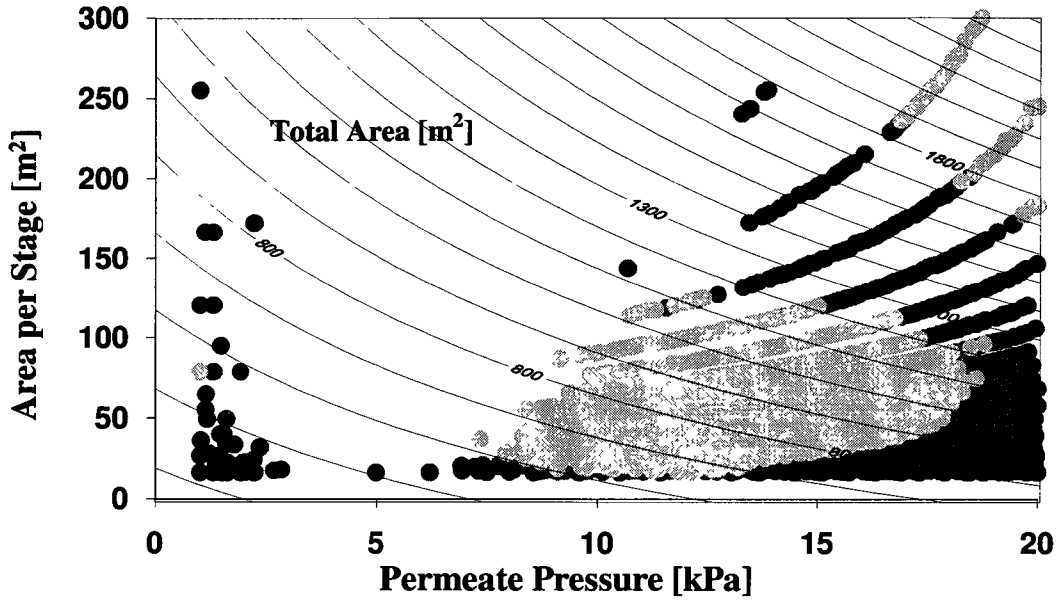

Figure 2.7 Pareto domain and contour plot of the total area as a function of the area per stage and the permeate pressure for a 3 atm feed pressure and operating variables defined in Table 2.4. (• – best solution; • – best 10% solutions; •- best 10% to 50% solutions; ◦ - remaining 50%).

On the other hand, a small membrane area per stage implies a smaller temperature drop per stage and, as a result, a higher average operating temperature and higher water permeation flux. Figure 2.10 shows the contribution of the membrane surface area per stage to the average water permeation flux as well as the permeation flux along the membrane. A smaller total membrane area is obtained when the area per stage is smaller. Figure 2.11 shows the variation of the membrane temperature as a function of the membrane area and shows that the average temperature of each module is higher for a smaller area per stage. Because of the decrease in the permeation flux with an increase in ethanol concentration, the temperature drop per stage will also decrease.

The domains of Figures 2.8 and 2.9 show that the best solution found by NFM is located at a medium values of energy consumption and a medium exergy loss. The right portion of the

best 10% of the Pareto-optimal solutions minimizes both the energy consumption and the exergy loss. When comparing the results of the four figures (Figures 2.6-2.9), the best point of the Pareto domain as identified by the NFM provides a reasonable compromised solution that corresponds to an optimum value for the total membrane area and intermediate values for the other three criteria. The left portion in the best 10% of the solutions of the Pareto domain are located where the energy consumed and the exergy loss are at their minimum values at the expense of increasing slightly the total membrane area and sacrificing the total number of stages. NFM is able to suggest more than one desirable operating state based on the preference made by the decision-maker. The influence of the weight factors used in NFM can be found in Appendix E.

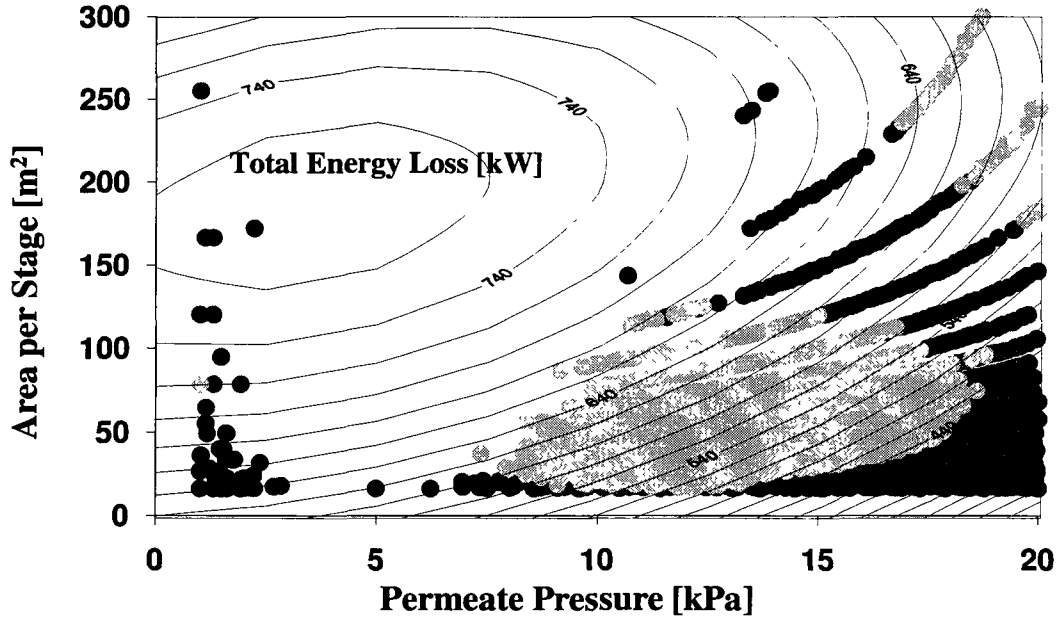

Figure 2.8 Pareto domain and contour plot of the total energy loss as a function of the area per stage and the permeate pressure for a 3 atm feed pressure and operating variables defined in Table 2.4. (• – best solution; • – best 10% solutions; •- best 10% to 50% solutions; · - remaining 50%).

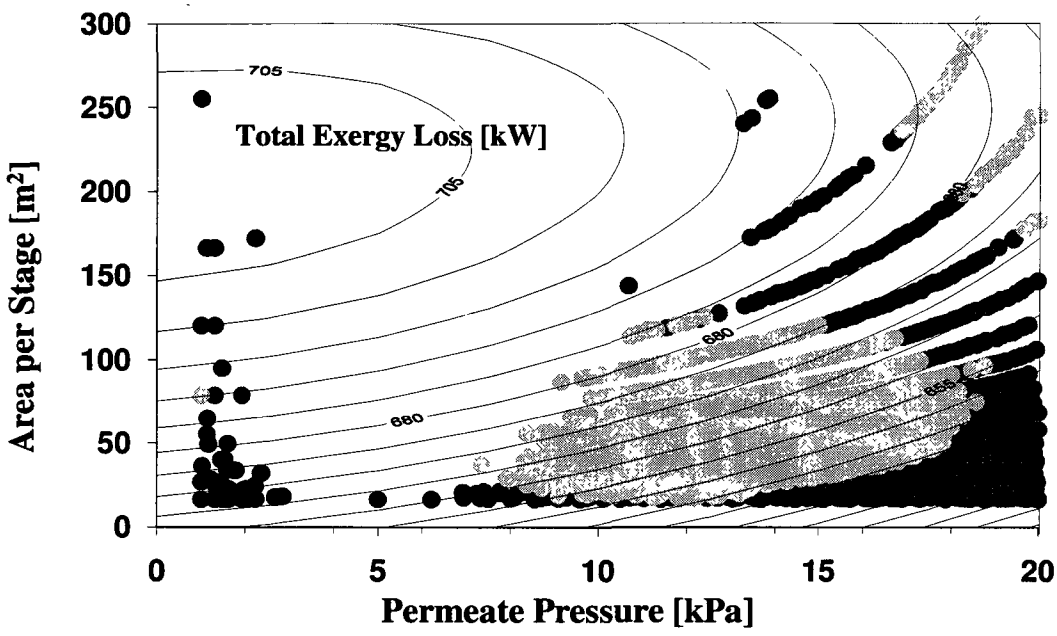

Figure 2.9 Pareto domain and contour plot of the exergy loss as a function of the area per stage and the permeate pressure for a 3 atm feed pressure and operating variables defined in Table 2.4. (● – best solution; ● – best 10% solutions; ●- best 10% to 50% solutions; ◦ - remaining 50%)

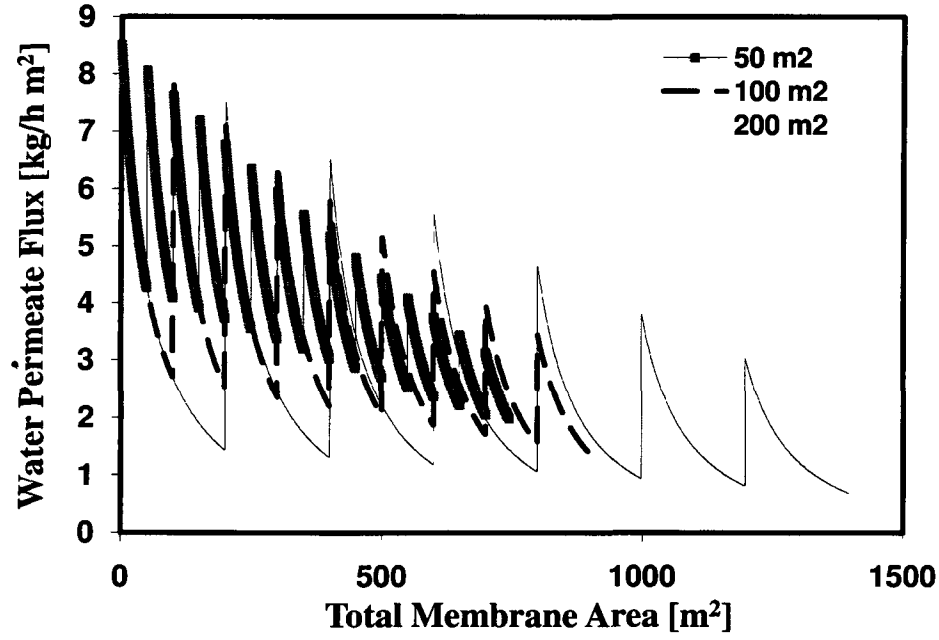

Figure 2.10 Water permeate flux as a function of the total membrane area for an area per stage of 50, 100 and 200 m^2 for a fixed area per stage.

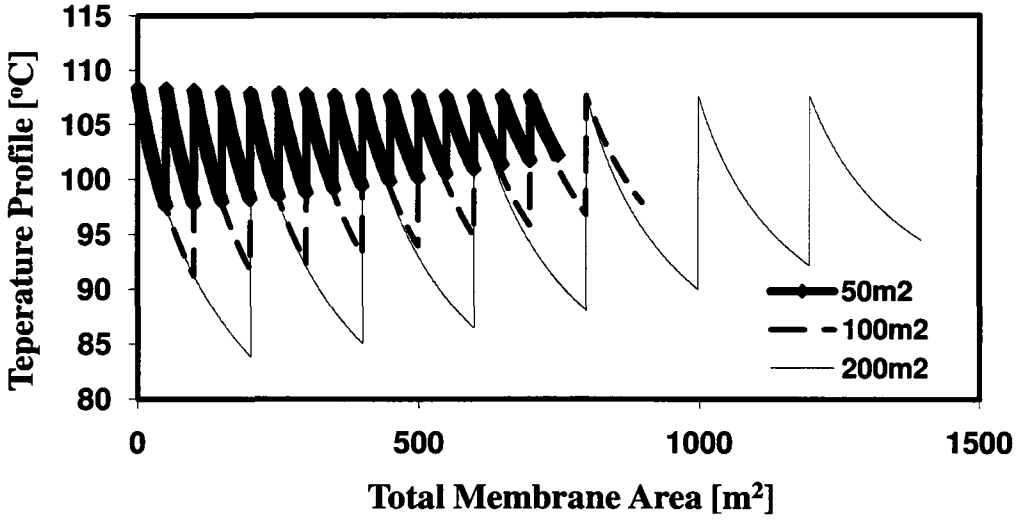

Figure 2.11 Temperature profile as a function of the total membrane area for an area per stage of 50, 100 and 200 m^2 for a fixed area per stage.

2.4.4 Optimization of an industrial-scale ethanol dehydration pervaporation process when the two input variables are the temperature drop per stage and the permeate pressure

A similar optimization study was performed for the case where a temperature drop was specified for each stage. This implies that the membrane surface area of each stage will be different. The varying input variables for this case study are therefore the temperature drop per stage and the permeate pressure. These two input variables were varied between 5 to 20°C and 2 to 25 kPa, respectively. Other operating conditions are the same as defined in Table 2.4. The total number of stages, the total membrane area, the total energy consumed and the total exergy loss were calculated for 2500 sets of input variables equally distributed on a 50x50 grid and contour plots of the four objective criteria were drawn. A series of simulations were also performed using the diploid genetic to circumscribe the Pareto domain for the minimization of the four objective criteria. The NFM was then used along with the parameters of Table 2.5 to rank all solutions of the Pareto domain. The ranked Pareto domain is superimposed onto the contour plots. Results of this optimization study are shown in Figures 2.12 to 2.15.

Based to the contour plot of Figure 2.12, the total number of stages is clearly dominated by the temperature drop per stage. When the temperature drop per stage is below 15°C, the total number of stages is nearly independent of the permeate pressure. Figure 2.13 shows that the total membrane area is strongly dependent on both the permeate pressure and the temperature drop per stage. To minimize the total membrane area, it is required to operate at both low permeate pressure and low temperature drop per stage. The total membrane area becomes very sensitive at higher permeate pressure and temperature drop per stage whereas the dependence is much weaker for low values of the input variables. Figure 2.14 highlights that the minimum energy consumption is observed at small temperature drop per stage and large permeate pressure. At low permeate pressures, there exists a temperature drop per stage for which the total energy consumed is maximum. The reason for the presence of the maximum is the same as previously discussed Figures 2.8 and 2.9 in Section 2.4.3. Figure 2.15 shows that the exergy loss will also be minimized with high permeate pressure and low temperature drop per stage.

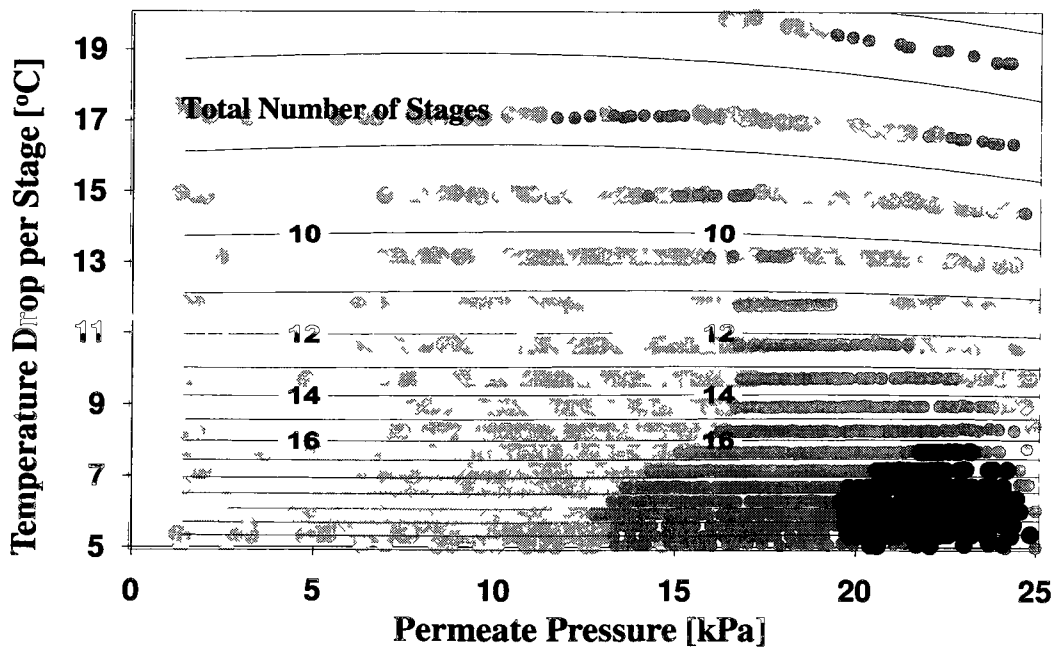

Figure 2.12 Pareto domain and contour plot of total number of stages as a function of the temperature drop per stage and the permeate pressure for 3 atm feed pressure and operating variables defined in Table 2.4. (● – best solution; ● – best 10% solutions; ● - best 10% to 50% solutions; - remaining 50%).

The ranked Pareto domains of Figures 2.13-2.15 show a very well defined zone of optimal operation. The best solution, based on the NFM parameters of Table 2.5, is obtained for a low temperature drop per stage and a high permeate pressure. The zone of the best 10% solutions is very well defined and surrounds the best solution. In this case, the multicriteria optimization satisfies perfectly the total energy consumed and the total exergy loss whereas the total membrane area is relatively well satisfied. On the other hand, the total number of stages has been completely sacrificed because the best solution is located where its value is close to the maximum. It is possible that the decision-maker would not be satisfied to have a very large number of stages because each stage requires a heat exchanger to increase the temperature of the retentate to its saturated liquid value. An optimization process is an iterative process where the expert or decision-maker needs to be involved. The decision-maker could increase the relative weight and modify the threshold values of this criterion but at the expense of not satisfying as well the other three criteria. Inevitably, some compromises need to be made because it is not possible to minimize all criteria at the same time.

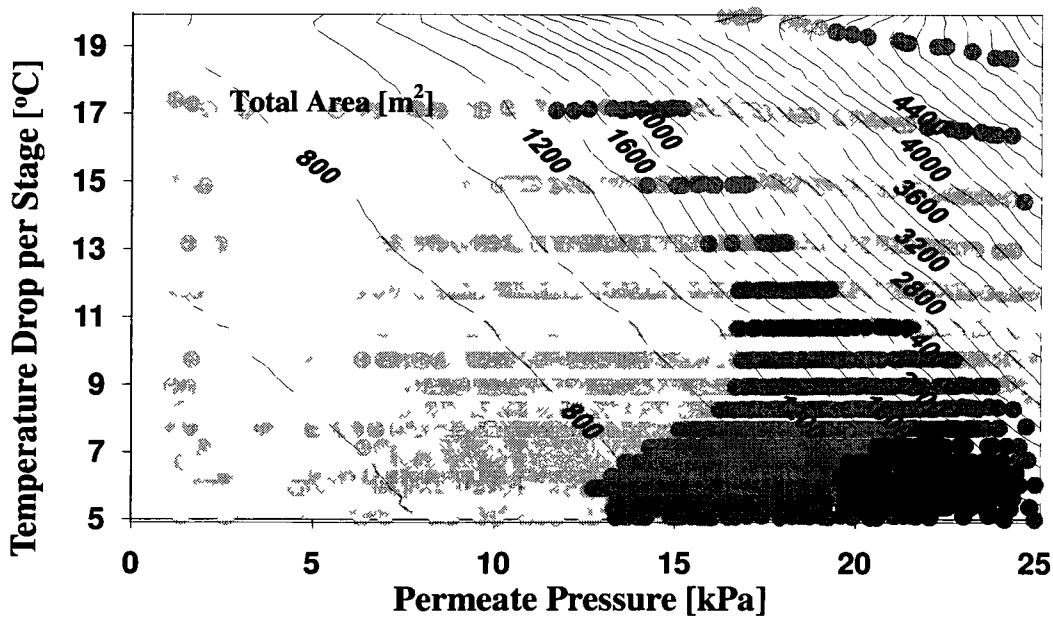

Figure 2.13 Pareto domain and contour plot of total membrane area as a function of the temperature drop per stage and the permeate pressure for 3 atm feed pressure and operating variables defined in Table 2.4. (• – best solution; • – best 10% solutions; •- best 10% to 50% solutions; • - remaining 50%).

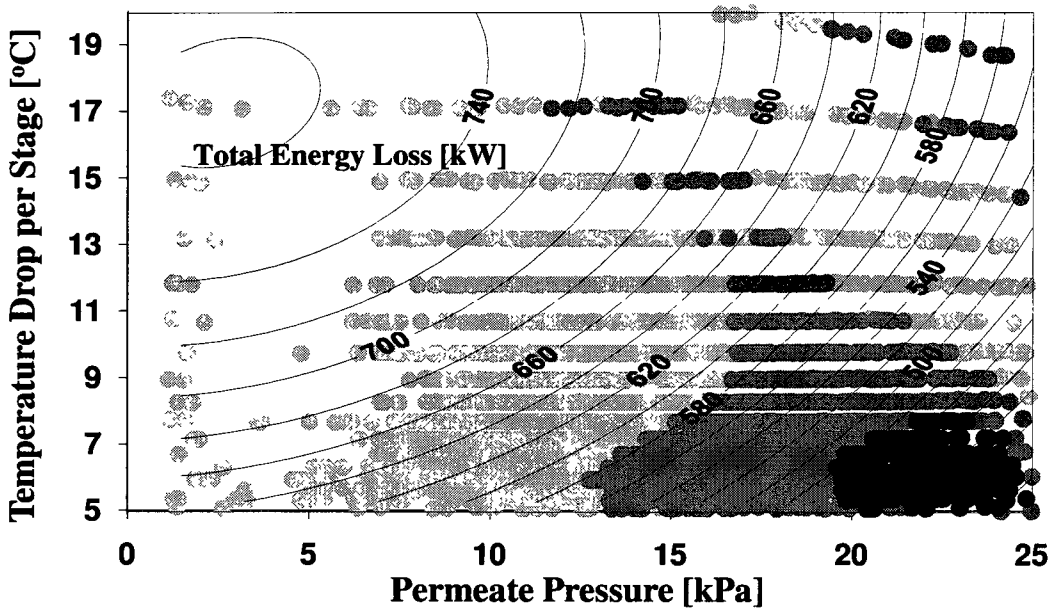

Figure 2.14 Pareto domain and contour plot of total energy consumed as a function of the temperature drop per stage and the permeate pressure for 3 atm feed pressure and operating variables defined in Table 2.4. (● – best solution; ● – best 10% solutions; ●- best 10% to 50% solutions; ● - remaining 50%).

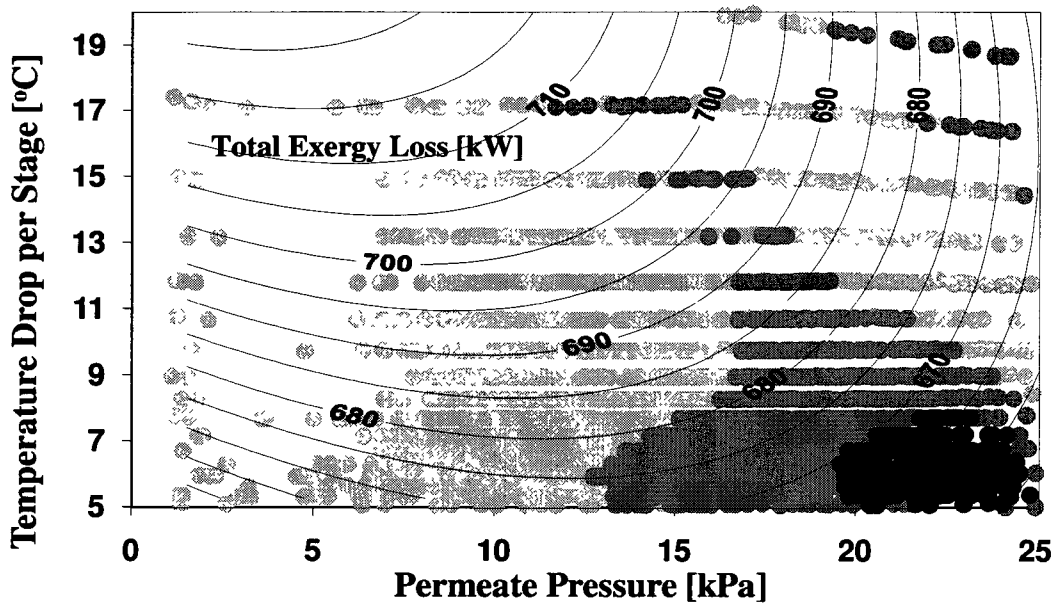

Figure 2.15 Pareto domain and contour plot of total exergy loss as a function of the temperature drop per stage and the permeate pressure for 3 atm feed pressure and operating variables defined in Table 2.4. (● – best solution; ● – best 10% solutions; ● - best 10% to 50% solutions; ● - remaining 50%).

2.4.5 Optimization of an industrial-scale ethanol dehydration pervaporation process when the two input variables are the permeate pressure and the retentate pressure

Another optimization study was performed for the case where the permeate pressure and the retentate pressure are varied whereas all the other operating variables are fixed and defined in Table 2.4. In addition, the temperature drop per stage is fixed at 10°C, which implies that the membrane surface area of each stage will be different. The varying input variables, the permeate and retentate pressures, were varied between 2 to 25 kPa and 1.01 to 5.05 bars, respectively. The total number of stages, the total membrane area, the total energy consumed and the total exergy loss were calculated for 2500 sets of input variables equally distributed on a 50x50 grid and contour plots of the four objective criteria were drawn. The Pareto domain for the minimization of the four objective criteria was obtained and ranked with NFM. The ranked Pareto domain was superimposed onto the contour plots. Results of this optimization study are shown in Figures 2.16 to 2.19.

Figure 2.16 shows that the total number of stages is a very weak function of the permeate and retentate pressure. Indeed, in the whole range of pressures tested, the total number of stages is between 11 and 13. The number of stages, as shown in Section 2.4.4, is dictated by the temperature drop per stage and is relatively insensitive to permeate pressure. A higher pressure driving force across the membrane will affect the permeation flux such that a smaller area will be required and the 10°C temperature drop will be achieved more rapidly but essentially the same number of stages is required. The small observed difference is due to the effect of pressure on the temperature profile along the membrane. Figure 2.17 shows, as expected, a strong dependence of the pressure difference on the total membrane area. Indeed, a small membrane area will be obtained for the lowest permeate pressure and the highest retentate pressure. The effect of the pressure difference on the total area is non linear and becomes very pronounced as the pressure difference is reduced. Since either increasing the retentate pressure or decreasing the permeate pressure is energy consuming, a higher pressure difference leads to a higher energy consumption and exergy loss as depicted Figures 2.18 and 2.19. Both criteria are minimized for a high permeate pressure and low retentate pressure.

The ranked Pareto domain shows that the best point is at the low permeate pressure and the low retentate pressure which provide the smallest total membrane area, an intermediate value of the energy consumption and an intermediate value of the exergy loss. However, the majority of the best 10% of Pareto-optimal solutions are in a zone of a high permeate pressure and high retentate pressure with essentially the same low total membrane area and intermediate energy consumption and energy loss. The different zones of the Pareto domain are well defined and it appears that the best zone is a diagonal band where the three sensitive criteria are essentially equal. In this case, the number of stages could almost be removed as an active criterion because of its relatively low sensitivity.

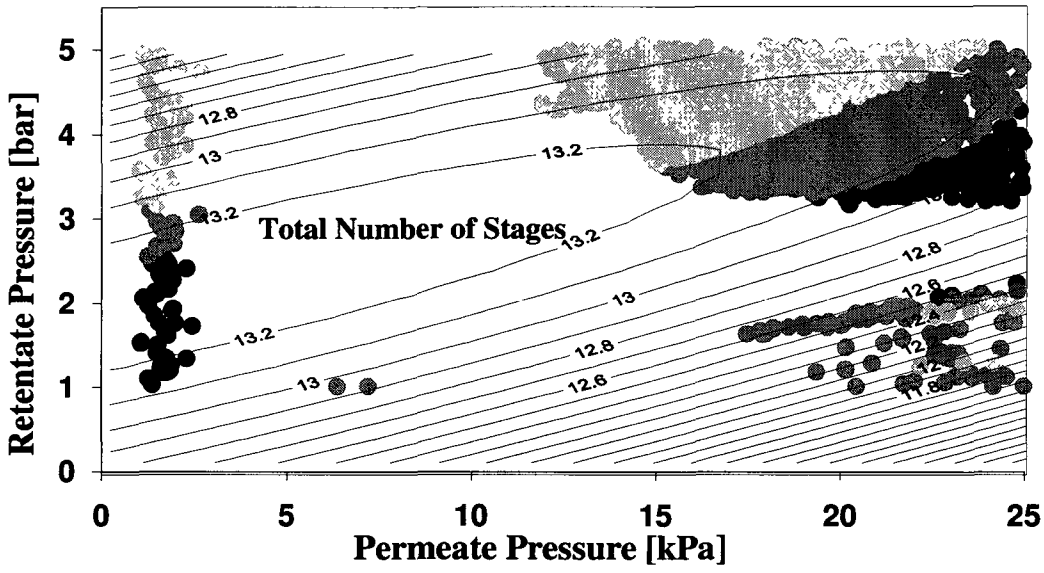

Figure 2.16 Pareto domain and the contour plot of the total number of stages as a function of the retentate pressure and the permeate pressure for a 10°C temperature drop per stage and for the operating variables defined in Table 2.4. (● – best solution; ● – best 10% solutions; ●- best 10% to 50% solutions; ● - remaining 50%).

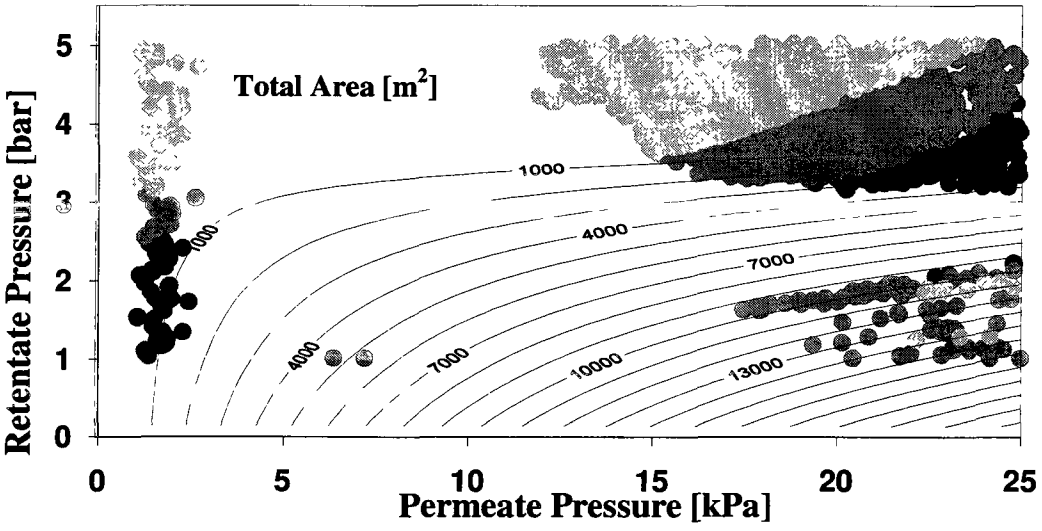

Figure 2.17 Pareto domain and the contour plot of the total area as a function of the retentate pressure and the permeate pressure for a 10°C temperature drop per stage and for the operating variables defined in Table 2.4. (● – best solution; ● – best 10% solutions; ●- best 10% to 50% solutions; ● - remaining 50%).

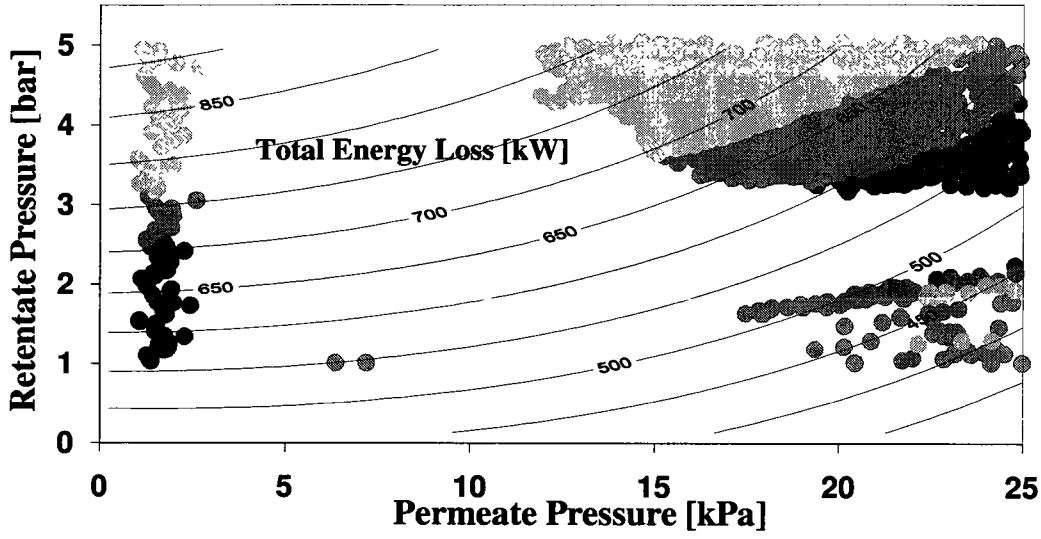

Figure 2.18 Pareto domain and the contour plot of the total energy consumed as a function of the retentate pressure and the permeate pressure for a 10°C temperature drop per stage and for the operating variables defined in Table 2.4. (● – best solution; ● – best 10% solutions; ◉- best 10% to 50% solutions; ◉ - remaining 50%).

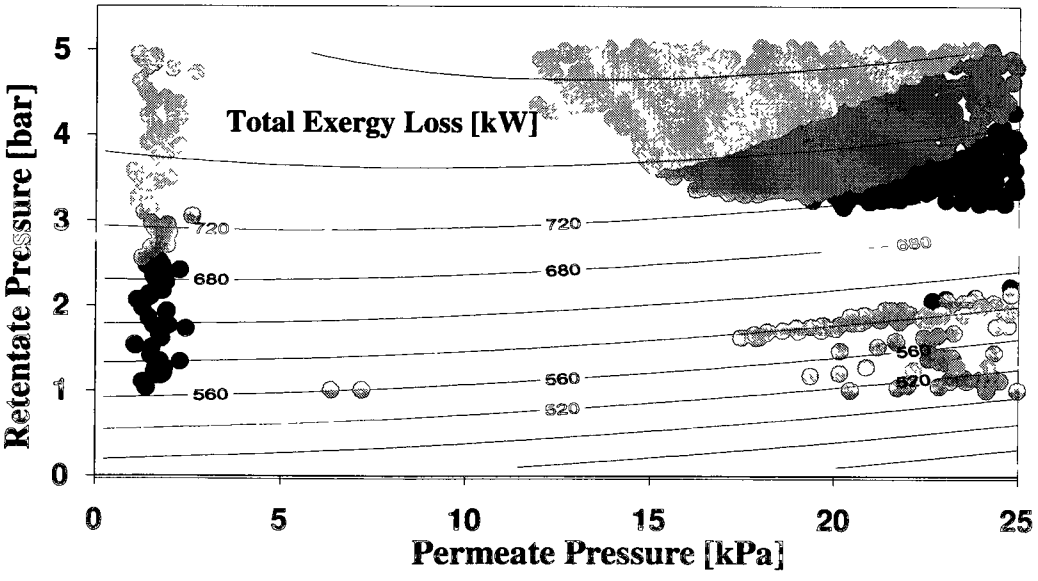

Figure 2.19 Pareto domain and the contour plot of the total exergy loss as a function of the retentate pressure and the permeate pressure for a 10°C temperature drop per stage and for the operating variables defined in Table 2.4. (● – best solution; ● – best 10% solutions; ◉- best 10% to 50% solutions; ◉ - remaining 50%).

2.5 Conclusion

The parametric analysis and the four-objective optimization were carried out for removal of water from ethanol/water mixture by A-type zeolite membrane modules. In the parametric analysis, besides pointing to optimal working conditions, it is shown that the minimum total membrane area and the minimum total number of stages are conflicting objectives. The four-objective optimization for the simultaneous minimization of the total membrane area, the total number of stages, the energy consumed, and the exergy loss are carried out using an approximation of the Pareto domain and the NFM for ranking the Pareto domain. Suitable compromises are identified among the four objective criteria. The area per stage and the temperature drop per stage are major contributors to the total number of stages to reach a desired separation. It is also found that the decision variables (the area per stage, the temperature drop per stage, and the retentate pressure) are shown to lie at their lower bound in the Pareto domain solutions, whereas the permeate pressure should lie either at its lowest or highest bound.

References

Bausa, J. and Marquardt, W. Shortcut Design Methods for Hybrid Membrane/Distillation Processes for the Separation of Nonideal Multicomponent Mixtures, Ind. Eng. Chem. Res. 39 (2000) 1658-1672.

Cojocaru, C., Khayet, M., Zakrzewska-Trznadel., G., Jaworska, A. Modeling and multi-response optimization of pervaporation of organic aqueous solutions using desirability function approach, J. Hazardous Materials 167 (2009) 52-63.

Couroux, P., Qannar, E.M., Melcion, J.P., and Morat, J. Optimisation multiréponse: Application à un procédé de granulation d'aliments, Récents Progrès en Génie des Procédés: Stratégie Expérimentale et Procédés Biotechnologiques, 36:9 (1995) 41-47.

Eldridge, R.B. and Seibert, A.F., Hybrid Separations/Distillation Technology Research Opportunities for Energy and Emissions Reduction, Separation Research Program University of Texas at Austin, 2005.

Fagen INC., http://www.fageninc.com/gallery/ethanol.htm, accessed June 2010

Fontalvo, J., Cuellar, P., Timmer, J. M. K., Vorstman, M. A. G., Wijers, J. G., and Keurentjes, J. T. F. Comparing Pervaporation and Vapor Permeation Hybrid Distillation Processes. Ind. Eng. Chem. Res., 44 (2005) 5259-5266.

Haelssig, J. B., Tremblay, A. Y., and Thibault , J., Technical and Economic Considerations for Various Recovery Schemes in Ethanol Production by Fermentation, Ind. Eng. Chem. Res., 47 (2008) 6185–6191

Halsall-Whitney, H., Taylor, D., and Thibault, J. Multicriteria optimization of gluconic acid production using Net Flow, Bioprocess and Biosystems Engineering, 25:5 (2003) 299-307.

Karaosmanoglu, F., Isigigur, A., and Aksoy, H. A., Effects of a new blending agent on ethanol-gasoline fuels, Energy & Fuels, 10 (1996) 816-820

Kita, H., Horii, K., Ohtoshi, Y., Okamoto, K. I., Tanaka, K. Synthesis of a zeolite NaA membrane for pervaporation of water/organic liquid mixtures. J. Material Science Letter 14 (1995) 206-208.

Kondo, M., Yamamura, T., Yukitake, T., Matsuo, Y., Kita, H., Okamoto, K.-I. IPA purification for lens cleaning by vapor permeation using zeolite membrane Separation and Purification Technology, 32 (2003) 191-198.

Morigami, Y., Kondo, M., Abe, J., Kita, H., and Okamoto, K. The first large-scale pervaporation plant using tubular-type module with zeolite NaA membrane. Sep. Purif. Technol. 25 (2001) 251-260.

Nemmani, G.R., Suggala, S.V., and Bhattacharya, P.K. NSGA-II for Multiobjective Optimization of Pervaporation Process: Removal of Volatile Organics from Water. Ind. Eng. Chem. Res. 48 (3) (2009) 1543-1550.

Perrin, E., Mandrille, A., Oumoun, M., Fonteix, C., and Marc I. Optimisation globale par stratégie d'évolution: Technique utilisant la génétique des individus diploïdes. RAIRO-Recherche Opérationnelle, 31 (1997) 161-201.

Renaud, J., Thibault, J., Lanouette, R., Kiss, L.N., Zaras, K., and Fonteix, C. Comparison of two multicriteria methods: Net Flow and Rough Set methods for aid to decision in a high yield pulping process. EJOR 177 (2007) 1418-1432.

Renewable Fuels Association (RFA), Fuel Ethanol Industry guidelines, specifications, and procedures. 2003.

RFA, http://www.ethanolrfa.org/industry/statistics/#A, accessed June 2010.

Richter, H., Voigt, I., Kühnert, J.-T., Dewatering of ethanol by pervaporation and vapour permeation with industrial scale NaA-membranes, Desalination 199 (2006) 92–93

Sommer, S., Melin, T., Influence of operation parameters on the separation of mixtures by pervaporation and vapor permeation with inorganic membranes. Part 1: Dehydration of solvents, Chem. Eng. Sci. 60 (2005) 4509 – 4523.

Thibault, J., Taylor, D., Yanofsky, C., Lanouette, R., Fonteix, C., and Zaras, K., Multicriteria optimization of a high yield pulping process with rough sets. Chem. Eng. Sci. 58 (2003) 203 – 213.

Thibault J. Net Flow and Rough Sets: Two Methods for Ranking the Pareto Domain. Chap. 7 in G.P Rangaiah, Ed.: Multi-Objective Optimization – Techniques and Applications in Chemical Engineering. Advances in Process Systems Engineering – Vol. 1, World Scientific (2009).

Tremblay, A., Thermodynamically Guided Integration of Distillation and Membrane Processes for Azeotropic Mixture Separation, Report submitted to NRCan. Department of Chemical Engineering, University of Ottawa, 2006.

United Nations Environment Programme (UNEP), Towards sustainable production and use of resources: Assessing biofuels, 2009

Yanofsky, C., Taylor, D. G., and Thibault, J. Novel methodology for assessing a ranked Pareto domain: Drift group analysis. Chem. Eng. Sci. 61 (2006) 1312-1320.

CHAPTER 3

Exergy Optimization of Bioethanol Dehydration using Hybrid Distillation/Membrane Systems

J. Yuan[1], J. Thibault[1], A. Tremblay[1] and Mikhael Sorin[2]

[1]Department of Chemical and Biological Engineering, University of Ottawa

Ottawa, Ontario, Canada K1N 6N5

[2]Canmet ENERGY, Natural Resources Canada Varennes, Quebec, Canada J3X 1S6

Abstract

The exergy requirements of a hybrid distillation/pervaporation hybrid system were studied for the separation of ethanol and water. The concentration of ethanol fed to the hybrid system was in the tangent pinch zone of the vapour –liquid equilibrium just below the azeotropic composition of ethanol. This composition is difficult to treat using distillation alone as a large number of trays are required to perform the separation. A pervaporation unit was fed liquid from various trays above the feed tray in the distillation column. Retentate from the pervaporation unit was sent back to the top of the column and the permeate sent below the feed tray to a tray having a similar liquid composition. The input and output compositions of ethanol to the hybrid system were kept constant for all experiments.

The exergy loss of the hybrid system was linearly correlated to the reflux ratio of the distillation column. For most trays, the exergy loss and reflux ratio exhibited a minimum for a draw ratio of 40%. The minimum value of exergy loss was 15.5 kJ/mole of ethanol product at a reflux ratio of 0.58 and a draw rate of 40%. However, the lowest exergy loss was

obtained by using the pervaporation unit alone with the same operating parameters. The exergy loss of pervaporation only was 3.8 kJ/mol of ethanol product compared to 38.5 kJ/mole of ethanol product, which is the exergy loss of distillation only. This represents a 10 fold decrease in exergy loss that was due the absence of a reflux in the membrane system. The combined hybrid system uses less membrane area than the pervaporation alone. The membrane area required for the membrane pervaporation is proportion to the draw ratio.

3.1 Introduction

Bioethanol is the most widely used gasoline oxygenate (RFA, 2003). Its production from cellulosic biomass has considerable green house gas reduction potential (UNEP, 2009). The demand and supply of bioethanol have nearly doubled in the past 5 years (RFA, 2010). However, its production requires considerable energy during the distillation process. Although distillation is still the dominant separation process in industry, there are several disadvantages in using a single distillation column to recover fuel grade bioethanol from fermentation broths. First, the single distillation column cannot overcome the azeotrope, which is at 95.6 wt% ethanol. Normally, the ethanol content is in the vicinity of 10 wt% ethanol from the beer column (Haelssig et al., 2008); however, the fuel grade ethanol contains less than 1 wt% water (Aventine renewable energy INC., 2009). Second, the separation of ethanol and water by distillation is very energy-intensive and costly (Eldridge & Seibert, 2005). Especially at high ethanol concentrations, the efficiency of distillation is very low. Many options have been studied to increase the energy-efficiency of distillation process, to replace it with alternative technologies, or to form more energy-efficient hybrid systems. At a low ethanol concentration, distillation is an unbeatable candidate for its flexibility, low investment, and low operational risk in industrial scale production (Eldridge & Seibert, 2005). However, above 70 wt% ethanol, two major problems exist: high energy input and a large number of trays. Many techniques have been introduced in the bioethanol dehydration process to solve these two major problems, such as: pressure-swing distillation, adsorption, extraction, pervaporation, and vapor permeation. Unfortunately, pressure-swing distillation is costly (Widagdo & Seider, 1996), adsorption requires more space and complex control systems for the paired columns to allow adsorbing and desorbing simultaneously (Cheah, 2010), extraction adds entrainers into the system that require a separation process,

and pervaporation and vapor permeation are low capacity (Will and Lichtenthaler, 1992; Sommer & Melin, 2005; Richter et al., 2006) and high capital cost (Sander & Soukup, 1988; Szitkai et al., 2002).

Presently one of the most attractive techniques for bioethanol dehydration is hybrid distillation. Haelssig (2008) simulated six alternative bioethanol recovery processes in Aspen HYSYS 2004.2 and investigated the economic and technical perspective of each process. The six processes include basic steam stripping distillation, flash fermentation distillation, single column distillation, two-column distillation, distillation with heat pump, and flash-vacuum distillation. After comparisons, two-column distillation operating at the different pressures and distillation with a vapor recompression system were recommended; however, from the energy saving standpoint, the flash fermentation process showed the highest efficiency. Fontalvo et al. (2005) compared the pervaporation and vapor permeation hybrid distillation processes for acetonitrile dewatering. They drew a conclusion that pervaporation or vapor permeation reduced the total cost between 25% and 60%. Although the capital cost of the membrane-distillation hybrid system is higher than the conventional distillation-based processes, the main reduction is due to the lower energy consumption of the membrane-distillation hybrid system (Fontalvo et al., 2005). Also, at a low water concentration, the pervaporation process saved more energy than vapor permeation process. Szitkai et al. (2002) studied a hybrid ethanol dehydration system. They connected a pervaporation unit to the top of distillation column to produce pure ethanol. Their studies showed that the hybrid system could be operated at a decreased reflux ratio and reduced the total annual cost of the separation process. In 2000, Bausa and Marquardt investigated distillation and membrane pervaporation individually, and introduced several possible configurations for a hybrid system. Unfortunately, they did not state a detailed design for the ethanol dehydration. Membrane pervaporation assisted systems have mainly focused on overcoming the azeotrope. In this work, the distillation-pervaporation hybrid system is operated in the tangent pinch zone of the ethanol/water VLE line, where the more energy consumption occurs. The focus of this work is to optimize exergy savings for the hybrid configuration.

3.2 Superstructure of the distillation-pervaporation hybrid system.

The pervaporation hybrid system consists in a traditional distillation column with 80 sieve trays and a series arrangement of membrane pervaporation units followed by a heating system. Figure 3.1 presents the superstructure of the pervaporation hybrid. In order to study this system at the tangent pinch for ethanol-water, a saturated mixture containing 80 wt% ethanol is fed to the distillation column at tray 65, where the ethanol concentration in the liquid phase is close to the feed concentration. Liquid flows down the column and is collected in the reboiler, where heat is supplied to generate vapor. The liquid removed from the reboiler is the bottom product. The vapor rises up the column and is cooled in a condenser at the top. The condensed liquid is stored in the reflux drum. A fraction of the condensate is recycled back to the top of the column as a reflux, and the rest of the liquid is removed from the column as the distillate. The intermediate liquid product drawn from the column to the pervaporation unit is removed from a tray located between the feed stage and the reflux. The drawn liquid flows through the membrane module where water is removed through a hydrophilic pervaporation membrane. The permeation decreases the retentate temperature due to the evaporation of the permeate flow. In order to maintain permeate evaporation, it is necessary to increase the retentate temperature before it enters the next membrane section. A liquid ring vacuum pump (LRVP) is used to keep a low pressure on the permeate side. A number of membrane sections are employed to achieve the desired retentate concentration. According to their concentration, the retentate and permeate flows are sent back to the distillation column at the trays with the closest concentration. The total permeate flow is recycled since it was shown to be optimal (Szitkai et al., 2002). Tables 3.1 and 3.2 list the geometric parameters of the membrane module and distillation column. The mathematical models for the distillation column (Bai, 2003) and the A-type zeolite membrane (Sommer & Melin, 2005) are described in Appendices A and C.

Table 3.1 Geometric parameters of A-type zeolite membrane module

Parameters	Values	Unit
Tube number	100	
Tube area	0.33	m^2

Table 3.2 Geometric parameters of distillation column

Parameters	Values	Unit
Diameter	1.5	m
Tray space	0.46	m
Total tray area	1.76	m^2
Net tray area	1.62	m^2
Bubbling area	1.48	m^2
Downcomer area	0.14	m^2
Weir length	1.00	m
Downcomer width	0.19	m
Hole diameter	0.005	m
Fractional hole area	0.1	m^2
Outlet weir height	0.05	m
Clearance under downcomer	0.038	m
Tray thick	0.003	m
Pitch	0.014	m
Reflux drum diameter	1.016	m

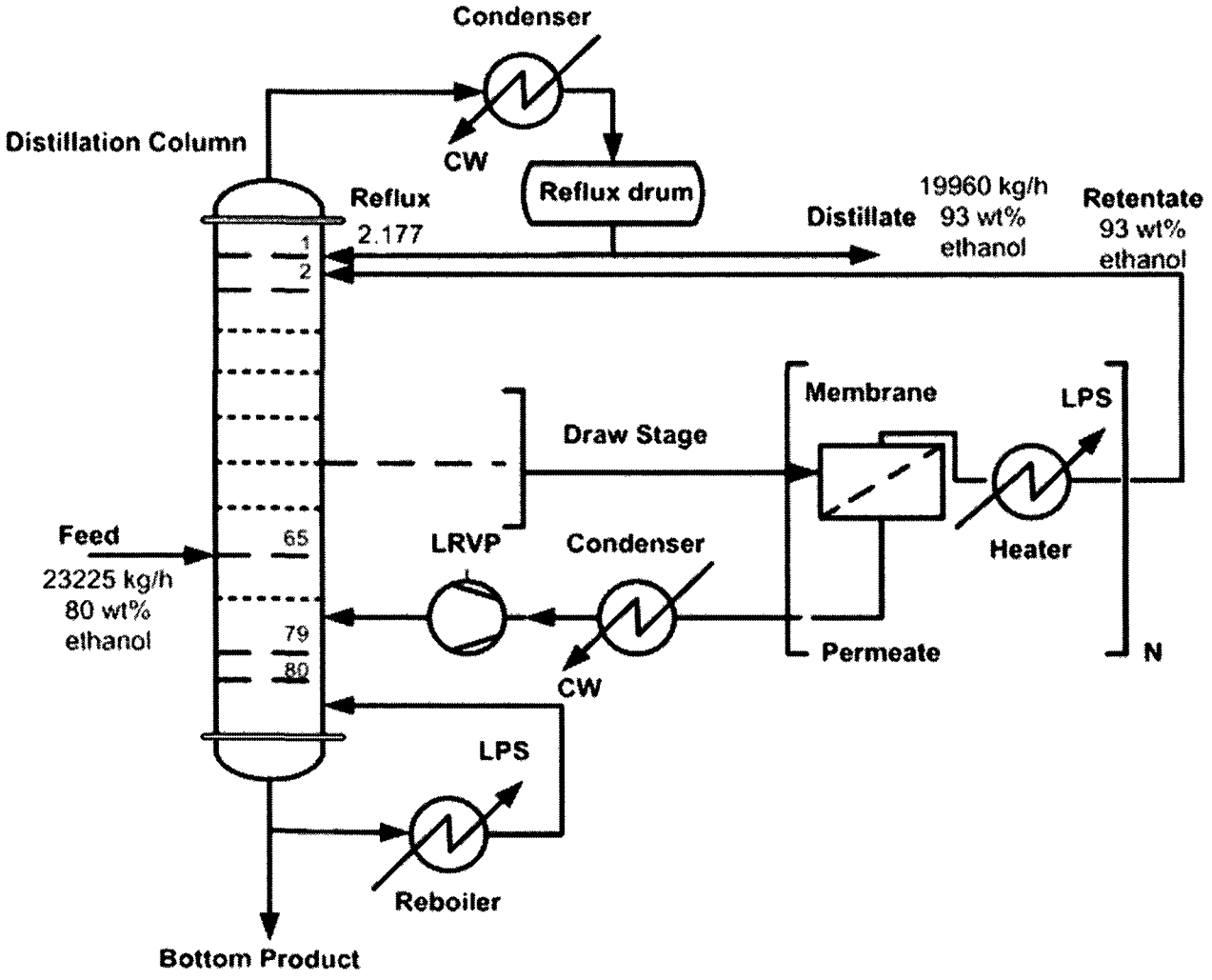

Figure 3.1 Superstructure of the hybrid system with draw stage at 65 and 30% draw ratio

3.3 Exergy loss optimization of the pervaporation hybrid for a tangent pinch on the VLE line

3.3.1 Tangent pinch on the VLE line

As a non-ideal mixture, ethanol/water has an azeotropic point on the equilibrium curve at 95.6 wt% under normal conditions. The inflection of the equilibrium curve before the azeotrope can give rise to the tangent pinch point, where the rectifying line is tangent to the equilibrium curve. The presence of the tangent pinch point indicates that the minimum reflux ratio evaluated by the feed pinch is not sufficient to make the desired separation. As a result, a higher reflux ratio and a large number of trays are expected. Furthermore, at the tangent pinch, distillation results in very small fractionation and would require an infinite number of stages to reach the azeotropic composition. If there are intermediate products drawn between the feed and the reflux stages, the reflux ratio can be changed by changing the slope of the rectifying line such that it is possible to reduce the reflux ratio by drawing part of liquid flow at the tangent pinch.

3.3.2 Exergy

Exergy is the useful energy that is not possible to recover in a process. After Keenan (1951) and Rant (1956) introduced exergy in process analysis, exergy has been taken as a more precise and adequate standard to evaluate process efficiencies (Araujo et al., 2007; Almeida-Rivera and Grievink, 2008; Faria and Zemp, 2005; Goff et al., 1996; Taprap and Ishida, 1996; Koeijer and Rivero, 2003; Liapis and Bruttini, 2008). Compared with the traditional energy balances analysis, the exergy balance analysis emphasizes the degradation of energy in a system based on the second law of thermodynamics. The general equation used to calculate the exergy of a stream is shown in Eq. 3.1

$$Exergy = H - T_{ref} S \tag{3.1}$$

Where H is the enthalpy of the stream [kJ]; S is the entropy of the stream [kJ/K]; T_{ref} is the reference temperature [K].

According to the second law of thermodynamics, the entropy change of a process can never be negative such that the exergy of a process is always depleted. The irreversible exergy loss is evaluated by the sum of the exergy of all streams (Eq. 3.2).

$$\left\{\begin{matrix}\text{exergy change} \\ \text{in a process}\end{matrix}\right\} = \left\{\begin{matrix}\text{sum of exergy} \\ \text{of outlet streams}\end{matrix}\right\} - \left\{\begin{matrix}\text{sum of exergy} \\ \text{of inlet streams}\end{matrix}\right\} \tag{3.2}$$

According to Figure 3.1, all the flows in the hybrid system that need to be considered in the exergy loss evaluation are summarized in Table 3.3.

Table 3.3 Mass and energy flows required in the exergy analysis of the hybrid system

	Inlet flows	Outlet flows
Distillation	Main feed	Distillate
	Cooling water (CW)	Bottom product
	Low pressure steam (LPS)	Cooling water (CW)
		Condensate Low pressure steam (LPS)
Pervaporation	Cooling water (CW)	Cooling water (CW)
	Low pressure steam (LPS)	Condensate Low pressure steam (LPS)
	Compressor power	

3.3.3 Investigation of an industrial-scale ethanol dehydration pervaporation hybrid system on a 5x9 grid simulation

The base case was selected as the Greenfield plant located in Johnstown Ontario (Canada). The plant has a rated production capacity of 200 MLPY (million liters per year) of fuel grade ethanol (<1% water in weight), (FAGEN INC., 2010). This capacity is common in plants within North America. A summary of the operating conditions of the distillation and the pervaporation membrane processes used to simulate the hybrid system are listed in Tables 3.4 and 3.5 respectively. In the Table 3.5, the optimal feed temperature, preheat temperature, feed pressure and permeate pressure determined in Chapter 2 were used for the pervaporation module.

Table 3.4 Operating conditions for an industrial-scale distillation column

Variables	Value	Unit
Feed flow rate	23225	kg/h
Feed ethanol concentration	80	wt%
Feed pressure	101.3	kPa
Feed temperature	Bubble point	
Feed tray	65	
Distillate	133	kg/h
Distillate concentration	93	wt%

Table 3.5 Operating conditions of fix area per module for an industrial-scale membrane pervaporation in a network structure

Variables	Value	Unit
Feed pressure	303.9	kPa
Feed temperature	Bubble point	
Preheat temperature	Bubble point	
Retentate concentration	93	wt%
Permeate pressure	13.3	kPa

Both the draw stage (tray to remove intermediate liquid product) and draw ratio (ratio of the removed intermediate liquid product to the feed flow) need to be set to determine the values of the reflux ratio and exergy loss. A 5x9 grid of these two operating conditions was generated based on the operating conditions of distillation and pervaporation defined in Tables 3.3 and 3.4. Simulations were performed to calculate the values of the reflux ratio and exergy loss.

The side draw stage and draw ratio of the feed to the pervaporation unit were used as input variables in the simulation, including using distillation alone and membrane pervaporation alone. Figure 3.2 presents the exergy loss of the hybrid system as a function of draw ratio for various draw stages. The exergy loss related to 0% draw ratio is the exergy loss from the distillation process only that is the highest exergy loss; the exergy loss corresponding to 100% draw ratio represents the exergy loss of membrane pervaporation only that is the lowest exergy loss. As expected, the exergy loss of the hybrid system is between these two values as

the draw ratio varies from 10% to 90%. Figure 3.3 is the contour plot of the exergy loss as a function of the draw stage and the draw ratio. For most trays, the minimum exergy loss occurs between 40% and 50% draw ratio. Since the exergy loss of pervaporation only is much smaller, the exergy loss of the hybrid system decreases initially with increasing draw ratio. However, as more separation is done by pervaporation, the rectification section does less work but consumes more energy. The exergy loss of the hybrid system starts increasing. With a 90% draw ratio, the exergy loss of the hybrid system is only half of the distillation column.

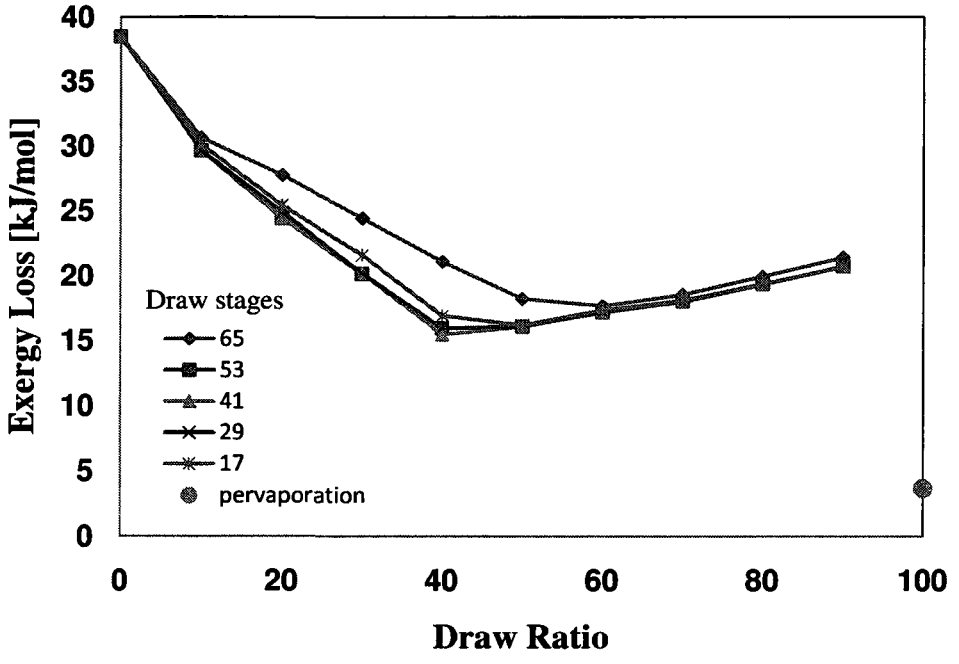

Figure 3.2 Exergy loss of hybrid system as a function of draw ratio for drawing at trays 17, 29, 41, 53 and 65.

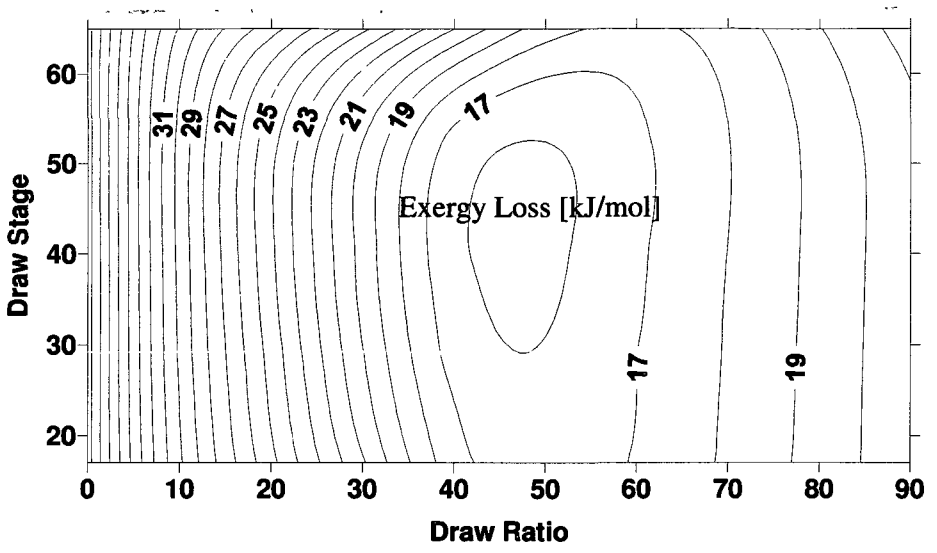

Figure 3.3 Contour plot of exergy loss of hybrid system as a function of draw stage and draw ratio.

Distillation at the tangent pinch requires a higher reflux ratio to perform separation, which implies a higher exergy loss. Figure 3.4 presents the reflux ratio as a function of the draw ratio for various draw stages; it shows a similar configuration to Figure 3.2. At approximately a 40% side draw ratio, the reflux ratio of the distillation column reaches the minimum value. Since the pervaporation is not designed to replace the column, the reflux ratio cannot decrease to zero. As the side draw ratio increases on the same draw position, more concentrated ethanol is sent to the top of the distillation column as the retentate return. As the distillate flow rate and concentration are fixed, the excess flow is sent back to the top of the column. Consequently, the reflux ratio has to increase after decreasing. On the other hand, the variation of draw stages shows a less significant influence on both the exergy loss and the reflux ratio in Figures 3.3 and 3.5. The different draw stages represent different concentration of draw flow in effect. At the tangent pinch, the concentration does not vary from one tray to the next. The liquid concentration drawn from different stages has also very similar concentration. Hence, with the same draw ratio, the exergy loss and the reflux ratio do not change much. Also, both the exergy loss and the reflux ratio have parallel lines of draw ratio in Figures 3.3 and 3.5. The minimum exergy loss and reflux ratio are located at 41 draw stage as shown in the Figures 3.2 and 3.5. Figure 3.6 presents the plot of the exergy loss of the

hybrid system as a function of the reflux ratio of the distillation at the 41st stage. The previous discussion is verified that the exergy loss of the hybrid system is correlated to the reflux ratio of the distillation column. In other words, the exergy loss saving of the hybrid system mainly lies in the exergy loss reduction of the distillation, which is dominated by the reflux ratio.

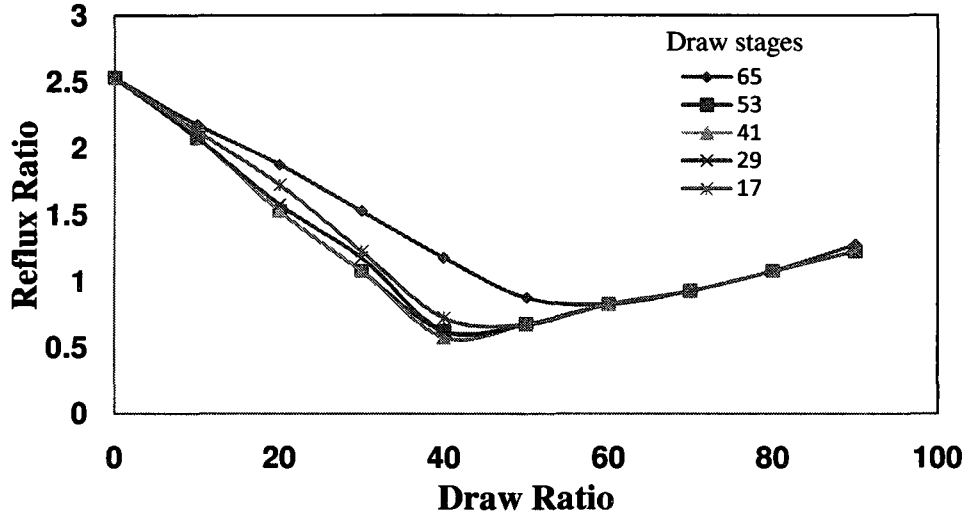

Figure 3.4 Reflux ratio of distillation column as a function of draw ratio at draw stages 17, 29, 41, 53 and 65.

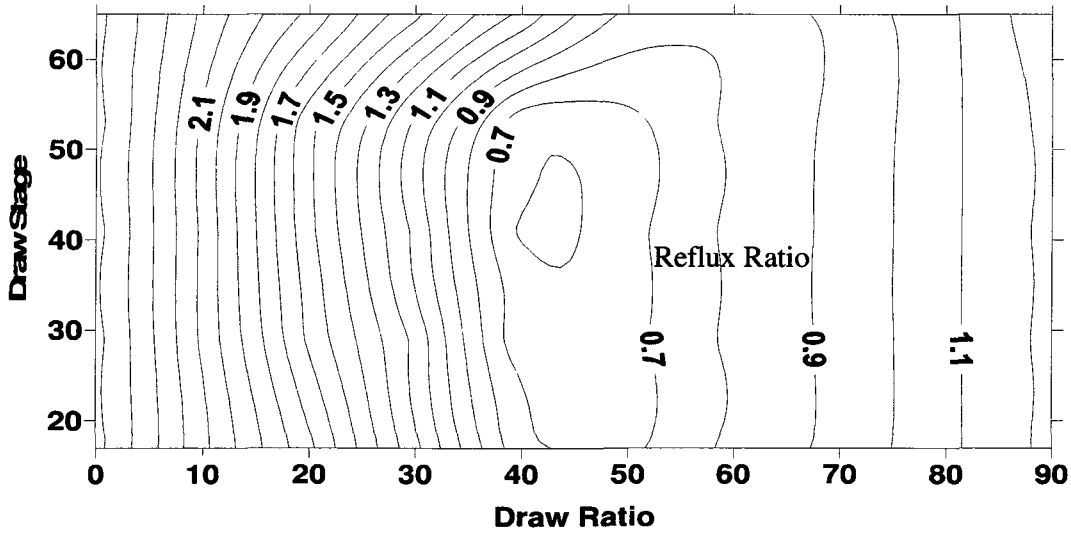

Figure 3.5 Contour plot of reflux ratio of distillation column correlating to draw ratio and draw stages.

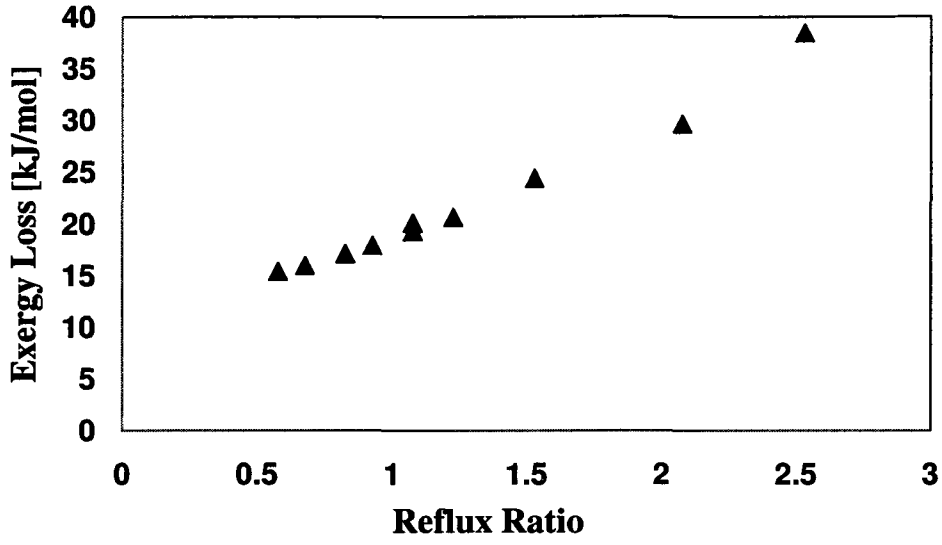

Figure 3.6 Exergy loss as a function of reflux ratio for draw at tray 41.

A greater insight can be gained by comparing the operating lines in Figures 3.7 and 3.8. Figure 3.7 is the operating lines of different draw ratio at draw stage 65. The ethanol concentration of the feed, the permeate, the distillate and retentate are labeled. As the draw ratio increases, the operating line rises close to the equilibrium curve initially, then flattens out. As expected, the variation of the operating lines leads to the change of the reflux ratio with the draw ratio. When the operating line is closer to the equilibrium curve, a lower reflux ratio is required; when the operating line moves away from the equilibrium curve, a large reflux ratio is required. The exergy loss of the distillation is dominated by the reflux ratio so that it is possible to minimize the exergy loss by decreasing the reflux ratio. The operating line with 40% draw ratio is the closest line to the equilibrium curve where the smallest reflux ratio is observed in Figure 3.4 above. Figure 3.8 presents the operating lines of various draw stages at a 40% draw ratio. The operating line variation for the selected draw stages is narrower than that of the draw ratio. Whereas the liquid concentration from various draw stages above the tangent pinch is relatively unchanged. This small change does not affect the reflux ratio significantly. Hence, the exergy loss of the hybrid system and the reflux ratio of the distillation column are more sensitive to the draw ratio than the draw stage.

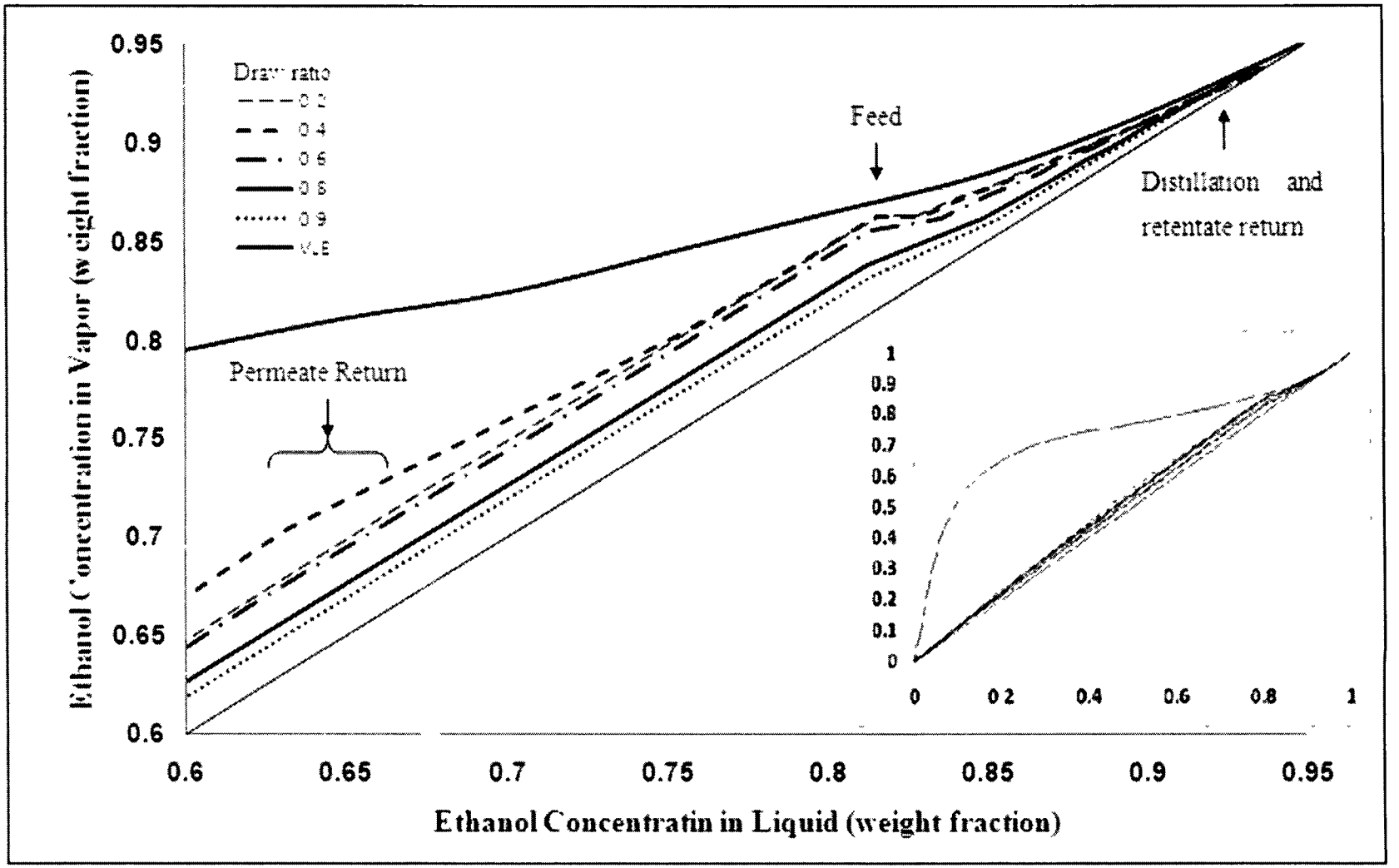

Figure 3.7 Operating line for various draw ratios drawing from tray 65

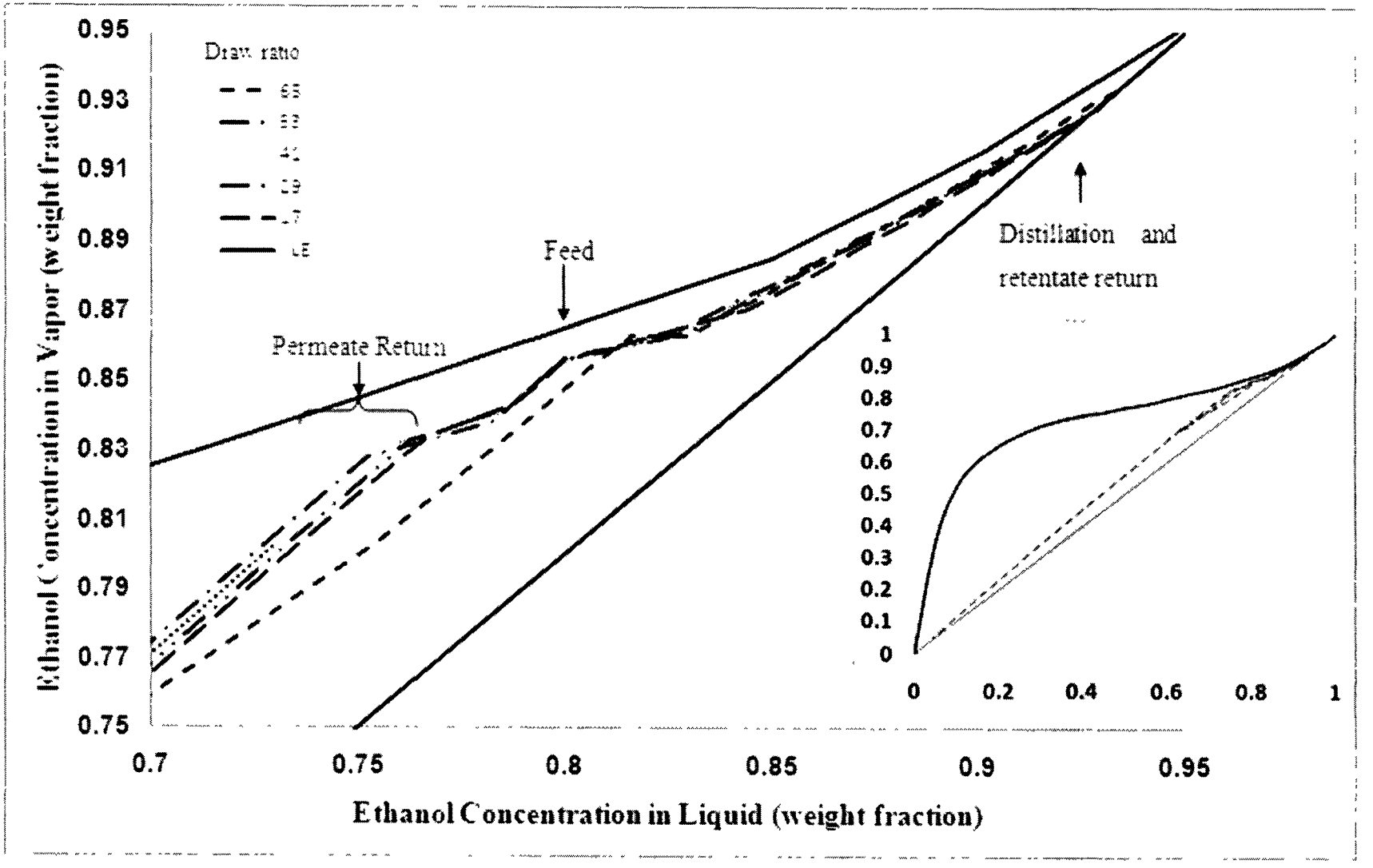

Figure 3.8 Operating line for various draw positions at a fixed draw ratio 0.4

Further investigation presented here is the membrane area required for pervaporation when the draw ratio and draw stage vary. Figure 3.9 presents the membrane area required for pervaporation as a function of draw ratio for various draw stages. The round dot corresponds to 4388 m^2, which is the membrane area for pervaporation alone using the same inputs. As expected, the membrane area is proportion to the draw ratio. As the draw ratio increases, more membrane area is required to reach the desired product concentration. Figure 3.10 is the contour plot of the membrane area required for pervaporation as a function of various draw ratios and draw stages. The membrane area is a strong positive linear function of the draw ratio. It only has a slight variation at different draw stages near the feed tray, which is indicated by the change of the slope. The reason is the ethanol concentration at the feed tray is a little bit lower than the ethanol concentration at the tangent pinch such that a little bit more membrane area is required for pervaporation to obtain the same retentate concentration. In addition, the concentration close to tangent pinch does not change significantly; as a result, the membrane area won't decrease very much by drawing the same amount of liquid flow from the trays at the tangent pinch. Figure 3.11 shows the exergy loss of the hybrid system as a function of the membrane area required for the pervaporation. For most draw stages, the exergy loss reaches the minimum value between 1100 and 1300 m^2, which is at 40% draw ratio. The relationships plotted in Figure 3.11 are similar to Figure 3.2 because the membrane area required for pervaporation has a strong linear relationship to the draw ratio.

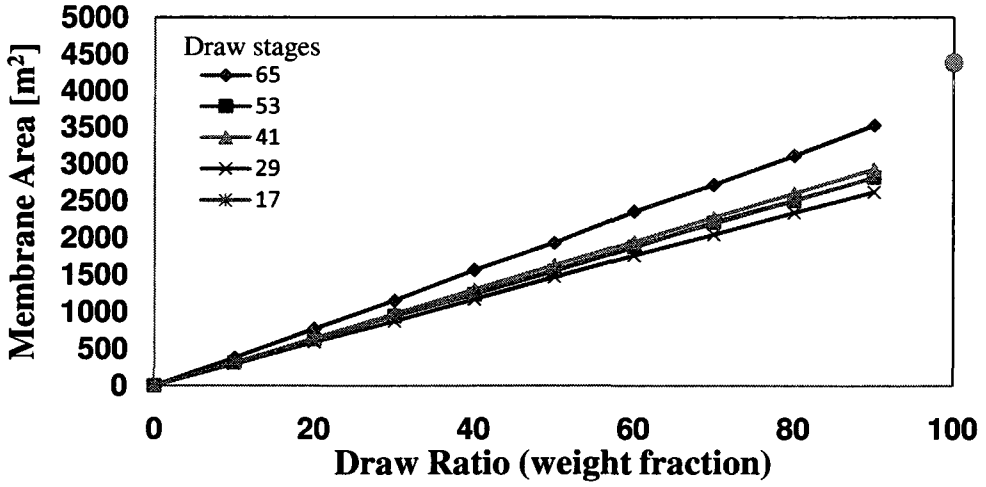

Figure 3.9 Membrane area required for pervaporation as a function of draw ratio for drawing at 17, 29, 41, 53, and 65 stages.

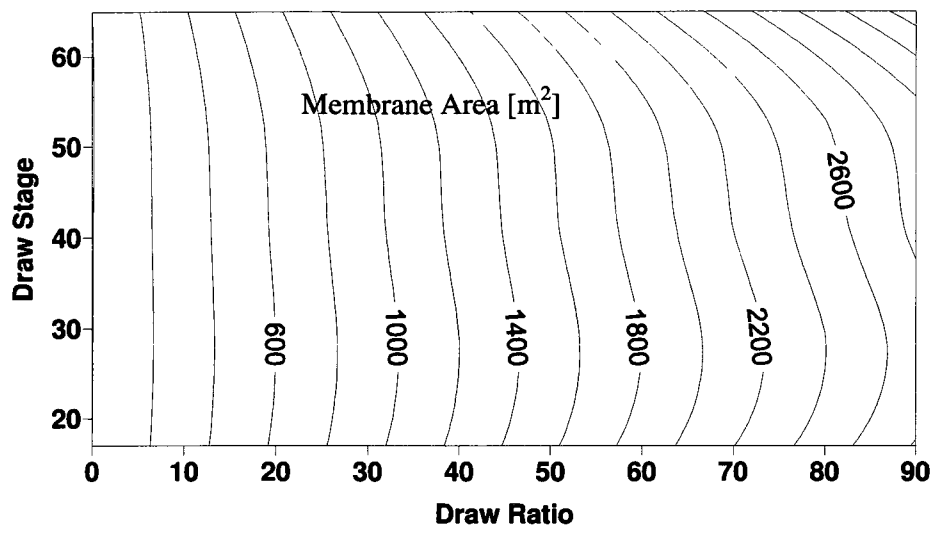

Figure 3.10 The contour plot of membrane area required for pervapoartion as a function of various draw ratio and draw stages.

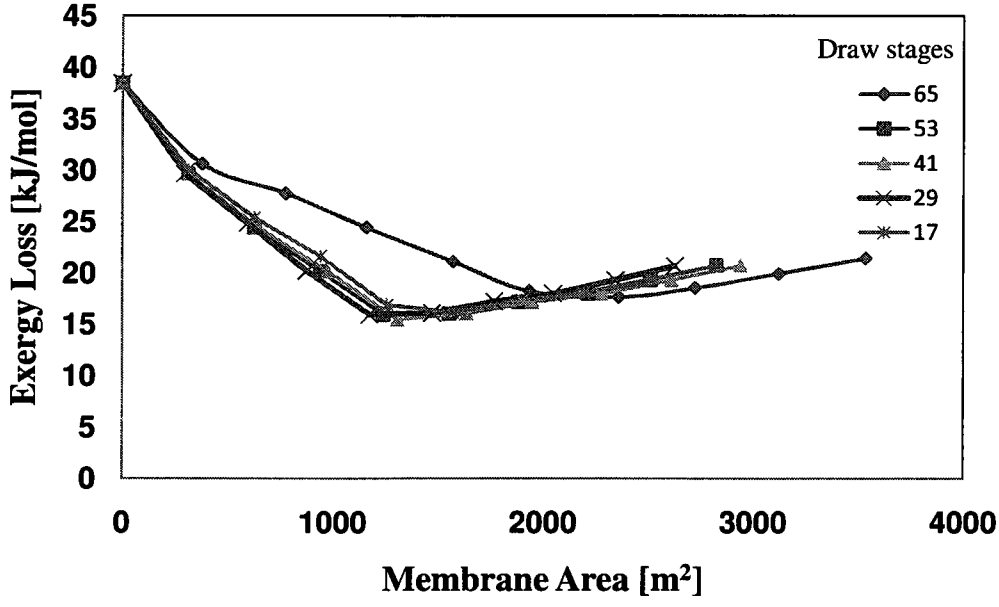

Figure 3.11 Exergy loss per mole of ethanol product of the hybrid system as a function of the membrane area required for pervaporation.

3.4 Conclusion

In this investigation, a pervaporation hybrid system operated at the tangent pinch of the equilibrium curve was modeled for the dehydration of bioethanol. A 5x9 grid of the draw ratio and draw stages was generated for each set of values and the reflux ratio and exergy loss determined. The exergy loss for all cases is between two boundaries, which are defined by two stand-alone units: distillation and pervaporation. The optimized draw stage is at tray 41 numbered from the top with a 40% draw ratio of liquid from the tray. At the optimal operating conditions, the minimum exergy loss of the hybrid system is 15.5 kJ/mol ethanol product, the minimum reflux ratio is 0.58, and the membrane area required is 1303 m^2. The exergy loss of the hybrid system is between 15.5 and 30.7 kJ/mol ethanol product. Compared with the traditional single distillation column (38.5 kJ/mol ethanol product), the reduction of the exergy loss is between 19% and 43%. The reflux ratio of the hybrid system is varied between 0.58 and 2.17. Compared with the reflux ratio of a single distillation column (2.53), the reflux ratio of the distillation in the hybrid system is decreased between 26% and 59%. Comparing the variation of the exergy loss and the reflux ratio, it is emphasized that the exergy loss of the hybrid system is dominated by the exergy loss of the distillation that follows the variation of the reflux ratio. Whereas the existing distillation column is not modified and the reflux ratio cannot be reduced to zero, the exergy loss of the hybrid system can never reach the lowest boundary set by using only pervaporation. Also, it is observed that the exergy loss of the hybrid system is more sensitive to the variation of the draw ratio than the variation of the draw stage at the tangent pinch.

References

Almeida-Rivera, C. P. and Grievink, J., Process Design approach for reactive distillation based on economics, exergy, and responsiveness optimization, Ind. Eng. Chem. Res., 47 (2008) 51-56

Araujo, A. C. B., Vasconcelos, L. G. S., Fossy, M. F., and Brito, R. P., Exergetic and economic analysis of an industrial distillation column, Brazilian J. Chem. Eng. 24 (2007) 461-469

Aventine renewable energy INC., Fuel-grade ethanol specifications, 2009

Bai, S., Assessment of Controller Performance with Embedded Data Reconciliation, PhD thesis, University of Ottawa, Canada, 2003

Bausa, J. and Marquard, W., Shortcut Design Methods for Hybrid Membrane/Distillation Processes for the Separation of Nonideal Multicomponent Mixtures, Ind. Eng. Chem. Res., 39 (2000) 1658-1672

Cheah, SM., http://www.separationprocesses.com/Adsorption, accessed June 2010

Eldridge, R. B., and Seibert, A. F., Hybrid Separations/ Distillation Technology Research Opportunities for Energy and Emissions Reduction, Separation Research Program University of Texas at Austin, 2005

FAGEN, INC., http://www.fageninc.com/gallery/ethanol.htm, accessed June 2010

Faria, S. H. B., and Zemp, R. J., Using exergy loss profiles and enthalpy-temperature profiles for the evaluation of thermodynamic efficiency in distillation columns, Therm. Eng. 4 (2005) 76-82

Fontalvo, J., Cuellar, P., Timmer, J. M. K., Vorstman, M. A. G., Wijers, J. G., and Keurentjes, J. T. F., Comparing Pervaporation and Vapor Permeation Hybrid Distillation Processes, Ind. Eng. Chem. Res, 44 (2005) 5259-5266

Goff, P., Cachot, T. and Rivero, R., Exergy analysis of distillation processes, Chem. Eng. Technol. 19 (1996) 478-485

Haelssig, J. B., Tremblay, A. Y., and Thibault , J., Technical and Economic Considerations for Various Recovery Schemes in Ethanol Production by Fermentation, Ind. Eng. Chem. Res. 47 (2008) 6185–6191

Keenan, J. H., Availability and irreversibility in thermodynamics, Br. J. Appl. Phys., 2 (1951) 183-192

Kita, H., Horii, K., Ohtoshi, Y., Okamoto, K. I., Tanaka, K., Synthesis of a zeolite NaA membrane for pervaporation of water/organic liquid mixtures. J. Mater. Sci. Lett. 14 (1995) 206-208

Koeijer, G. and Rivero, R., Entropy production and exergy loss in experimental distillation columns, Chem. Eng. Sci., 58 (2003) 1587-1597

Kondo, M., Komori, M., Kita, H., Okamoto, K., Tubular-type pervaporation module with zeolite NaA membrane. J. of Membr. Sci. 133 (1997) 133-141

Liapis, A. I. and Bruttini, R., Exergy analysis of freeze drying of pharmaceuticals in vials on trays, International J. Heat and Mass transfer, 51 (2008) 3854-3868

Mustapha, D., Sabria, T., and Fatima, O., Distillation of a complex mixture. Part II: performance analysis of a distillation column using exergy, Entropy 9 (2007) 137-151

Rant, Z., Exergy, a new world for "Technical available work", Forsch. Ingenieurwes, 22 (1956) 36-37

Richter, H., Voigt, I., Kuhnert, J.-T., Dewatering of ethanol by pervaporation and vapour permeation with industrial scale NaA-membranes, Desalination 199 (2006) 92-93

Renewable Fuels Association (RFA), Fuel Ethanol Industry guidelines, specifications, and procedures. 2003.

RFA, http://www.ethanolrfa.org/industry/statistics/#A, accessed June 2010.

Sander, U., and Soukup P., Design and Operation of a Pervaporation Plant for Ethanol Dehydration, J. of Membr. Sci., 36 (1988) 463-475

Sommer, S., and Melin, T., Influence of operation parameters on the separation of mixtures by pervaporation and vapour permeation with inorganic membranes. Part 1: Dehydration of solvents, Chem. Eng. Sci. 60 (2005) 4509-4523

Szitkai, Z., Lelkes, Z., Rev, E., and Fonyo, Z., Optimization of hybrid ethanol dehydration systems, Chem. Eng. Process., 41 (2002) 631-646

Taprap, R. and Ishida, M., Graphic exergy analysis of processes in distillation column by energy-utilization diagrams, AIChE J. 42 (1996) 1633-1641

United Nations Environment Programme (UNEP), Towards sustainable production and use of resources: Assessing biofuels, 2009

Widagdo, S., and Seider, W. D., "Azeotropic Distillation - A Review," AIChE J., 42:1 (1996) 96-130.

Will B., and Lichtenthaler, R. N., Comparison of the separation of mixtures by vapor permeation and by pervaporation using PVA composite membrane. I. Binary alcohol-water systems, J. Membr. Sci., 68 (1992) 119-125

CHAPTER 4

Conclusions and Recommendations

This thesis was primarily devoted to the exergy loss minimization of a hybrid bioethanol dehydration process. The exergy loss was significantly decreased by implanting a membrane pervaporation process into an existing distillation column. The following aspects were investigated: the parametric analysis of membrane pervaporation for ethanol/water separation at a high ethanol concentration, multiple objective optimizations of membrane pervaporation, and the exergy optimization of pervaporation hybrid system at a tangent pinch on the VLE line.

4.1 Conclusions

In the parametric analysis of membrane pervaporation, it was observed that the minimization of the total membrane area and the minimization of the number of stages are conflicting objectives such that a trade-off solution was expected to balance these two objectives. When looking at the the stage inlet temperature and the ethanol concentration in the feed, it was preferred that the retentate flow should be at its saturated temperature for higher flux and a decrease in the number of stages. This is an important consideration because temperature affects one of the driving forces (saturated vapour partial pressure on the retentate side) significantly.

Second, suitable compromised solutions were identified among the four objectives for the optimization of the membrane pervaporation where it was desired to minimize these four objective functions simutaneously: the total membrane area, the total number of stages, the energy consumed, and the exergy loss. It was spotted that the total number of stages was dominated strongly by the area per stage and the temperature drop per stage. Also, for the optimized solutions, the decision variables were located at their lower bounds (area per stage is 20 m^2; temperature drop per stage is 6 °C; retentate pressure is 1.2 bar), except permeate pressure that was at its both lowest (2 kPa) and highest bounds (23 kPa).

Finally, the exergy loss of a hybrid pervaporation-distillation system was found to be limited by the boundaries between the exergy loss of pervaporation and the exergy loss of a simple distillation. The optimal solution for the hybrid system reduced the distillation reflux ratio up to 59% compared to the simple distillation. As a result, the total exergy loss was reduced by 43% compared to the simple distillation. In addition, it is concluded that the total exergy loss reduction is dominated by the drop in reflux ratio.

4.2 Recommendations

A number of recommendations can be made based on the work that was achieved in this thesis.

1. Saturated liquid temperature is preferred for the feed temperature of the membrane pervaporation (Chapter 2).

2. Increasing membrane feed pressure is a better choice than decreasing permeate pressure, especially when the vacuum pump cannot provide sufficiently low pressure on the permeate side (Chapter 2).

3. Applying the membrane pervaporation at the tangent pinch of equilibrium curve can reduce the total exergy loss, where the distillation separation efficiency is very low (Chapter 3).

4. Changing the side draw ratio from the column to the membrane is a more effective solution to reduce the exergy loss than changing the draw stage.

APPENDIX A Modeling of Membrane

A.1 Models Used in the Simulation of the Membrane Pervaporation

Modeling and simulation of the membrane separation process have been widely studied during the past decades. Spiegler and Kedem (1966) tried to model the membrane hyperfiltration by differential membrane layer. Bakker et al. (1996) built the gas permeation model through a membrane as a function of temperature based on diffusion and adsorption. Carmo and Gubulin (1997) investigated the kinetic and thermodynamic data of commercial 3A zeolite on the ethanol water adsorption process. Chen et al. (1997) and Yang et al. (2007) studied and simulated the adsorption and diffusion behaviours of silicalite membrane for water/ethanol mixture. Sommer and Melin (2005) investigated various operation parameters on commercial inorganic membranes and introduced a simple transport model for both pervaporation and vapor permeation. P. Titus et al. (2008) introduced pervaporation model for NaA zeolite membrane in dehydration ethanol according to the diffusion and adsorption. In this part, the permeate transportation of single membrane module is set up on differential segments for the ethanol/water binary system. Highly hydrophilic membrane (A-type zeolite) is used. In the pervaporation process, water preferentially permeates the membrane and evaporate at the permeate side. Most ethanol is retained in the retentate flow. Membrane tubes or sheets are used to construct modules in order to isolate the retentate and the permeate flow. The following assumptions have been generally made in modeling of membrane:

- On the permeate side, vapour are considered well mixed, and the concentration of permeate components are constant in the membrane.
- In pervaporation, on the retentate side, there is a temperature and concentration gradient along the membrane. Therefore, the permeate flux is varying correspondingly.
- The temperature, the permeate flux and the retentate concentration all vary along the membrane. However, for each segment, the mixture is assumed uniform.

- The heat transfer coefficient of the membrane layer can be neglected.
- The pressure on both sides of membrane remains constant.
- Since the heat of mixing is negligible, the evaporation heat, the heat capacity and the liquid enthalpy of the mixture are considered ideal.

The single membrane module is illustrated as Figure A.1. F_i is the feed mixture to the membrane; x_{ei} and x_{wi} are the ethanol and water fraction in the feed flow representatively; T_i is the feed temperature. F_o is the flow leaving membrane from the retentate side; x_{eo} and x_{wo} are the ethanol and water concentration in the retentate flow; T_{out} is the temperature of retentate flow. F_p is the flow rate of permeation through the membrane; x_{ep} and x_{wp} are the permeate concentration for ethanol and water separately. P_m is the pressure of membrane, and P_p is the permeate pressure.

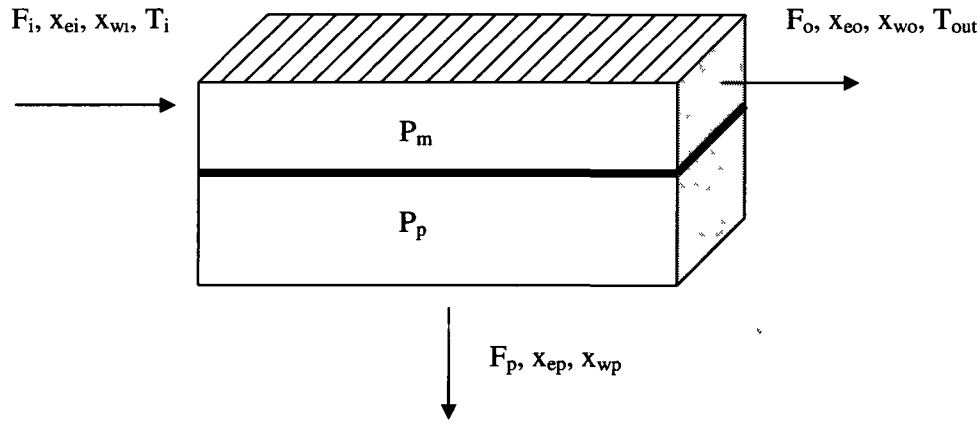

Figure A.1Schematic representation of single membrane module for ethanol-water system

In this study, the initial settings for membrane module are 27 m^2 in area (Tremblay, 2006), 1.0135 bar (Sommer and Melin, 2005) as membrane pressure and 0.133 (POMPETRAVAINI S.p.A, 2009) bar as permeate pressure. The entire membrane sheet is divided into small slices (0.05 m^2) for permeate flow rate, temperature and retentate concentration calculations (as shown in Figure A.2).

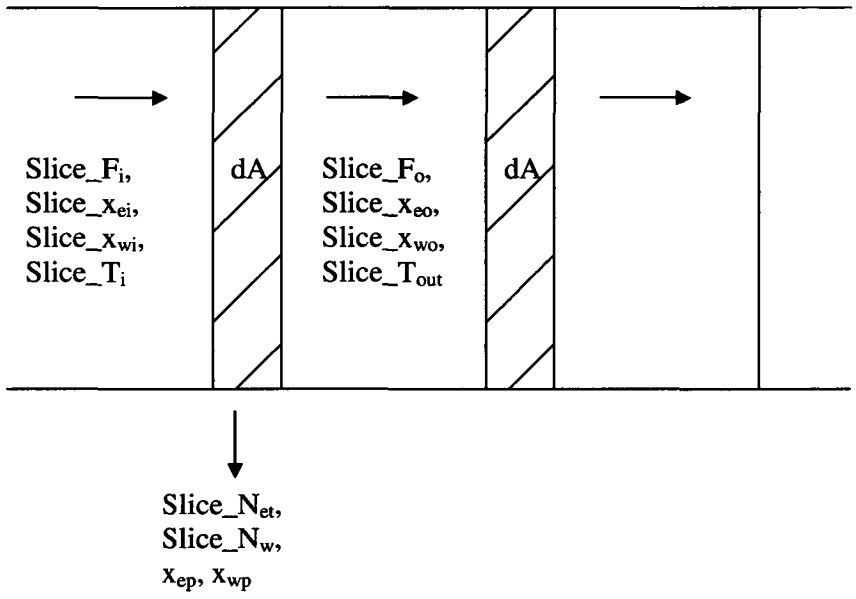

Figure A.2 Schimatic diagram of membrane segments

Permeate flow rate

As shown in Figure A.2 the total permeate flow of the membrane module is the sum of each slice.

$$N_{tot} = \sum Slice\_N_{et} + \sum Slice\_N_w \qquad (1)$$

Where N_{tot} is total permeate flow rate of membrane module [kg/h], Slice_N_{et} is ethanol permeate flow rate of membrane slice [kg/h], Slice_N_w is water permeate flow rate of membrane slice [kg/h]

The permeate flow rate of sliced membrane is given as

$$Slice\_N_{et} = J_{et,PV} \times dA \qquad (2a)$$

$$Slice\_N_w = J_{w,PV} \times dA \qquad (2b)$$

Where $J_{et,PV}$ is permeate flux of ethanol [kg/m^2 h], $J_{w,PV}$ is permeate flux of water [kg/m^2 h], dA is slice area [m^2]

For each component, the flux is calculated by (Sommer and Melin, 2005),

$$J_{j,PV} = Q_{j,ref} \exp\left[\frac{E_j}{R_{gas}}\left(\frac{1}{T_{ref}} - \frac{1}{T_F}\right)\right] \times \left(x_{jF}\gamma_j p_{jF}^{sat} - x_{jP} p_P\right) \quad (3)$$

Where $J_{j,PV}$ is pervaporation integral transport of component j [kg/m^2 h], $Q_{j,ref}$ is permeance of component j at reference temperature [kg/m^2 h bar], E_j is activation energy [J/mol], R_{gas} is ideal gas constant [J/molK], T_{ref} is reference temperature [K], T_F is feed temperature [K], x_{jF} is feed concentration of component j [wt%], γ_j is activity coefficient of component j, p^{sat}_{jF} is saturate pressure of component j in feed [bar], x_{jp} is permeate concentration of component j [wt%], p_p is permeate pressure [bar], and j is ethanol or water.

The commonly used empirical model of activation coefficients for a binary solution is defined by Margules equations (4a and 4b): (Smith et al., 2005)

$$\ln\gamma_{et} = x_w^2\left[A_{et,w} + 2\left(A_{w,et} - A_{et,w}\right)x_{et}\right] \quad (4a)$$

$$\ln\gamma_{w} = x_{et}^2\left[A_{w,et} + 2\left(A_{et,w} - A_{w,et}\right)x_{w}\right] \quad (4b)$$

Arrange the equations:

$$\gamma_{et} = e^{x_w^2\left[A_{et,w} + 2\left(A_{w,et} - A_{et,w}\right)x_{et}\right]} \quad (5a)$$

$$\gamma_{w} = e^{x_{et}^2\left[A_{w,et} + 2\left(A_{et,w} - A_{w,et}\right)x_{w}\right]} \quad (5b)$$

Where γ_{et} is activation coefficient of ethanol to water, γ_w is activation coefficient of water to ethanol, $A_{w,et}$ is interaction parameters of water to ethanol (1.4177), and $A_{et,w}$ is interaction parameters of ethanol to water (1.0574)

Saturation partial pressure is calculated by the Antoine equation (Smith, 2005),

$$P_i^{sat} = 10^{A_i - \frac{B_i}{C_i + T}} \quad (5)$$

Where P_i^{sat} is the saturated partial pressure of component i [bar], A, B and C are parameters of component i in the Antoine equation, and T is the temperature [K].

Permeate concentration calculation

Based on the mass balance, the permeate concentration is calculated by:

$$x_{ep} = \frac{F_i \cdot x_{ei} - F_o \cdot x_{eo}}{F_i - F_o} \quad (6a)$$

$$x_{wp} = \frac{F_i \cdot x_{wi} - F_o \cdot x_{wo}}{F_i - F_o} \quad (6b)$$

However, the retentate flow and its concentration are determined by the permeate flow and concentration

$$F_o = F_i - N_{tot} \quad (7)$$

$$F_o \cdot x_{eo} = F_i \cdot x_{ei} - N_{tot} \cdot x_{ep} \quad (8a)$$

$$F_o \cdot x_{wo} = F_i \cdot x_{wi} - N_{tot} \cdot x_{wp} \quad (8b)$$

Unfortunately, permeate flow rate is related to the permeate concentration as well. The solution is to estimate a permeate concentration and calculate the permeate flow rate on all membrane slices, then re-calculate the permeate concentration with the mass balance; by iterating the permeate concentration until the estimated concentration is close enough to the calculated one, the real permeate concentration is determined (Tremblay, 2006).

The one dimension Golden search method (Cambridge University, 2010; University of Illinois, 2005) is applied to find the permeate concentration. Figure A.3 is the flow chart of Golden search method algorithm. X_3 and X_0 is the upper boundary and lower boundary respectively. Two new interpoints X_1 and X_2 are estimated by Golden ratio (0.61803). The four points are kept tracking and minimize the preceding intervals. The process

continuous till the bracketing interval is acceptable small (http://www.mpi-hd.mpg.de/astrophysik/HEA/internal/Numerical_Recipes/f10-1.pdf, 2010). The function served in Golden search method is defined as,

$$dif = \left(x_{ep-est} - x_{ep-cal}\right)^2 \qquad (9)$$

Where dif is difference between estimate value and the calculated value, $x_{ep\text{-}est}$ is estimation of ethanol permeate concentration, and $x_{ep\text{-}cal}$ is re-calculated ethanol permeate concentration.

A detailed algorithm for the minimization function design is illustrated in Figure A.4.

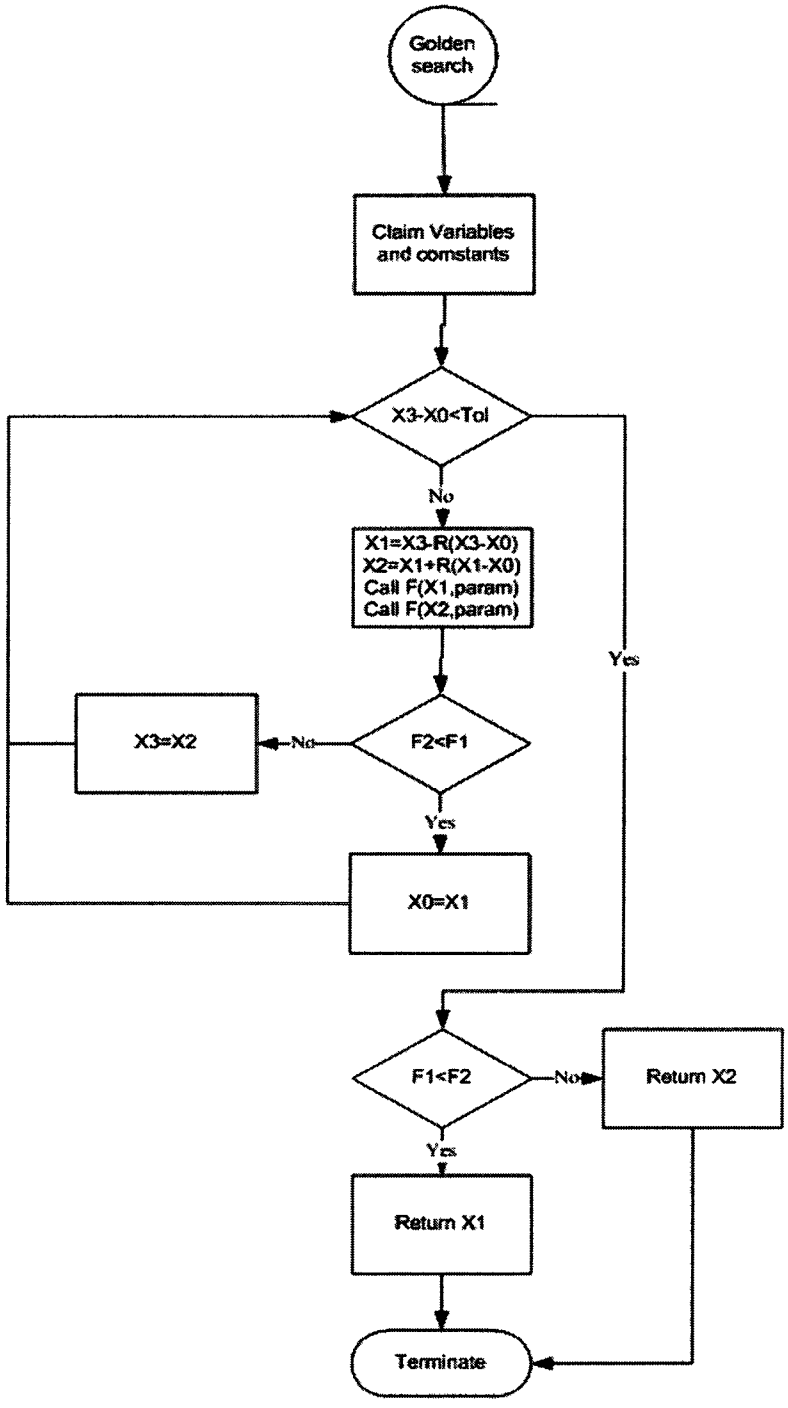

Figure A.3 Flow chart of one dimension Golden search method algorithm

The interpoints X_1 and X_2 are calculated by,

$$X_1 = X_3 - R(X_3 - X_0) \tag{10a}$$

$$X_2 = X_1 + R(X_1 - X_0) \tag{10b}$$

Where R is the Golden ratio.

Comparing function value F_1 and F_2 for the two interpoints, if F_2 is smaller than F_1, then set the X_1 as the new lower boundary; otherwise, set the X_2 as the new upper boundary. Hence, the minimum value is always inside the interval. Until the interval size is small enough, the solution is obtained.

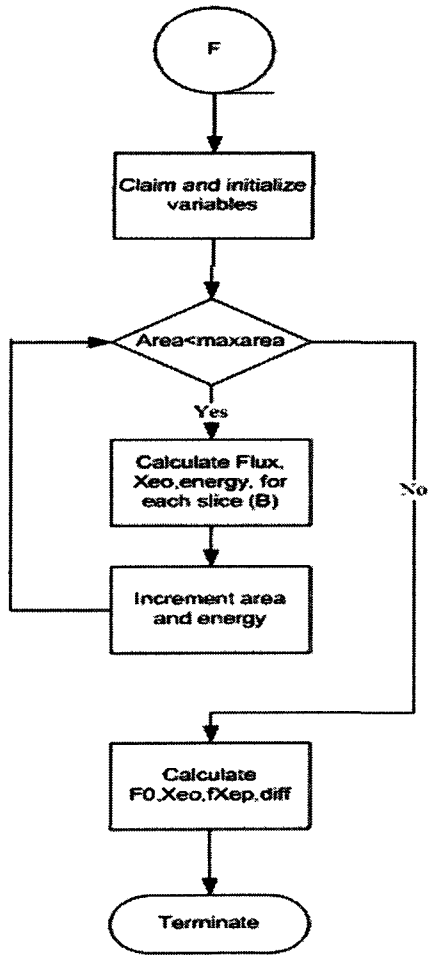

Figure A.4 Minimization function algorithm for Golden search method

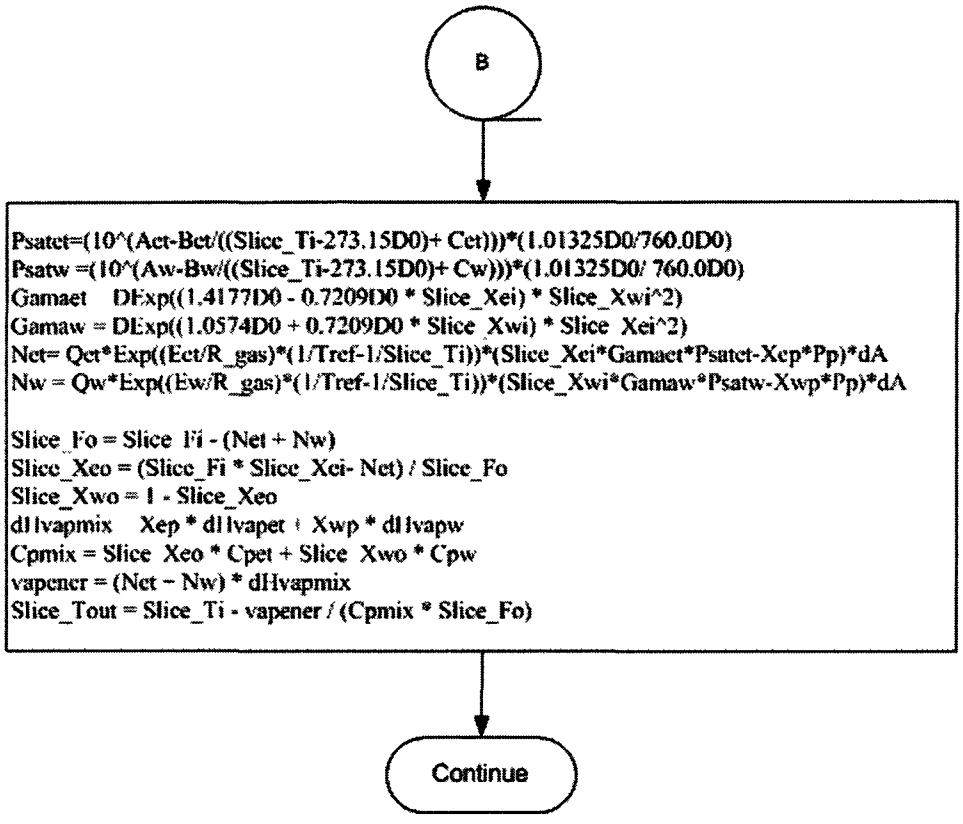

Figure A.5 The B part in minimization function algorithm

The upper boundary and lower boundary of ethanol permeate concentration is important for Golden search method. Between the two boundaries, there should be one and only one minimum (maximum) value (as shown in Figure A.6.) The smaller the interval size, the more accurate is the obtained minimum (maximum). According to previous settings, for ethanol permeate concentration, it is always between 0 and the ethanol feed concentration; it increases as the pervaporation process going on. For highly hydrophilic membrane, water flux is non-negative value, in other words, no water goes through membrane from bottom to top side. Set the equation (3) to 0, a lowest possible value of ethanol permeate concentration is estimated except pure ethanol feed.

$$J_{w,PV} = Q_{w,ref} \exp\left[\frac{E_w}{R}\left(\frac{1}{T_{ref}} - \frac{1}{T_F}\right)\right] \times \left(x_{wF}\gamma_w p_{wF}^{sat} - x_{wP} p_P\right) = 0$$

Derive the equation above,

$$x_{wF}\gamma_w p_{wF}^{sat} - x_{wP} p_P = 0$$

The estimate ethanol permeate concentration by zero water flux is

$$x_{eP} = 1 - \frac{x_{wF}\gamma_w p_{wF}^{sat}}{p_P}$$

This value can be negative, since the permeate pressure is much smaller than the saturated partial pressure. In that case, 0 is set to the lower boundary and the upper boundary is still the feed concentration of ethanol; otherwise, the estimate ethanol permeate concentration based on zero water flux is set to the lower boundary. Positive water flux is guaranteed if ethanol concentration is in the interval.

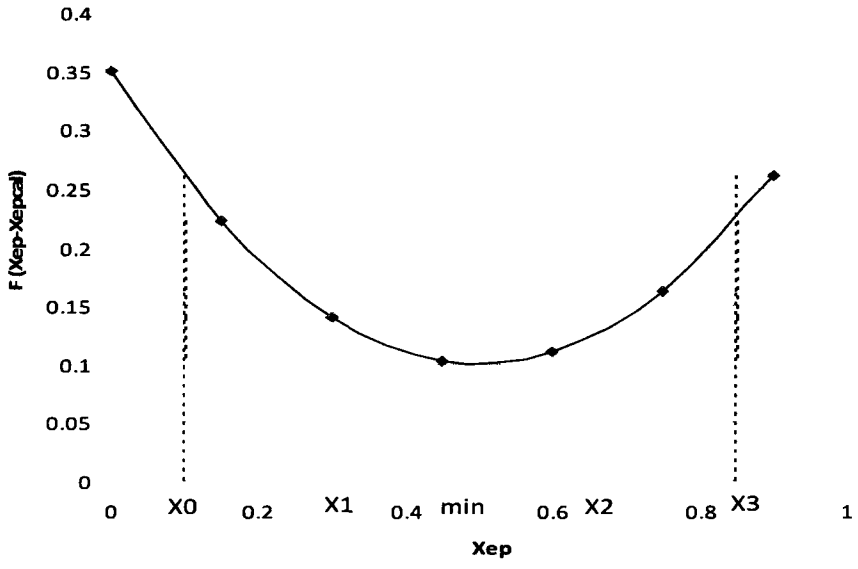

Figure A.6 Golden search boundary decision

Temperature drop calculation

Temperature changing estimation is based on energy balance. There is no heat source inside the membrane module, and no heat loss through membrane module to surrounding. The permeate flow evaporates on the bottom side for the very low permeate pressure. This causes the temperature reduction across the membrane.

The evaporation heat is estimate by

$$E_{vap} = N_{tot} \cdot H_{vap-mix} \tag{11}$$

Where E_{vap} is the evaporation heat [W], and $H_{vap-mix}$ is the latent heat of mixture [J/kg]

Latent heat of mixture is given by,

$$H_{vap-mix} = H_{vap-et} \cdot x_{eP} + H_{vap-w} \cdot x_{wP} \tag{12}$$

The heat supplied by retentate flwo is,

$$E = F_o \cdot Cp_{mix} \cdot (T_i - T_{out}) \tag{13}$$

Where E is energy [W], and Cp_{mix} is heat capacity of liquid mixture [J/kgK]

Heat capacity of liquid mixture is given by,

$$Cp_{mix} = Cp_{et} \cdot x_{eo} + Cp_w \cdot x_{wo} \tag{14}$$

Combine equation (11) and (13),

$$E_{vap} = Cp_{mix} \cdot (T_i - T_{out})$$

$$T_{out} = T_i - \frac{E_{vap}}{F_o \cdot Cp_{mix}} \tag{15}$$

Energy and exergy evaluation

Exergy is unrecoverable work. Exergy is always a loss for a process due to the increasing in entropy. Exergy [kJ] is evaluated by equation (16)

$$Exergy = H - T_{ref} S \tag{16}$$

Without entropy term, equation (16) can evaluate energy of each stream.

Exergy change for a process is calculated by equation (17)

$$\begin{Bmatrix}\text{exergy change}\\ \text{in a process}\end{Bmatrix} = \begin{Bmatrix}\text{sum of exergy}\\ \text{of outlet stream}\end{Bmatrix} - \begin{Bmatrix}\text{sum of exergy}\\ \text{of inlet stream}\end{Bmatrix} \tag{17}$$

For membrane pervaporation process with heat exchanger between stages and a vacuum pump, the outlet streams and inlet streams are specified in table 1.

Table A.1 Inlet and outlet stream specification of membrane pervaporation process

Inlet streams	Outlet streams
Feed (F)	Retentate (R)
Cooling water to condenser (CW,in)	Permeate (P)
Low pressure steam to heater (LPS,in)	Cooling water leaving condenser (CW,out)
Vacuum pump power (Pvp)	Low pressure steam leaving condenser (CW,out)

General equation for energy and exergy change in membrane process is shown below,

$$X_T = \left(X_R + X_P + \sum X_{CW,out} + \sum X_{LPS,out}\right) - \left(X_F + \sum X_{CW,in} + \sum X_{LPS,in} + Pvp\right) \tag{18}$$

Where X coulde be exergy (B) or energy (E).

References

Bakker W.J.W., v.d. Broeke L.J.P., Kapteijn F., Moulijn J.A., Temperature dependence of one-component permeation through a silicalite-1 membrane. A.I.Ch.E. 43 (1997) J., 2203–2215.

Cambridge University Press, Numerical recipes in Fortran 77: the art of scientific computing, 1992

(http://www.mpi-hd.mpg.de/astrophysik/HEA/internal/Numerical_Recipes/f10-1.pdf, accessed April 2010)

Carmo, M.J., and Gubulin, J.C., Ethanol-water adsorption on commercial 3A zeolites: Kinetic and thermodynamic data, Braz. J. Chem. Eng. 14:3 (1997) Sept.

Chen, X., Ping, Z., Long, Y., Separation Properties of Alcohol–Water Mixture through

Silicalite-I-Filled Silicone Rubber Membranes by Pervaporation, J. Appl. Polymer Sci., Vol. 67 (1998) 629–636

Smith, J. M., V. Ness, H. C., Abbott, M. M., Introduction to chemical engineering thermodynamics, 2005

Sommer S., Melin T., Influence of operation parameters on the separation of mixtures by pervaporation and vapor permeation with inorganic membranes. Part 1: Dehydration of solvents", Chem. Eng. Sci. 60 (2005) 4509 – 4523

Spiegler, K. S., Kedem, O., Thermodynamics of hyperfiltration (reverse osmosis): criteria for efficient, Desalination, 1 (1966) 311-326

P. Titus, M., Fite, C. Sebastian, V., Lorent, E., Llorens, J., and Cunill, F., Modeling Pervaporation of Ethanol/Water Mixtures within 'Real' Zeolite NaA Membranes, Ind. Eng. Chem. Res. 47 (2008) 3213-3224

POMPETRAVAINI S.p.A., Operating manual liquid ring vacuum pumps and compressors, 2009

Tremblay, A. Y., Thermodynamically Guided Integration of Distillation and Membrane Processes for Azeotropic Mixture Separation, 2006

University of Illinois at Chicago, The Golden section search method, Department of Mathematics, Statistics and Computer Science, 2005

APPENDIX B Validation of Membrane

Selectivity and total permeate flux

Membrane selectivity and permeate flux vary for membrane types, operating conditions and mixture. For A-type zeolite membrane, the selectivity of water over ethanol and water flux are listed in Table B.1. The operating conditions provided by Kita et al. (1995) are 30-37 cm^3/min flow rate, 13.3Pa as permeate pressure, and 47 cm^2 effective membrane area.

Table B.1 Separation factor of water over ethanol and water flux of A-type zeolite membrane

Temperature [·C]	Feed water [wt%]	Flux [kg/m^2h]	Separation factor
75	10.3	2.15	10000
75	5.1	1.1	16000

(Kita et al., 1995)

Figure B.1 shows the pervaporation flux and separation factor related to feed ethanol concentration of A-type zeolite membrane for water ethanol mixture. Comparing to the simulation results (as shown in Figure B.2), both flux and separation factor are smaller than Kita's data; however, both show the same trends. Pervaporation flux is reduced from 3.1 kg/m^2h to 0.0023 kg/m^2h as the ethanol feed concentration increases from 40 wt% to 99 wt%. Separation factor is going up to its maximum value around 92 wt% then decreasing gradually. The simulation operating conditions are: 1175 kg/h feed flow rate, ethanol concentration from 40 wt% to 99 wt%, 1 atm feed pressure, 13.3 Pa permeate pressure, and saturate feed temperature in K. Also, membrane area is changed to guarantee the temperature drop is less than 10 °C over the stage.

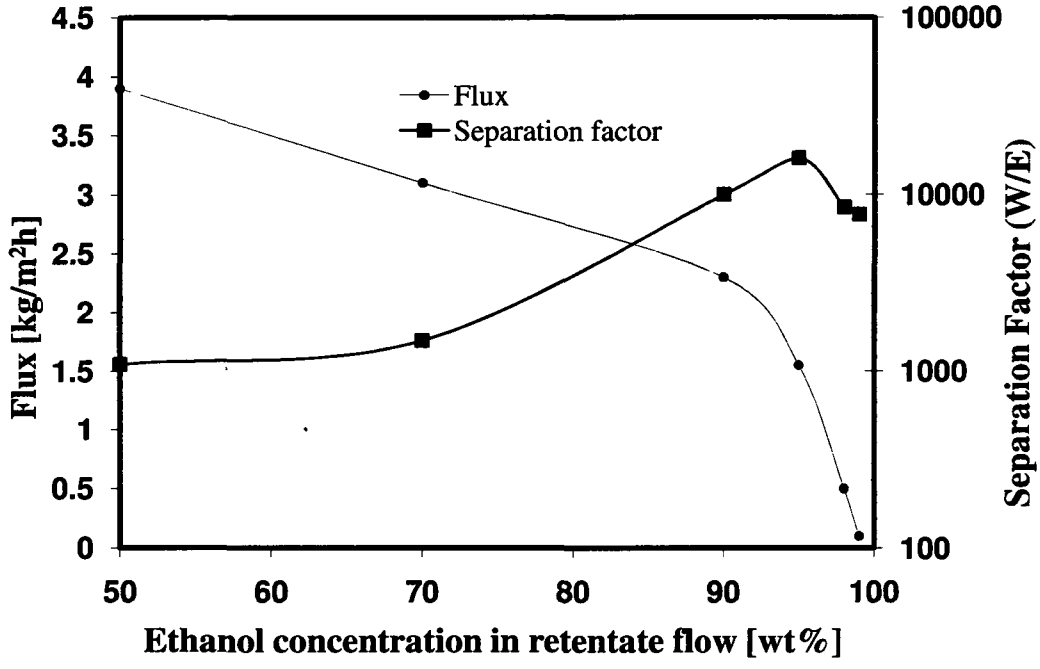

Figure B.1 Permeate Flux and separation factor as function of ethanol feed concentration
(Kita et al., 1995)

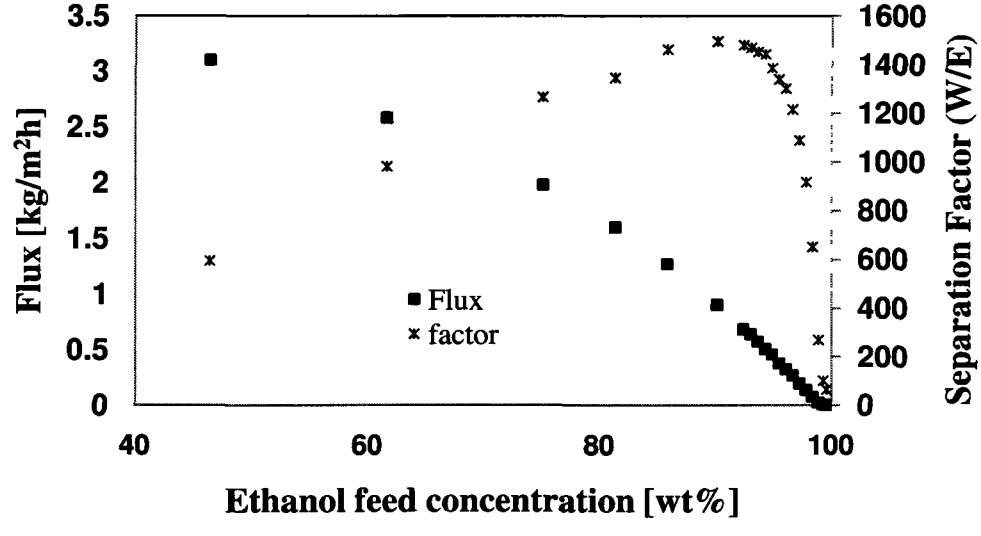

Figure B.2 Average pervaporation flux and separation factor as function of ethanol feed concentration from simulation
Temperature drop profile

For membrane module, two major simulations are taken. One is fix membrane area per stage; the other is fix temperature drop per stage. In Figure B.3, fix membrane are per stage is illustrated. The flow sent into each membrane module in series after it is preheated to certain temperature. The permeate side pressure is kept at 133Pa, and the retentate pressure is at 101.3kPa. Water is going through the membrane and evaporated at the surface. The evaporation heat taken by flux water flow will drop down the flow temperature. In Figure B.3, temperature drop for each stage will decrease since the less water flux through the certain area membrane as the ethanol concentration going up.

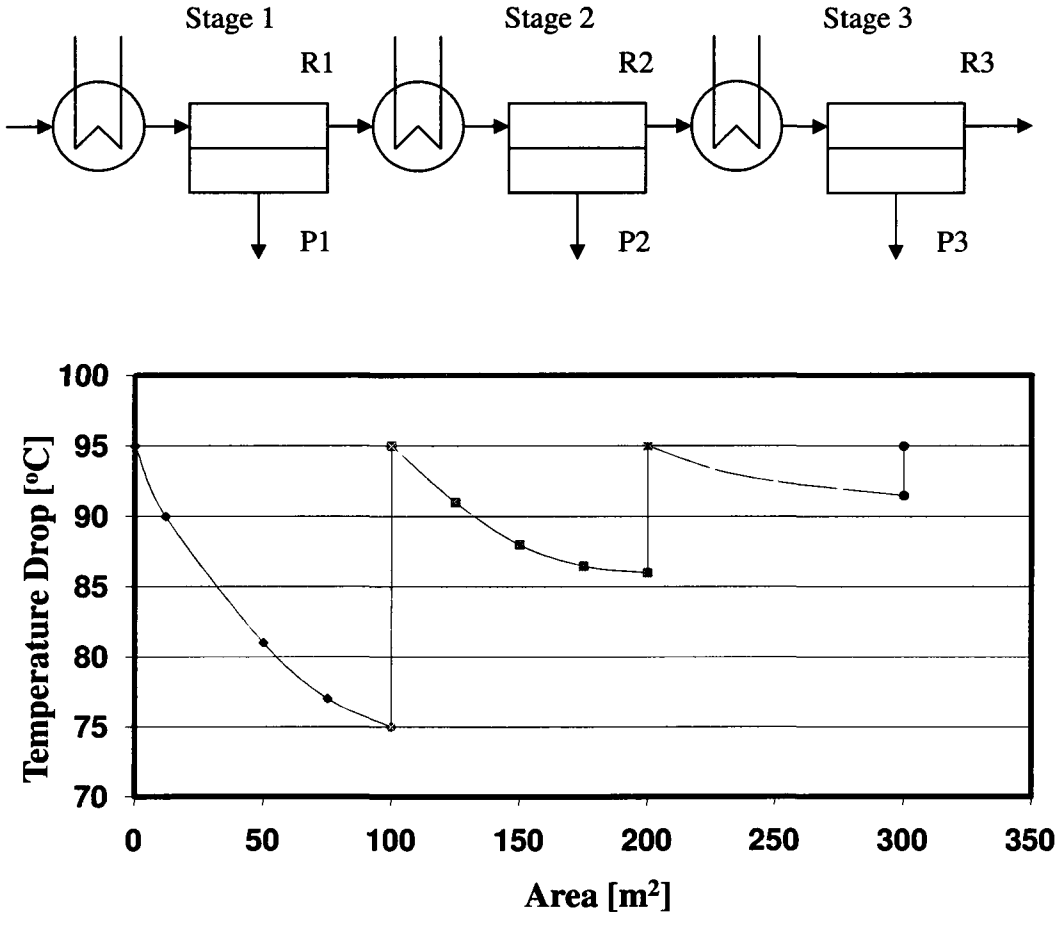

Figure B.3 Temperature profile for fixed stage area of PVA/PAN membrane
(Bausa and Marquardt, 2000)

In Bausa and Marquardt (2000) simulation, higher feed temperature and PVA/PAN membrane are applied. For A-type zeolite membrane simulation, the operating conditions are: 100kg/h feed flow rate, 40 wt% ethanol in feed, saturate feed temperature (around 80 °C), 1 atm feed pressure, 27 m^2 membrane area, and 0.02 bar permeate pressure. Figure B.4 is the simulation result of temperature drop for fixed stage area. Comparing Figure B.3 and Figure B.4, they have exactly the same trend. The preheat temperature is drop down to 78.7°C, then the temperature drop for each stage much faster than higher inlet temperature flow. That means, for pervaporation, the separation is more efficient at higher temperature. This result agrees with the module; temperature is one of the driving forces of pervaporation and has exponential effect on the flux value.

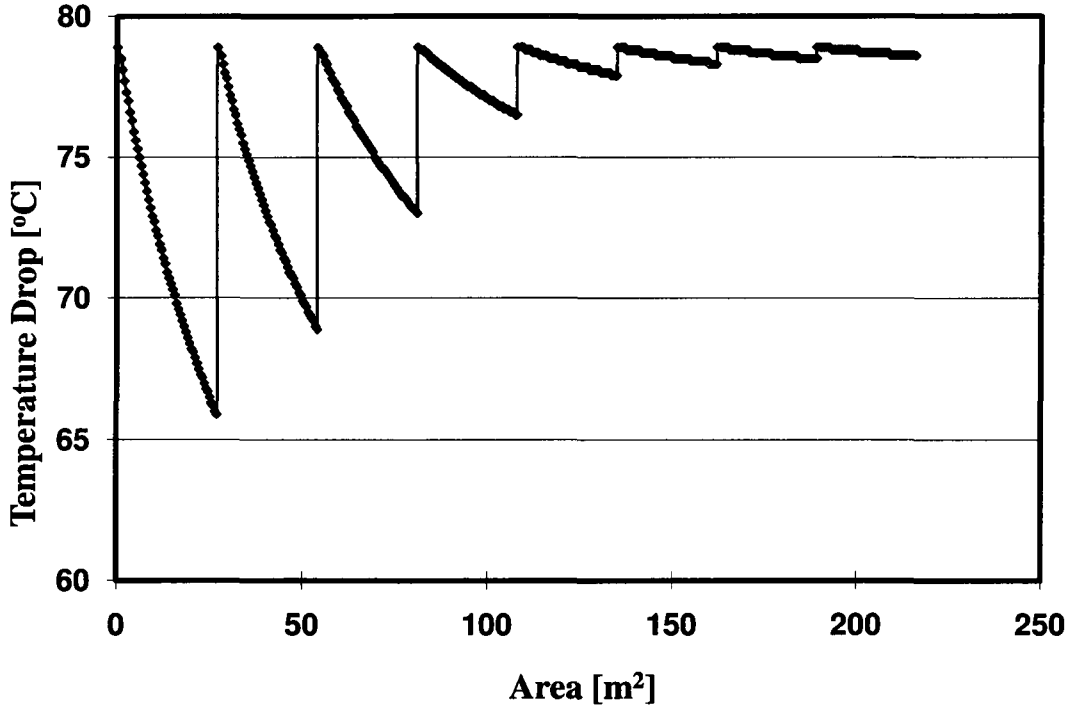

Figure B.4 Simulation of temperature drop profile for fixed stage area

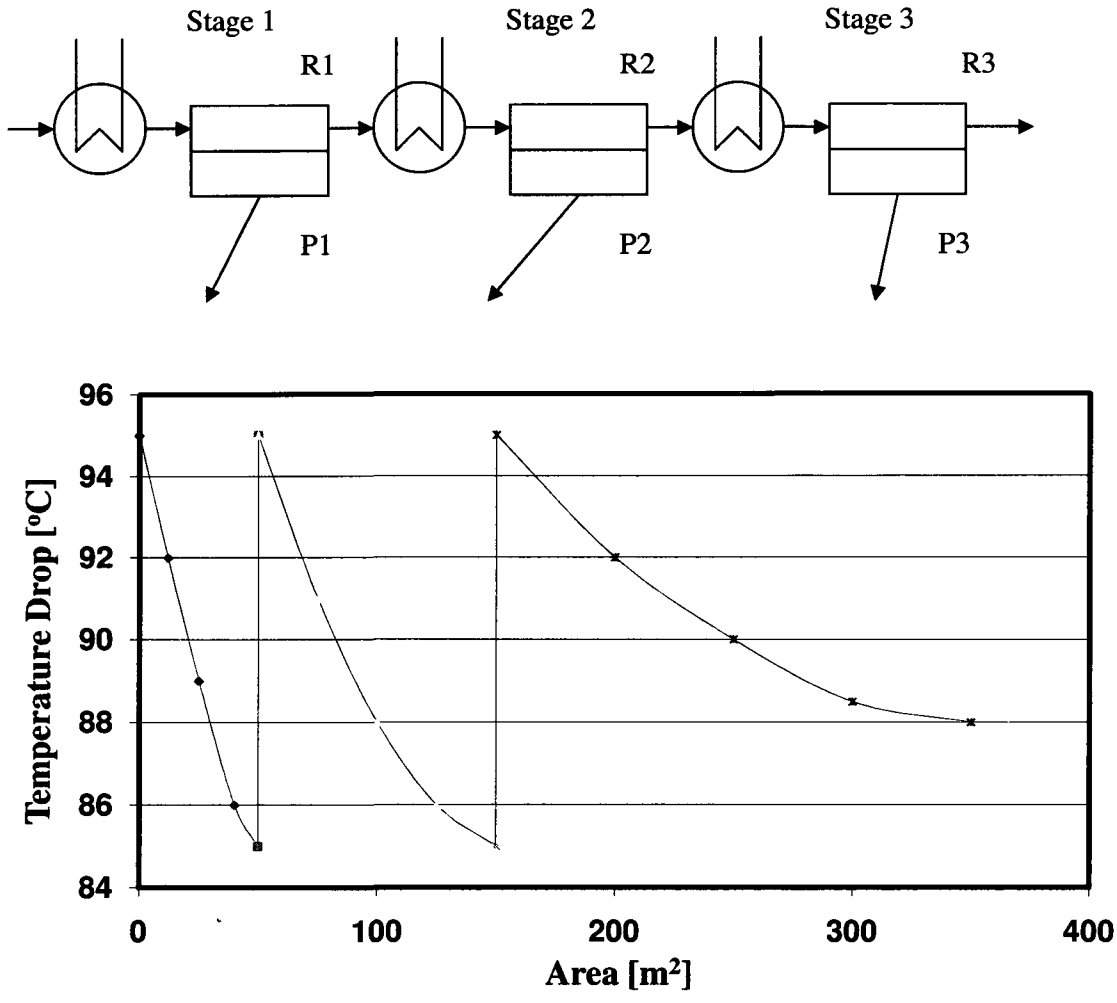

Figure B.5 Temperature profile for fixed temperature drop
(Bausa and Marquardt, 2000)

Figure B.5 shows the membrane modeling of fixed temperature drop per stage. For given temperature drop (10-15 °C in normal), the demand membrane area is increasing as the water concentration going down and less water flux through the membrane. It may go to infinity as no enough water flux evaporated. Comparing with Figure B.6, the simulation temperature profile shows the same trend as Bausa and Marquardt's paper. The operating conditions are: 100kg/h feed flow rate, 40 wt% ethanol in feed, saturate feed temperature (around 80 °C), 1 atm feed pressure, 10 °C temperature drop of each membrane module, and 0.02 bar permeate pressure.

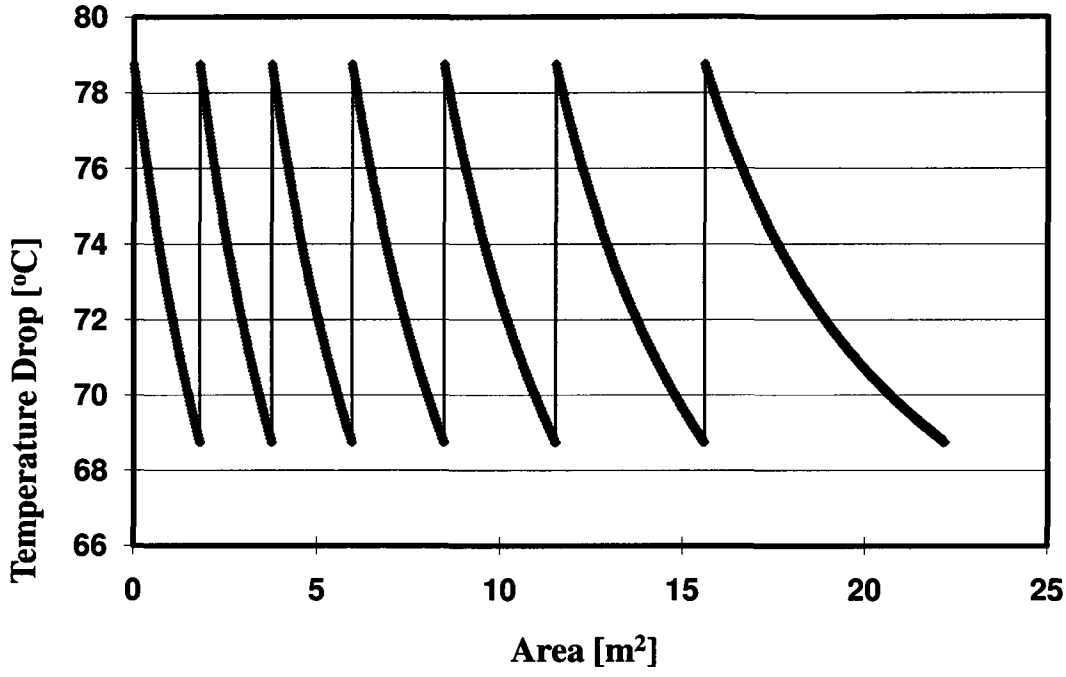

Figure B.6 Teperature drop profile for fixed temperature drop per stage

Permeate water flux

Figure B.7, is the permeate water flux as a function of inlet water concentration. The solid markers are experimental data for 90°C and 110 °C provided by Sommer and Merlin (2005). The lines represent the simulation results for both temperatures. The lines are fitted to the makers very well. The operating conditions are: 100kg/h feed flow rate, 40 wt% ethanol in feed, 90 °C and 110 °C feed temperature respectively, 1 atm feed pressure, 27 m^2 membrane area, and 0.02 bar permeate pressure.

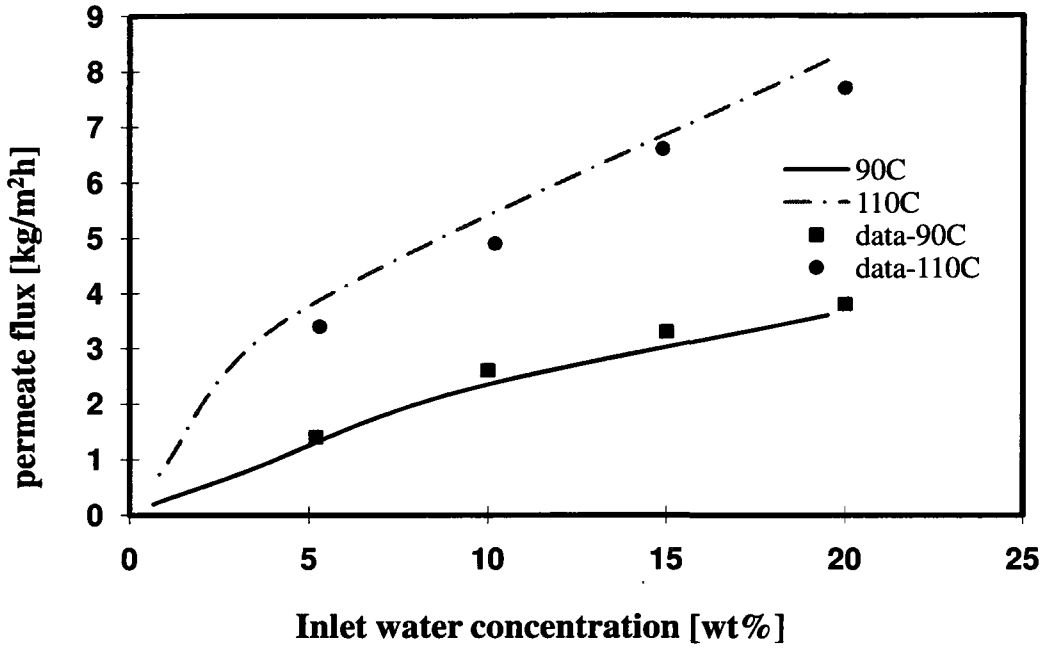

Figure B.7 Permeate flux as a function of water inlet concentration
(Sommer and Melin, 2005)

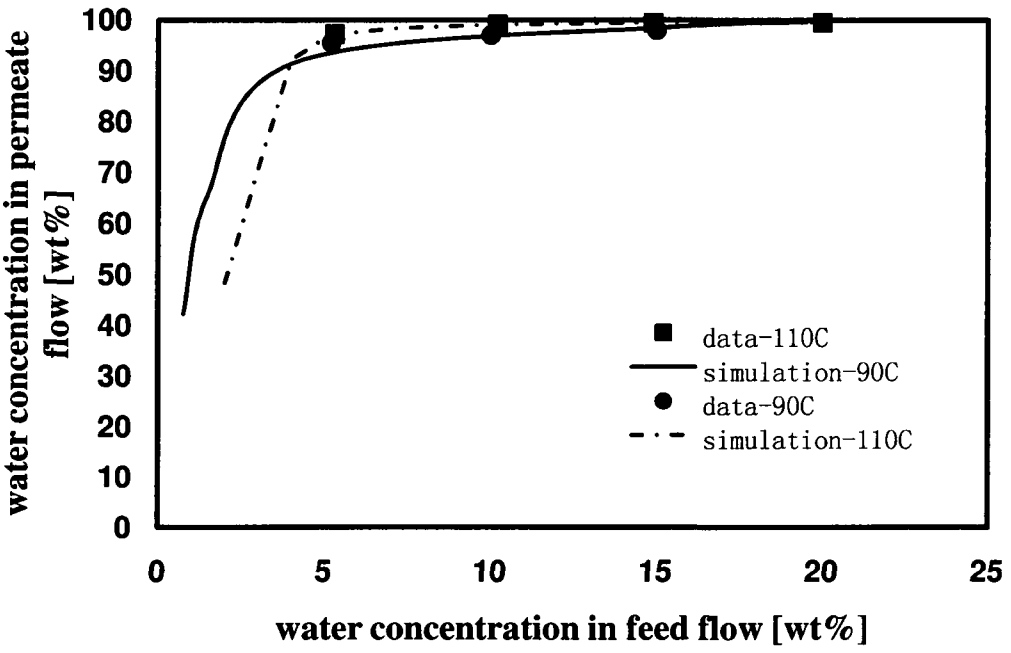

Figure B.8 Permeate flux and water concentration as a function of water inlet concentration
(Sommer and Melin, 2005)

Figure B.8 illustrates the relationship between permeate water concentration and inlet water concentration. It is obvious that when inlet water concentration is higher than 5 wt%, the permeate water concentration is above 90 wt%; if the inlet water concentration is above 10 wt%, the permeate flow are almost pure water. Since there is no experimental data available below 5 wt% water inlet, the simulation will focus on above 5 wt% inlet.

Energy validation by Hysys

Table B.2 Energy balance validation by Hysys

Unit [kW]	Feed	Retentate	Permeate	Cooling water	Low pressure steam	Liquid ring vacuum pump	Total energy
simulation	841.4	684	9.96	1047.7	1342.7	2.51	-2540.35
Hysys	-24808.25	-1766.96	-11489.88	1019.84	1463.56	0.77	-2604.45
	Heat loss in process					-1151.7	

The reference conditions for enthalpy calculation in Hysys are 25 °C and 1 bar. For compounds, the enthalpy is including formation heat. The reference conditions for simulation are 25 °C and 1 atm. For compound enthalpy evaluation, formation heat is not considered. From table 2, the total energy change is very close between simulation results and Hysys; difference is 4%, which is inside 5%.

References

Bausa, J., and Marquardt, W., Shortcut Design Methods for Hybrid Membrane/ Distillation Processes for the Separation of Nonideal Multicomponent Mixtures, Ind. Eng. Chem. Research, 39 (2000) 1658-1672

Sommer, S., Melin, T., Influence Of Operation Parameters On The Separation Of Mixtures By Pervaporation And Vapor Permeation With Inorganic Membranes. Part 1: Dehydration of Solvents, Chem. Eng. Sci., 60 (2005) 4509-4523

Kondo, M., Yamamura, T., Yukitake, T., Matsuo, Y., Kita, H., Okamoto, K., IPA purification for lens cleaning by vapor permeation using zeolite membrane, Separation and Purification Technology, 32 (2003) 191-198

Kita, D., Horii, K., Ohtoshi Y., Tanaka, K., Okamoto K., Synthesis of a zeolite NaA membrane for pervaporation of water/organic liquid mixtures, J. Mater. Sci. Lett. 14 (1995) 206-208

APPENDIX C Modeling of Distillation Column

Nowadays, dynamic modeling and simulation are widely applied to industrial processes. Distillation column is one of them. In the 1980's, many scientists tried to introduce numerical methods to model distillation processes and verified assumptions. In this project, an ideal distillation column is applied and following assumptions are used to set up the model:

- A continuous binary distillation column is employed.
- Only one feed flow, the feed flow is at bubble temperature.
- Only dynamics of distillation column is taken into consideration.
- Low pressure operation along the column (1 atmosphere).
- No pressure drop along the column.
- No heat lost through column wall.
- Tray efficiencies are assumed to be 1.
- Heat transfer efficiencies of condenser and reboiler are assumed to be 1.
- Liquid holdups on each tray are well mixed.
- Water and ethanol are the only components in the separation process.
- Mixture temperature on each tray is at saturation temperature.

Based on above assumptions, only the liquid holdup on each tray is considered since at low pressure, vapor holdup can be neglected for ethanol/water system. Mass and energy transfer only occur between the vapor and liquid phase on the tray. Ethanol and water mixture have an azeotropic point at 96.4 wt%. Below azeotropic point, ethanol is the more volatile component and is rich in vapor phase. Above azeotropic point, water will be more volatile than ethanol and accumulate in vapor phase. If feed and product ethanol concentration are both below azeotropic point, ethanol rich flow will be recovered at the top of the column as distillate; on the other hand, water will be accumulated at the bottom. If both feed and product ethanol concentration are above azeotrop point, ethanol will be collected at the bottom and water will be accumulated at the top. If the feed ethanol concentration is below azeotrop point but product requirement is above azeotropic point,

it cannot be solved by single distillation column. In this part, the distillation column is modeled for ethanol/ water system, which is below azeotropic point.

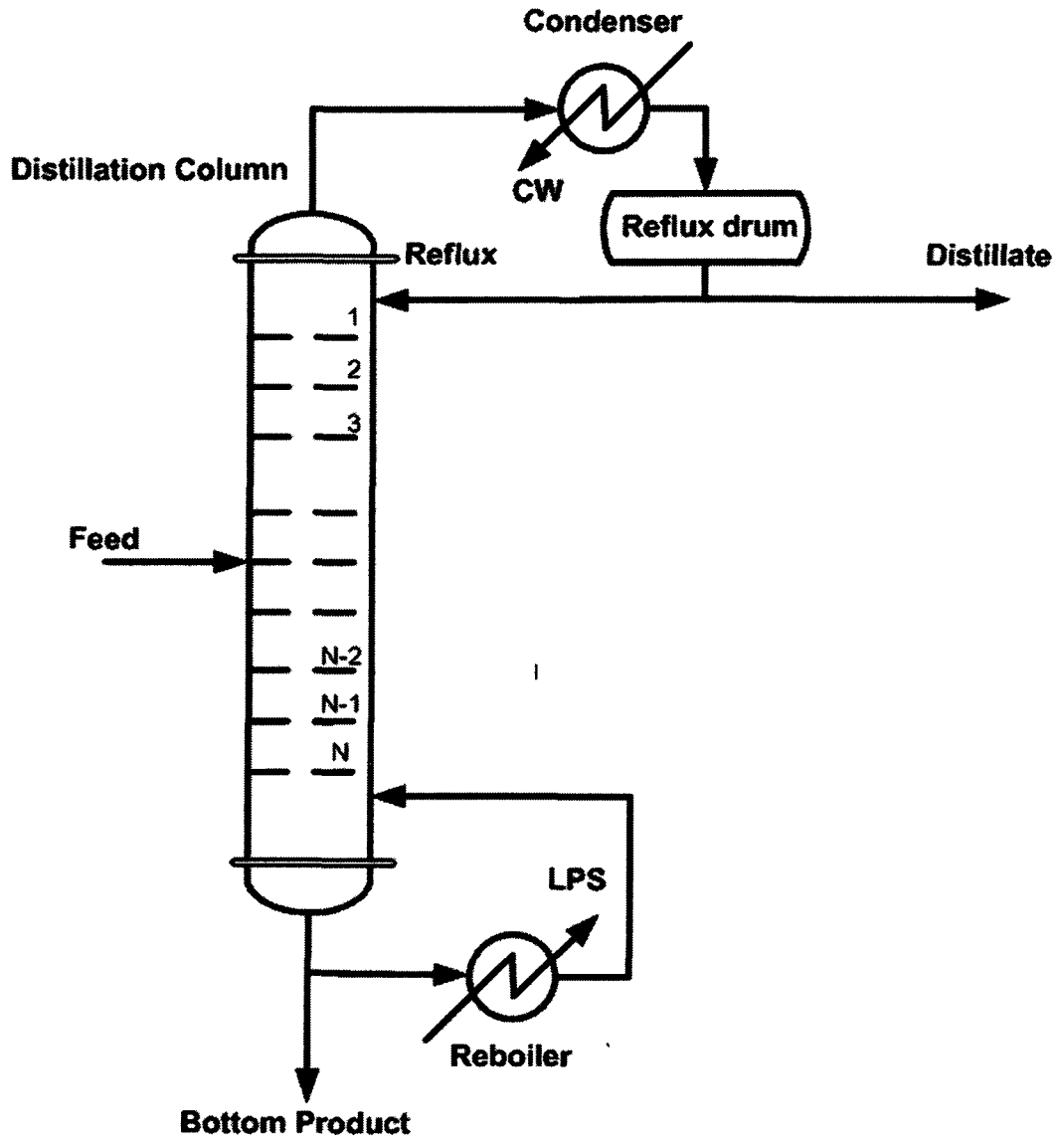

Figure C.1 Distillation column model

The distillation column model is as shown in Figure C.1. The major components are column, reboiler, condenser and a reflux drum.

Mass balance

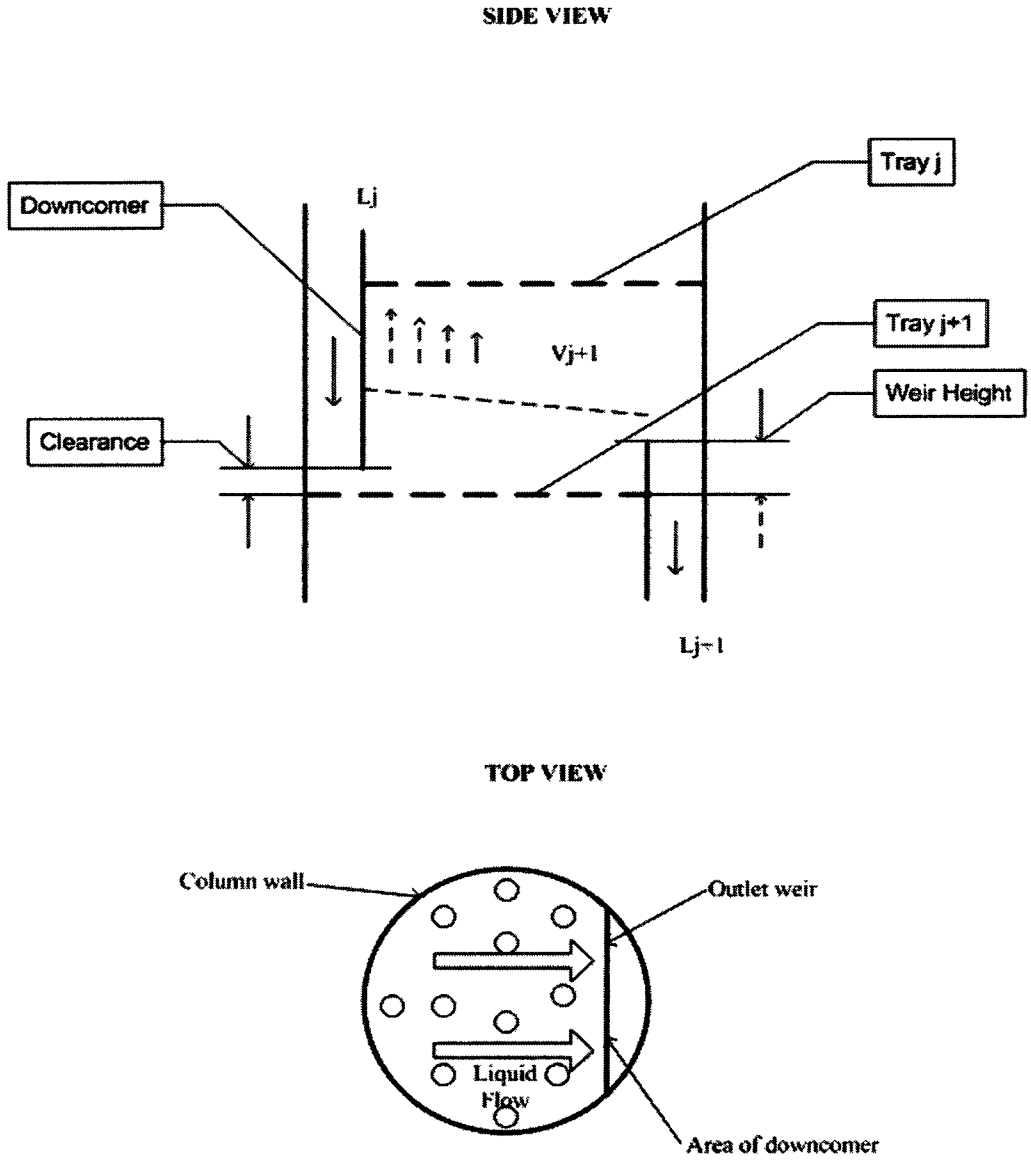

Figure C.2 Tray model for distillation column

The mass transfer and energy transfer occur on reboiler, condenser and each tray. The general equations for mass/ energy transfer are,

Inlet +Generation-Consumption-Outlet=Accumulation [1]

There is no reaction along the column; therefore, there is no generation or consumption. When the process reaches steady state, there is no accumulation any more. The differential equations for mass and energy on condenser, reboiler and each tray are shown in detail.

The overall mass balance for condenser

$$\frac{dM_1}{dt} = V_2 - (L_1 + D) \quad [2]$$

Where M_1 is the fixed molar liquid holdup in reflux drum [mol], L_1 is the molar reflux flow back to distillation column [mol/s], D is the molar distillate flow; [mol/s], V_2 is the molar vapor flow entering the condenser [mol/s]

Ethanol mass balance in condenser

$$\frac{d(M_1 x_{1,1})}{dt} = V_2 y_{1,2} - (L_1 + D)x_{1,1} \quad [3]$$

Where $x_{1,1}$ is the molar concentration of ethanol in the liquid phase in reflux drum [mol%], $y_{1,2}$, is the molar concentration of ethanol in vapor phase in V_2 flow [mol%]

According to Figure C.2, overall mass balance on tray i, $(2 \leq i \leq n-1)$

$$\frac{dM_i}{dt} = V_{i+1} - V_i + L_{i-1} - L_i + F_i \quad [4]$$

Where Mi is the liquid holdup on tray i [mol], L_i is the liquid flow leaving tray i [mol/s], V_i is the vapor flow leaving tray i [mol/s], F_i is the feed flow to tray i [mol/s]

The ethanol mass balance on tray i, $(2 \leq i \leq n-1)$

$$\frac{d(M_i x_{1,i})}{dt} = V_{i+1} y_{1,i} - V_i y_{1,i} + L_{i-1} x_{1,i-1} - L_i x_{1,i} + F_i x_{F,i} \quad [5]$$

Where $x_{1,i}$ is liquid concentration of ethanol leaving tray i [mol%], $y_{1,i}$ is the vapor concentration of ethanol leaving tray i [mol%], $x_{F,i}$ is the liquid concentration of feed flow to tray i [mol%]

The overall mass balance on reboiler (i = n):

$$\frac{dM_n}{dt} = L_{n-1} - (V_n + B) \qquad [6]$$

Where B is the bottom product flow. [mol/s]

Ethanol mass balance on reboiler

$$\frac{d(M_n x_{1,n})}{dt} = L_{n-1}x_{1,n-1} - (V_n y_{1,n} + Bx_{1,n}) \qquad [7]$$

Where $x_{1,n}$ is the ethanol concentration in liquid phase in reboiler [mol%], $y_{1.n}$ is the ethanol concentration in vapor phase in reboiler [mol%]

Energy balance

Energy balance on condenser

$$\frac{d(M_1 h_1)}{dt} = V_2 H_2 - (L_1 + D)h_1 - Q_c \qquad [8]$$

Where h_1 is the liquid specific molar enthalpy of flow L_1 [kJ/mol], H_2 is the vapor specific molar enthalpy of flow V_2 [kJ/mol], Q_c is the heat load of condenser [kJ/s]

The energy balance on tray i, ($2 \leq i \leq n-1$):

$$\frac{d(M_i h_i)}{dt} = V_{i+1}H_{i+1} - V_i H_i + L_{i-1}h_{i-1} - L_i h_i + F_i h_F \qquad [9]$$

Where h_i is the liquid specific molar enthalpy for liquid flow L_i [kJ/mol], H_i is the vapor specific molar enthalpy for vapor flow V_i [kJ/mol], h_F is the liquid specific molar enthalpy for feed flow [kJ/mol]

The energy balance on reboiler i=n

$$\frac{d(M_n h_n)}{dt} = L_{n-1}h_{n-1} - V_n H_n - Bh_n + Q_B \qquad [10]$$

Where Q_B is the heat load of reboiler [kJ/s]

Vapor-liquid phase equilibrium

A shortcut model is applied to generate vapor and liquid equilibrium based on liquid concentration at saturated temperature. This model is generated on experimental data (Perry's hand book) by using natural net work method. The vapor liquid equilibrium correlation is verified by both experimental data and Hysys.

Physical properties

Enthalpy

Normally, enthalpy of ethanol-water mixture at fixed pressure is determined by Ponchon-Savarit plot (Bosnjakovic et al., 1935). In this part, the mixture enthalpy is evaluated for liquid phase and vapor phase respectively. Liquid enthalpy and vapor enthalpy are generated on experimental data from Cornell and Montonna (1933) and Noyes and Warfel (1901). Both liquid and vapor enthalpy experimental data are correlated to the ethanol concentration at saturated temperature.

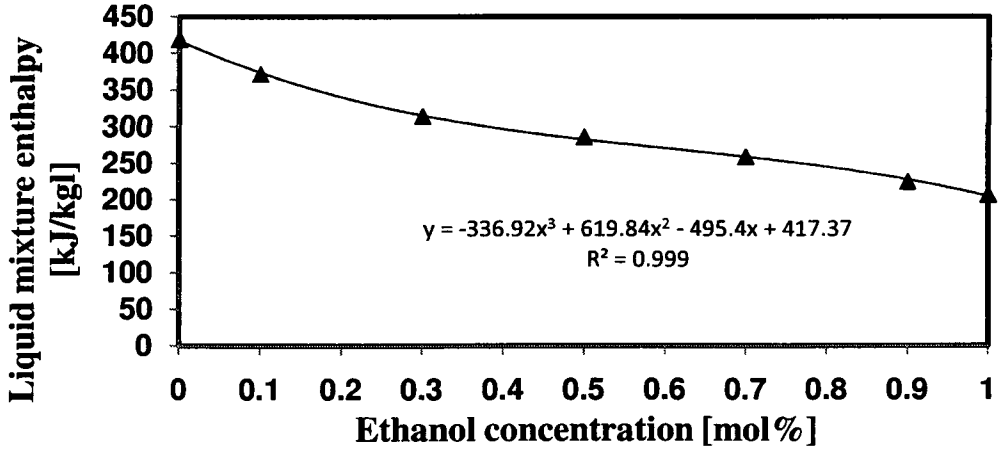

Figure C.3 Liquid mixture enthalpy as a function of ethanol concentration at saturate temperature

According to Figure C.3, correlation between ethanol concentration and liquid mixture enthalpy can be illustrated by equation [11], and the R-squared value of fitted line equation to the experimental data is 0.999.

$$h = (-336.92x_1^3 + 619.84x_1^2 - 495.4x_1 + 417.37) \times [MW_{ethanol} \cdot x_1 + MW_{water} \cdot (1 - x_1)]/1000 \quad [11]$$

Where, h is representing the liquid mixture enthalpy [kJ/mol], x_1 is the ethanol concentration in liquid, $MW_{ethanol}$ is the molecular weight of ethanol [mol/g], MW_{water} is the molecular weight of water [mol/g]

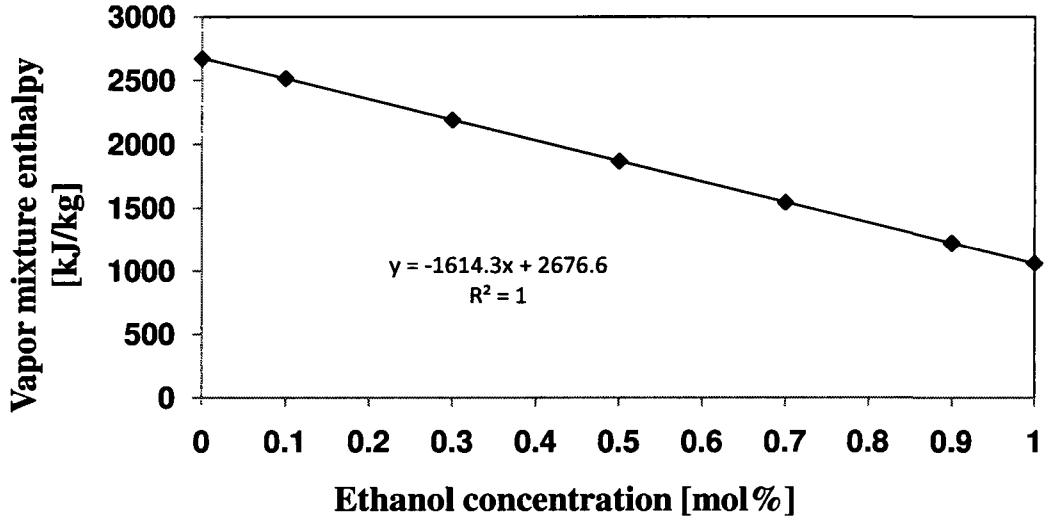

Figure C.4 Vapor mixture enthalpy as a function of ethanol concentration at saturate temperature

From Figure C.4, the correlation between ethanol concentration and vapor mixture enthalpy is a straight line with a negative slop. The linearized relationship is shown as equation [12] with a R-squared value as 1.

$$H = (-1614.3y_1 + 2676.6) \times [MW_{ethanol} \cdot y_1 + MW_{water} \cdot (1 - y_1)]/1000 \quad [12]$$

Where H is the vapor mixture enthalpy [kJ/mol], y_1 is the ethanol concentration in vapour.

Density

Ethanol and water density is estimated in two parts. One is in vapor, and the other is in liquid. Although ethanol and water solution is nonideal, the difference is very small between the experimental data and that calculated as ideal solution. The comparison shown following are generated from experimental data (CRC Handbook, 2005) and estimation as ideal solution.

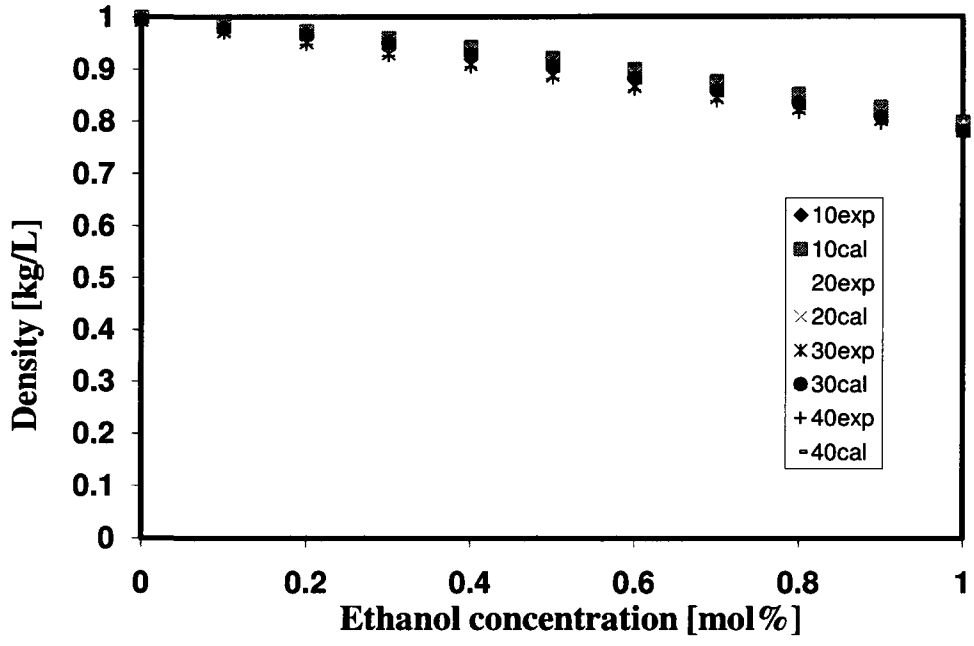

Figure C.5 Comparison of estimate density to experimental data of ethanol solution at different temperature

Figure C.5 is the comparison of estimated density to experimental data at different temperature. At each temperature, the estimated density is very close to the experimental data. Figure C.6 is the comparison of estimated density to experimental data at different composition. At each composition, the estimated density is very close to the experimental data as well. Hence, the estimated density is chosen in the distillation column modeling.

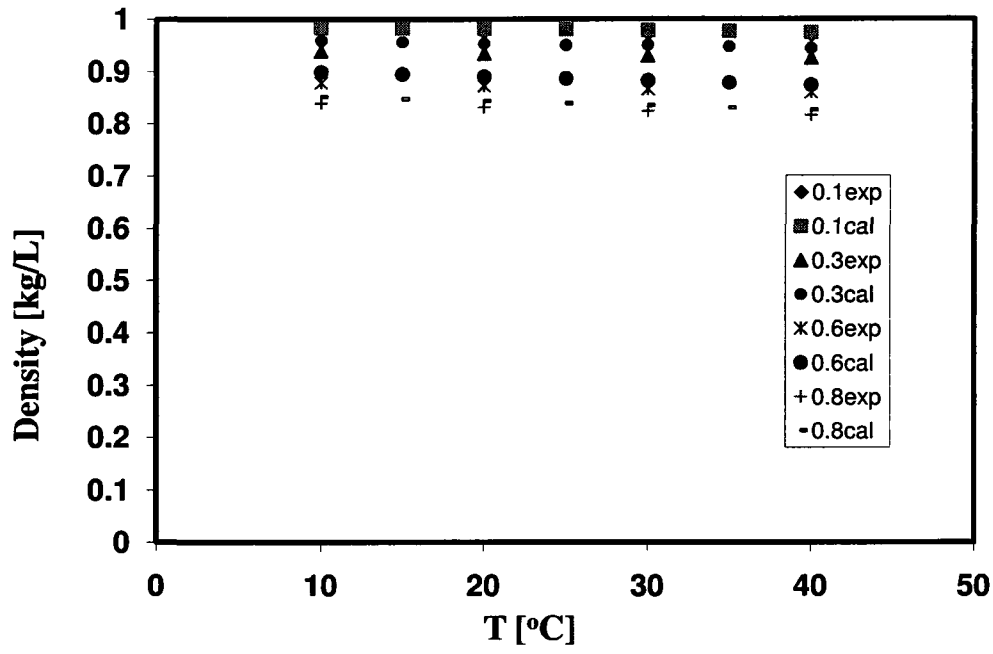

Figure C.6 Comparison of estimate density to experimental data of ethanol solution at different composition

The ethanol solution density is estimated by pure component density and its composition. Pure component density is provided in CRC handbook (2005), shown as equation [13],

$$\rho = \frac{C_1}{C_2^{\left[1+\left(1-\frac{T}{C_3}\right)^{C_4}\right]}} \times MW \qquad [13]$$

Where ρ is the density [kg/m^3], T is the temperature [K], and C_1, C_2, C_3, C_4 are parameters

Table C.1 Parameters for ethanol and water density

component	C_1	C_2	C_3	C_4
Ethanol	1.648	0.27627	513.92	0.2331
Water	5.459	0.30542	647.13	0.081

(CRC Handbook, 2005)

The liquid density is estimated by equation [14],

$$\rho_{Liq} = \rho_{ethanol} \cdot x_1 + \rho_{water} \cdot x_2 \qquad [14]$$

Where ρ_{Liq} is the density of liquid phase [kg/m^3], ρ_{water} is the density of liquid water [kg/m^3], $\rho_{ethanol}$ is the density of liquid ethanol [kg/m^3], x_1 is the composition of liquid ethanol, and x_2 is the composition of liquid water

Density of vapor phase is consider as ideal gas mixture density and is derived from idea gas law. It is shown as equation [15],

$$\rho_{Vap} = \frac{P}{R \cdot T} \times (MW_{ethanol} \cdot y_1 + MW_{water} \cdot y_2) \qquad [15]$$

Where ρ_{Vap} is the density of vapor phase [kg/m^3] , P is the pressure of column [kPa], T is the temperature [K], $MW_{ethanol}$ is the molecular weight of ethanol [g/mol], MW_{water} is the molecular weight of water [g/mol], y_1 is the ethanol composition in vapor, y_2 is the water composition in vapor, R is gas constant 8.314 [Pa m^3/mol K]

Viscosity

Vapor and liquid mixture viscosities are evaluated on pure components' viscosities. At low pressure, vapor viscosity can be considered as a function of temperature only. The equation is given below (Yaws, 1999),

$$\eta^V = A + BT + CT^2 \qquad [16]$$

Where η^V is the viscosity of vapor [μP], and A, B, and C are parameters.

Table C.2 Parameters for ethanol and water vapor viscosity (Yaws, 1999)

component	A	B	C
Ethanol	1.499	0.30741	-4.4479e-5
Water	-36.826	0.429	-1.62e-5

The vapor mixture viscosity is not linear to concentration. For a binary system, the vapor mixture viscosity can be determined by equation [17] (Reid and Sherwood, 1966),

$$\eta^V_{Mix} = \frac{\eta^V_1}{1+\frac{y_2}{y_1}F_{12}} + \frac{\eta^V_2}{1+\frac{y_1}{y_2}F_{21}} \quad [17]$$

Where η^V_{Mix} is the viscosity of vapor [μp], η^V_1 is the viscosity of ethanol vapor [μp], η^V_2 is the viscosity of water vapor [μp], y_1 is the ethanol composition in vapor, y_2 is the water composition in vapor, F_{12} is the coefficient of ethanol to water, F_{21} is the coefficient of water to ethanol

$$F_{12} = \frac{\left[1+\left(\frac{\eta^V_1}{\eta^V_2}\right)^{0.5}\cdot\left(\frac{MW_2}{MW_1}\right)^{0.25}\right]^2}{\sqrt{8}\left[1+\frac{MW_1}{MW_2}\right]^{0.5}} \quad [18]$$

$$F_{21} = \frac{\left[1+\left(\frac{\eta^V_2}{\eta^V_1}\right)^{0.5}\cdot\left(\frac{MW_1}{MW_2}\right)^{0.25}\right]^2}{\sqrt{8}\left[1+\frac{MW_2}{MW_1}\right]^{0.5}} \quad [19]$$

Where MW_1 is the ethanol molecular weight [g/mol], and MW_2 is the water molecular weight [g/mol]

Also the pure liquid component viscosity is provided by Yaws, C. L. It is only correlated to temperature as well.

$$\eta^L = 10^{A+\frac{B}{T}+CT+DT^2} \quad [20]$$

Where η^L is the viscosity of liquid [cp], and A, B, C, and D are parameters

Table C.3 Parameters for ethanol and water liquid viscosity (Yaws, 1999)

Component	A	B	C	D
Ethanol	-6.4406	1.1176×10^{3}	1.3721×10^{-2}	-1.5465×10^{-5}
Water	-10.2158	1.7925×10^{3}	1.773×10^{-2}	-1.2631×10^{-5}

The viscosity of binary mixture is defined in equation [21] (Rein and Sherwood, 1966),

$$\eta_{Mix}^{L} = \left(x_1\sqrt{\eta_1^{L}} + x_2\sqrt{\eta_2^{L}}\right)^2 \qquad [21]$$

Where η^{L}_{Mix} is the viscosity of liquid mixture [cp]

Surface tension

The pure liquid surface tension is a function of temperature at low pressure. According to Reid and Sherwood (1966), the pure liquid surface tension can be calculated by equation [22],

$$\sigma = A\left(1-\frac{T}{T_C}\right)^{n} \qquad [22]$$

Where σ is the liquid surface tension [mN/m], T_C is the critical temperature [K], and A and n are specific constants

Table C.4 Parameters for ethanol and water liquid surface tension (Yaws, 1999)

component	A	T_C	n
Ethanol	67.036	516.25	1.2222
Water	132.674	647.13	0.955

The liquid mixture surface tension is considered proportion to component concentration.

$$\sigma_{Mix} = \sigma_1 \cdot x_1 + \sigma_2 \cdot x_2 \qquad [23]$$

Where σ_{Mix} is the liquid mixture surface tension [mN/m], σ_1 is the liquid ethanol surface tension [mN/m], and σ_2 is the liquid water surface tension [mN/m]

Modeling of tray hydraulics

The purpose to model tray hydraulics is to obtain liquid flow rate of each tray. As shown in Figure C.7, the liquid flow rate on each tray is related to liquid height over weir, height of weir, hydraulic gradient, and liquid height in downcomer. Except height of weir, the

other three parameters are related to total pressure drop across a tray. For sieve trays, the total pressure drop is determined by the sum of the pressure drop across the dry hole and through the aerated mass, as shown in equation [24] (Kister, 1992).

$$h_t = h_d + h_l \qquad [24]$$

Where h_t is the total tray pressure drop [in], h_d is the pressure drop through dry hole [in], and h_l is the pressure drop through aerated mass [in]

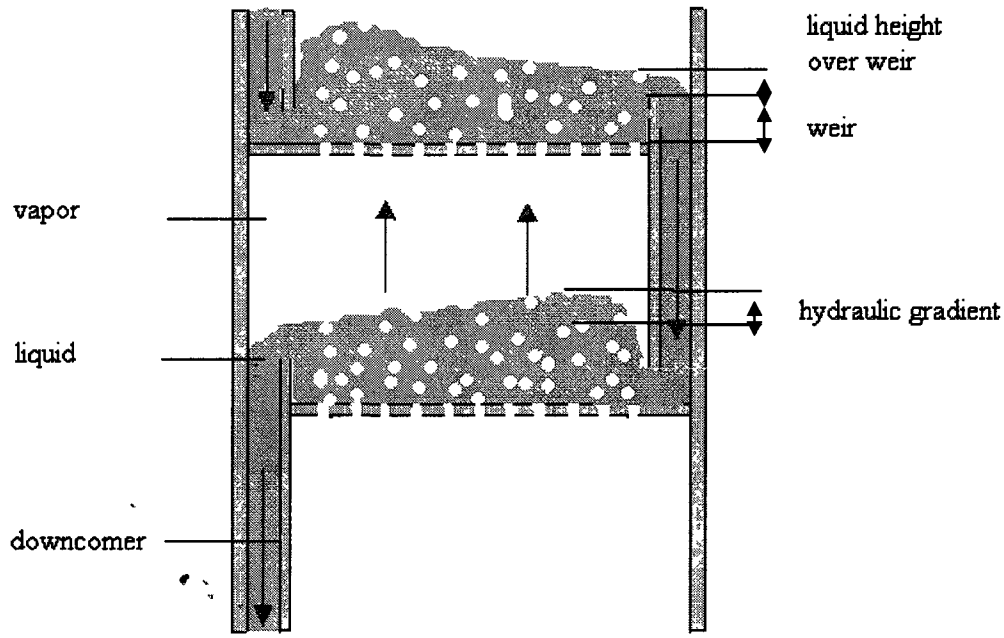

Figure C.7 Tray geometry illustration

The dry pressure drop across holes is given by Kister (1992)

$$h_d = K \frac{\rho_G}{\rho_L} u_h^2 \qquad [25]$$

For a sieve tray,

$$K = \frac{0.186}{C_v^2} \qquad [26]$$

Where ρ_G is vapor mixture density [lb/ft^3], ρ_L is liquid mixture density [lb/ft^3], u_h is the vapor hole velocisty [ft/s], C_V is the discharge coefficient

According to Kister (1992), the C_V value is 0.77 for sieve tray.

The pressure drop through aerated mass is calculated by equation [27],

$$h_l = \beta h_C \qquad [27]$$

Where β is aeration factor, h_C is height of clear liquid [in]

A short cut model can be applied,

$$h_l = 0.6(h_w + h_{ow}) \qquad [28]$$

For sieve trays, height of clear liquid is determined by height of weir, height of liquid over weir, and hydraulic gradient.

$$h_C = h_w + h_{ow} + \frac{h_g}{2} \qquad [29]$$

Where h_w is height of weir [in], h_{ow} is height of liquid over weir [in], and h_{hg} is hydraulic gradient [in]

For segmental weirs, liquid height over the weir is estimated by (Kister, 1992),

$$h_{ow} = 0.48 F_w (Q_L)^{\frac{2}{3}} \qquad [30]$$

Where F_w is a correction term, Q_L is liquid load on the tray [gal/min]

When weir length is 0.67 of column diameter, F_w can be estimated by equation [31]

$$F_W = 0.9815 + 0.0955 \log K \qquad [31]$$

Where $K = \left(\frac{Q_L}{L_w}\right)^{2.5}$

Hydraulic gradient is calculated by equation [32] (Kister, 1992)

$$h_g = \frac{12 f U_f^2 L_f}{g R_h} \quad [32]$$

Where f is friction factor, U_f is clear liquid velocity [gal/min], L_f is the length of flow path across the tray, equal to L_w [in], g is gravity coefficient, and R_h is the hydraulic radius of the aerated mass [in]

Friction factor is a function of Reynolds number and can be estimated by (Bai, 2003),

$$f = \frac{10^{3.3816}}{R_e^{1.0003}} \quad [33]$$

Where $R_e = \frac{R_h U_f \rho_L}{\eta^L}$

Velocity of the aerated mass is determined by (Kister, 1992; Bai, 2003),

$$U_f = \frac{1}{37.4} \frac{Q_L}{h_l} \frac{L_w}{D_f} \quad [34]$$

Where $D_f = 0.5(D_t + L_W)$, and D_t is the column diameter [in]

Hydraulic radius of the aerated mass is given by (Kister, 1992; Bai, 2003)

$$R_h = \frac{h_f D_f}{2h_f + 12D_f} \quad [35]$$

Where $h_f = 2.78(h_w + h_{ow})$

For segmental downcomers, the friction loss under downcomer apron is given as (Kister, 1992)

$$h_{da} = 0.03\left(\frac{Q_L}{100 A_{da}}\right)^2 \quad [36]$$

Where A_{da} is the area under downcomer [ft^2]

The total liquid on a tray is the sum of liquid on the tray and liquid in downcomer (Bai, 2003),

$$V = A_b\beta(h_w + h_{ow} + 0.5h_g) + A_d h_{dc} \qquad [37]$$

Where V is the total liquid volume on a tray [ft^3], A_b is the active area on the tray [ft^2], and A_d is the area of downcomer [ft^2]

Combining equation [37] to [30], Q_L is determined by,

$$Q_L = \left[\frac{\frac{(V - A_d h_{dc})}{A_b\beta} - h_w - 0.5h_g}{0.48F_w}\right]^{1.5} L_w \qquad [38]$$

Where $V = \frac{M}{\rho_L}$, and M is molar holdup on the tray

References

Bai, S., Assessment of controller performance with embedded data reconciliation, PhD thesis, University of Ottawa, Canada, 2003.

Bosnjakovic, F., Techische Thermodynamik, T. Steinkopff, Leipzig, 1935

Cornell, L. W. and Montonna, R. E., Ind. Eng. Chem., 25 (1933) 1331

CRC handbook, 2005

Kister, H. Z., Distillation design, Brown & Root Braun, Alhambra, California, 1992

Noyes, W. A. and Warfel R. R. J. Am. Chem. Soc., 23 (1901) 463

Reid, R. C. and Sherwood, T. K., The properties of gases and liquid, 2ne Ed., McGrawHill, 1996

Yaws, C. L., Chemical Properties Handbook, McGrawHill, 1999

APPENDIX D Validation of Distillation Column

Simulation of distillation column in moderate scale

In order to validate distillation column simulator, moderate scale and industrial scale are chosen in this part. For both simulations, the column calculation is terminated at steady state. The input variables are feed flow rate, feed composition, reflux ratio, distillate flow rate, number of trays, and feed tray. Time step is set to 0.0002 s; the convergence is set as 10^{-6} for sum of liquid flow change, sum of temperature change, and sum of vapor flow change; the convergence is set as 10-5 for the ratio of outlet flow to inlet flow. Aspen Hysys is used to compare the simulation result with the same initial settings, and NTRL-extended thermodynamic package is chosen.

For moderate scale settings are list in Table D.1. The calculated distillate concentration is 80.15 mol%.

Table D.1 Settings for moderate scale distillation simulation

Input variables	value	unit
Feed flow rate	100	mol/s
Feed concentration	40	mol%
Reflux ratio	1.58	
Distillate flow rate	48.15	mol/s
Number of trays	31	
Feed tray	26	

The comparison of simulation results to Aspen Hysys is shown in Figure D.1. The solid markers are results from Hysys, and the solid line is simulation result. Both simulation result and Hysys results show the exactly same trend. The difference between these two results is due to the thermodynamics. In Hysys, extended-NTRL package is chosen; in simulation, a short cut model is applied for vapor-liquid equilibrium, and some mixture properties are simplified as ideal mixture.

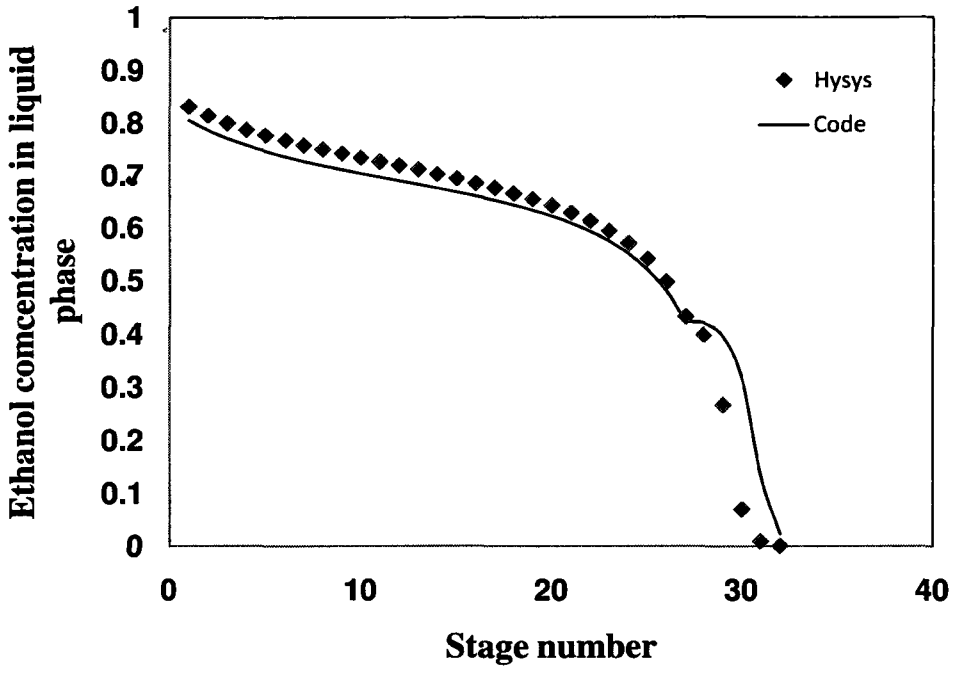

Figure D.1 Comparison of moderate scale distillation simulation to Aspen Hysys: Ethanol composition in liquid phase as a function of stage number

Simulation of industrial scale distillation column

Table D.2 Settings for moderate scale distillation simulation

Input variables	value	unit
Feed flow rate	183.88	mol/s
Feed concentration	61.01	mol%
Reflux ratio	1.3	
Distillate flow rate	133.01	mol/s
Number of trays	80	
Feed tray	75	

The calculated distillate concentration is 81.8 mol%. The comparison to Aspen Hysys is shown in Figure D.2.

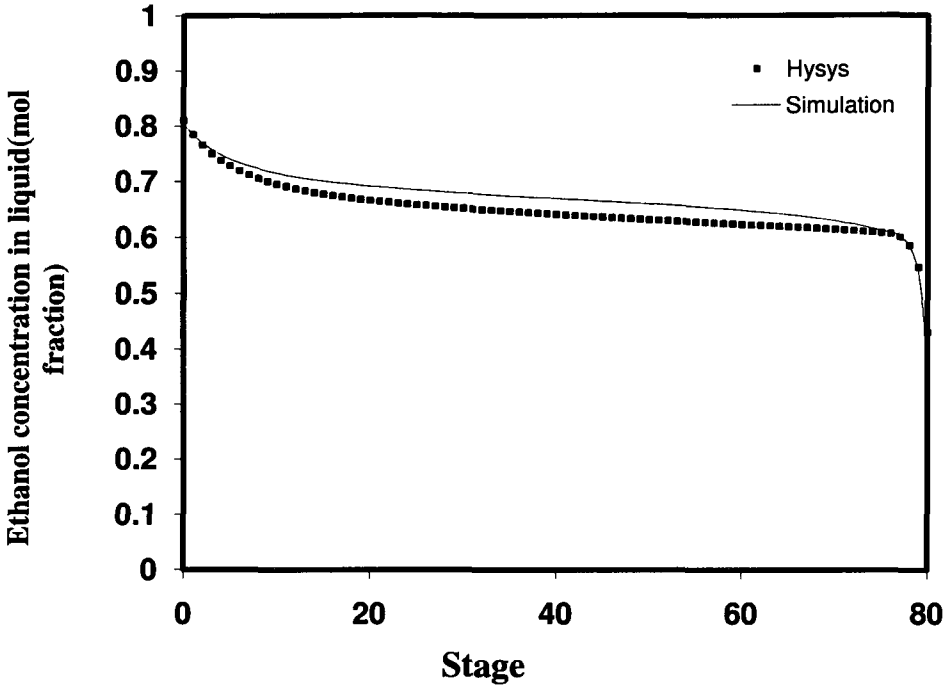

Figure D.2 Comparison of industrial scale distillation simulation to Aspen Hysys: Ethanol concentration in liquid phase as a function of stage number

APPENDIX E Weight Factor on the Pareto Domain Ranked by NFM

As discussed in Chapter 2, the compromised solutions from the ranked Pareto domain are mainly determined by the weight of each criterion. Decision makers can easily scarify one or several criteria by reduce their weight in purpose. In this section, a similar investigation was performed with different relative weight on an industrial-scale ethanol dehydration pervaporation process when the two input variables are the area per stage and the permeate pressure. A 50x50 grid of these two input variables was generated and, for each set of values, simulations were performed to calculate the four objective criteria (total number of stages, total membrane area required, total energy consumption, and total exergy loss) and to draw contour plots of these four objective criteria. The grid of solutions contains both dominated and non-dominated solutions. Then, for the same operating conditions, the Pareto domain was determined using the diploid genetic algorithm and ranked with NFM. The four NFM parameters for each criterion used to rank all points in the Pareto domain are list in Table E.1. Other operating conditions are the same as the Chapter 2.4.3.

Table E.1 NFM parameters used to rank the Pareto domain for relative weight investigation

Variable	Relative weight	Indifference threshold	Preference threshold	Veto threshold
Total number of stages	0.15	5	10	20
Total membrane area	0.15	200	400	1000
Energy consumed	0.35	50	100	200
Exergy loss	0.35	5	10	20

Figure E.1 presents the total number of stages as a function of the area per stage and the permeate pressure. Compared to Figure 2.6, the best solution identified using the NFM does minimize the total number of stages which is located at a low permeate pressure and relative large area per stage. The best 10% of all solutions of the Pareto domain are

obtained in two parts as well: (1) low permeate pressure and small area per stage – the same as Figure 2.6 and (2) high permeate pressure and intermediate area per stage. The best 10 to 50% of the Pareto domain are located at small to medium area per stage and medium to high permeate pressure.

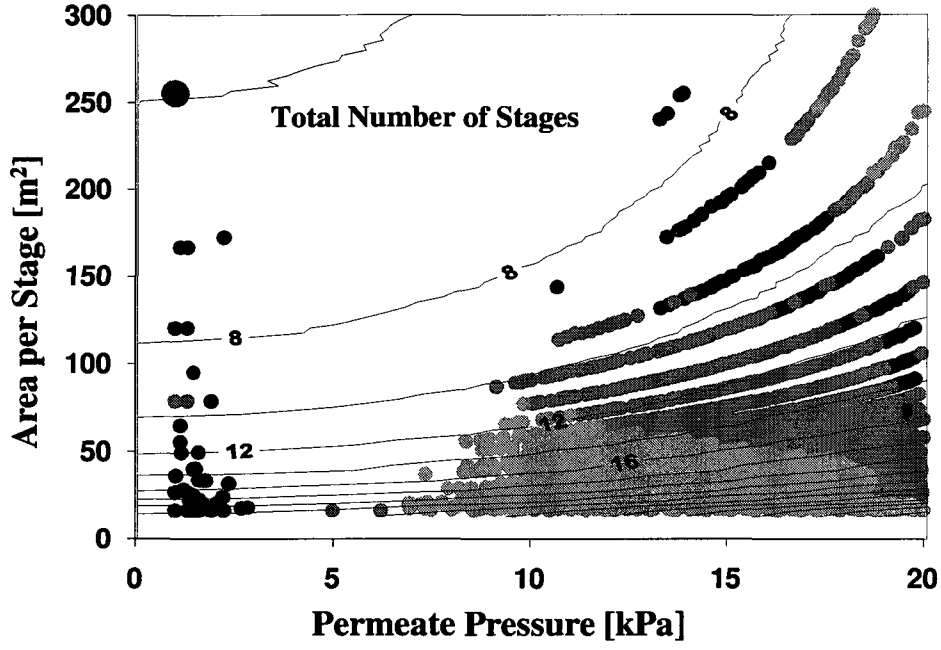

Figure E.1Pareto Domain solutions covered by contour plot of the total number of stages as a function of area per stage and permeate pressure at 3 atm feed pressure for industrial scale production as defined in Table 2.4 (• – best solution; • – best 10% solutions; • - best 10% to 50% solutions; • - remaining 50%)

Figure E.2 presents the contour plot of the total membrane area as a function of the area per stage and the permeate pressure. The best compromised solution is obtained for an intermediate total membrane area. Figures E.3 and E.4 present the contour plots of the total energy consumed and the exergy loss as a function of the area per stage and the permeate pressure. It is obvious that both the energy consumed and the exergy loss are sacrificed for the compromised solutions are located at the relative high values.

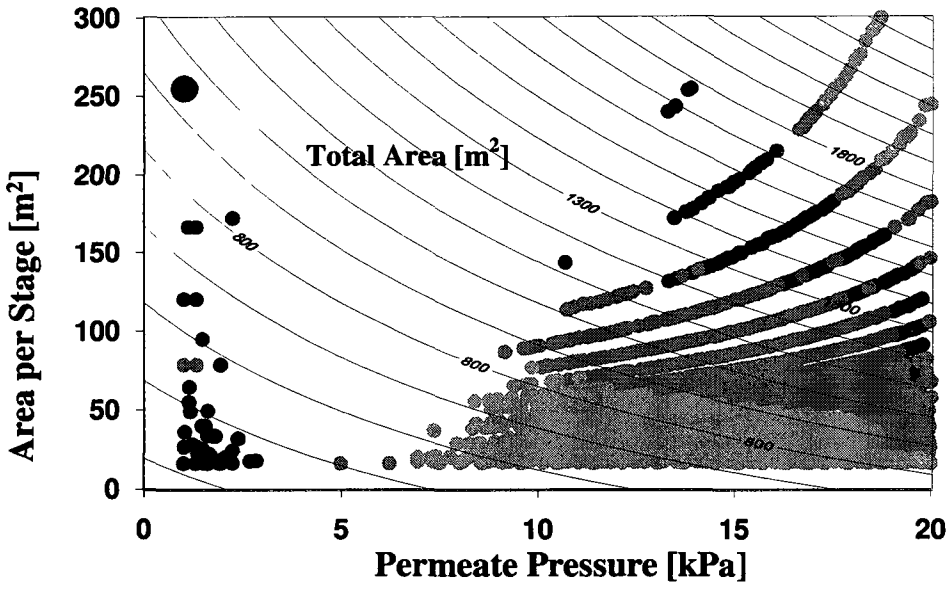

Figure E.2. Pareto Domain solutions covered by contour plot of the total membrane area as functions of permeate pressure and membrane area per stage at 3 atm feed pressure for industrial scale production as defined in Table 2.4 (● – best solution; ● – best 10% solutions; ●- best 10% to 50% solutions; ● - remaining 50%)

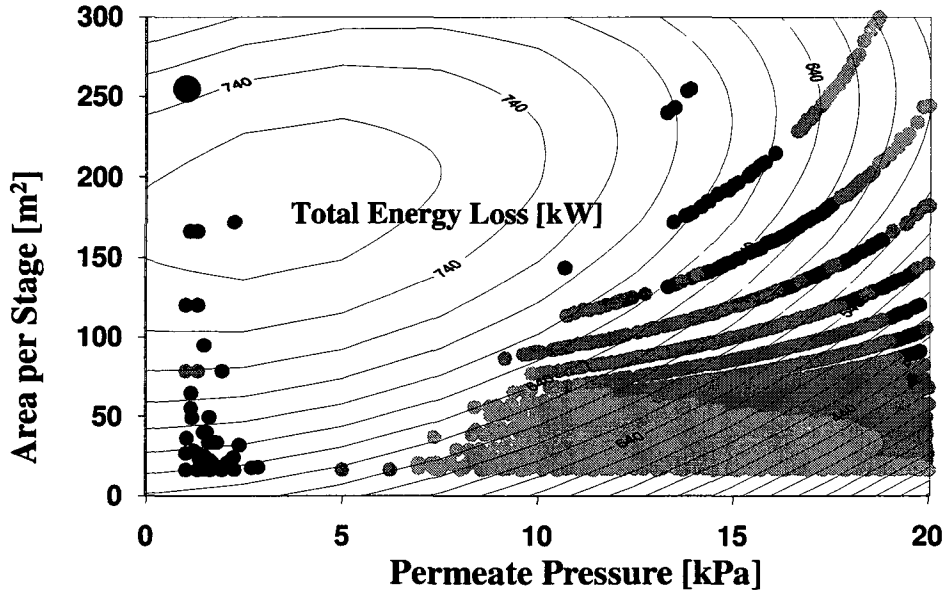

Figure E.3. Pareto Domain solutions covered by contour plot of the total energy loss as functions of permeate pressure and membrane area per stage at 3 atm feed pressure for industrial scale production as defined in Table 2.4 (● – best solution; ● – best 10% solutions; ●- best 10% to 50% solutions; ● - remaining 50%)

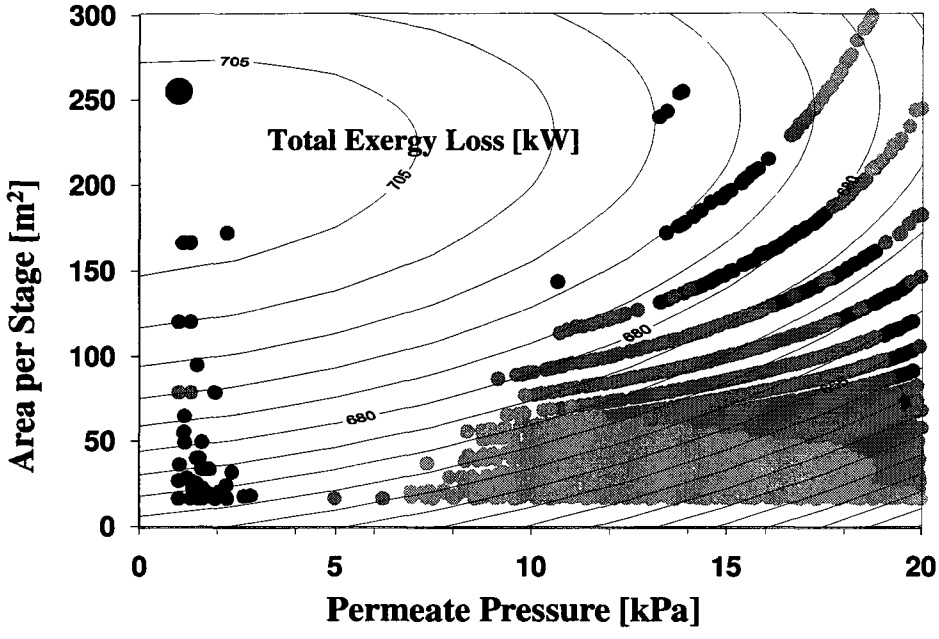

Figure E.4. Pareto Domain solutions covered by contour plot of the total exergy loss as functions of permeate pressure and membrane area per stage at 3 atm feed pressure for industrial scale production as defined in Table 2.4 (● – best solution; ● – best 10% solutions; ●- best 10% to 50% solutions; ○ - remaining 50%)

APPENDIX F Fortran Code for Hybrid System

```
Program main
        double precision Tf,Pp,F,Xef,Xer,Pm,maxarea, Ftest, Ytest, NumOfStages,xf, mF, Fperm, Xperm, Fpermol,
Xpermol,T1,TNTray, Pc, Pref, Tref, Tcin, Tcout, Tbin, Tbout, Pb
        double precision totarea, totrec, totstages,totenergy, Xeo, Fo, Feed1,xf1, Feed2,xf2,Fomol, Xeomol, FDist,
XDist, FDistOld, XDistOld,FBott
        double precision DifF, DifX, FMain, XMain, Tbw, Tbe, D, Tout, best_xep, Fdraw
        double precision totcostCap, CostCol, CostReb, CostCon, CostHex, totcostOp, COReb, COCon, COHex, QB,
QC, CapM, OpM, RefluxR,ELoss
        Real(8),Dimension(2,100)::y,x
        Real(8),Dimension(100):: T,L,FSideRate
        integer, dimension(100):: Ndraw
        integer i, j, NMainFeed, NRet, Nperm, NTray, Nruns, iread
        double precision exergDist, exergBott, exergFeed, exergCondin, exergCondout, exergCond, exergReboil,
exergReboilin, exergReboilout,Fcw,Flps, exergyLoss, Hw, Sw, He, Se
        open (11, FILE = 'draw.txt', status='old')          !input file
        open (2, FILE = 'results.txt', access='append')     !results
        Pp=0.133 !bar                                       !permeate pressure of the membrane process
        NTray = 82                                          !tray number of the distillation column
        NMainFeed = 66                                      !feed stage
        mF =183.8796 !mol/s                                 !feed flow rate to the distillation column
        xf=0.6102                                           !feed concentration to the distillation column
        D=133.0097                                          ! distillate flow rate of the distillation column
        Xer = 0.92D0                                        !ethanol concentration after the membrane process
        Pm = 1.01324D0                                      !base pressure of the membrane process
        maxarea =0.33D0                                     !tube area of the membrane fiber
        NumOfStages = 10                                    !stage number of the membrane section
        Pc=1.     !bar                                      !pressure of the column
        Pref=1.                                             !reference pressure
        Pb=2.                                               !pressure of the reboiler
        Tref=298.15                                         !reference temperature
        Tcin=293.15                                         !inlet temperature of the cooling water to heater exchanger
        Tcout=308.15                                        !outlet temperature of the cooling water
        Tbin=393.15                                         !inlet temperature of the low pressure steam
        Tbout=368.15                                        !outlet temperature of the low pressure steam
        Tbw=373.15                                          !boiling point of water at standard conditions
        Tbe=351.4                                           !boiling point of ethanol at standard conditions
        read (11,*) nruns
        print *, nruns
        Do iread = 1, nruns
                read (11,*) Ndraw(iread), FSideRate(iread)
                print *, 'Ndraw, Fsiderate', Ndraw(iread), Fsiderate(iread)
        end do
        Do iread =4, nruns
        totcostCap=0
        totcostOp=0
        Feed1=0.0
        xf1=0.0
        Feed2=0.0
        xf2=0.0
        Fdraw=0.0
        call GetInitialConditions(mF,xf,NTray,NMainFeed,D,Fdraw, Ndraw(iread), Feed1, xf1,13, Feed2, xf2, 82, FDist,
XDist, x, y, QB, QC, T, L,CostCol, totrec,RefluxR)
                Fdraw=L(Ndraw(iread))*FsideRate(iread)
                call MolToKg(Fdraw, x(1,Ndraw(iread)), F, Xef)
                Call TrayTemperature1(Xef,Tf)
                Tf=Tf+273.15
                Call  pervap(NumOfStages,Tf,Pp,F,Xef,Xer,Pm,maxarea,totarea,totrec,totstages,totenergy,Xeo,  Fo,
Tout, best_xep,CapM, OpM,ELoss)
                call KgToMol(Fo, Xeo, Fomol, Xeomol)
                Feed1 = Fomol
                xf1 = Xeomol
                Fperm = F - Fo
                Xperm = (F*Xef - Fo * Xeo)/(F-Fo)
                call KgToMol(Fperm, Xperm, Fpermol, Xpermol)
```

```
                Feed2 = Fpermol
                xf2 = Xpermol
                NRet=1                          !estimate stage number of the permeate and retentate return to column
                NPerm=NMainFeed
                Do i= NMainFeed, 1
                        if ( xf1 .GT. x(1, i) ) then
                                NRet = i
                        end if
                End do
                If (NRet .EQ. 1) then
                        NRet=2
                end if
                If (NRet .EQ. NMainFeed) then
                        NRet = NMainFeed -1
                end if
                Do i=NMainFeed, NTray
                        if (x(1, i) .GT. xf2) then
                                NPerm = i
                        end if
                End do
                If (NPerm .EQ. NMainFeed) then
                        NPerm = NMainFeed+1
                end if
                If (NPerm .EQ. NTray) then
                        Nperm=NTray-1
                end if
                call GetInitialConditions(mF,xf,NTray,NMainFeed,D,Fdraw, Ndraw(iread), Feed1, xf1,NRet, Feed2,
xf2, Nperm, FDist, XDist, x, y, QB, QC, T, L,CostCol, totrec,RefluxR)
        call HeatExchanger(1, QC, 1, CostCon, COCon)
        call HeatExchanger(2, QB, 2, CostReb, COReb)
        call ColumnCost(RefluxR, FDist, XDist, NTRAY, CostCol)
        totcostCap=937.61/280*(CostCon+CostReb+CapM)+CostCol+1616.1*totarea+775*totarea/3
        totcostOp=COCon+COReb+OpM
        totrec=FDist*XDist/mf/xf
        call MolToKg(mF, xf, F, Xef)
        call TrayTemperature1(xef,Tf)
        Tf=Tf+273.15                            !estimate exergy loss and energy comsuption
        call HWater(Tf, Tref, Tbw, Hw, 1)
        call HEthanol(Tf, Tref, Tbe, He, 1)
        call SWater(Tf, Tref, Tbw,Pc, Pref, Sw, 1)
        call SEthanol(Tf, Tref, Tbe, Pc, Pref, Se, 1)
        exergFeed=mF*xf*(He-Tref*Se)+mF*(1-xf)*(Hw-Tref*Sw)
        call MolToKg(FDist,XDist,F,Xef)
        call TrayTemperature1(Xef,Tf)
        Tf=Tf+273.15
        call HWater(Tf, Tref, Tbw, Hw, 1)
        call HEthanol(Tf, Tref, Tbe, He, 1)
        call SWater(Tf, Tref, Tbw, Pc, Pref, Sw, 1)
        call SEthanol(Tf, Tref, Tbe, Pc, Pref, Se,1)
        exergDist=FDist*XDist*(He-Tref*Se)+FDist*(1-XDist)*(Hw-Tref*Sw)
        !exergy of bottom
        call MolToKg(L(NTray),x(1,NTray),F,Xef)
        call TrayTemperature1(Xef,Tf)
        Tf=Tf+273.15
        call HWater(Tf, Tref, Tbw, Hw,1)
        call HEthanol(Tf, Tref, Tbe, He,1)
        call SWater(Tf, Tref, Tbw, Pc, Pref, Sw,1)
        call SEthanol(Tf, Tref, Tbe, Pc, Pref, Se,1)
        exergBott=L(NTray)*x(1,NTray)*(He-Tref*Se)+L(NTray)*(1-x(1,NTray))*(Hw-Tref*Sw)
        call HWater(Tcout, Tcin, Tbw, Hw,1)
        Fcw=Qc/Hw*1000
        !exergy of cooling water enter condenser
        call HWater(Tcin, Tref, Tbw, Hw,1)
        call Swater(Tcin, Tref, Tbw, Pc, Pref, Sw,1)
        exergcondin=Fcw*(Hw-Tref*Sw)
        call HWater(Tcout, Tref, Tbw, Hw,1)
        call Swater(Tcout, Tref, Tbw, Pc, Pref, Sw,1)
        exergcondout=Fcw*(Hw-Tref*Sw)
        !Low pressure steam flow rate
        call HWater(Tbin, Tbout, Tbw, Hw,0)
```

```
        Flps=QB/Hw*1000
        call HWater(Tbin, Tref, Tbw, Hw,0)
        call Swater(Tbin, Tref, Tbw, Pb, Pref, Sw,0)
        exergReboilin=Flps*(Hw-Tref*Sw)
        call HWater(Tbout, Tref, Tbw, Hw,1)
        call Swater(Tbout, Tref, Tbw, Pb, Pref, Sw,1)
        exergReboilout=Flps*(Hw-Tref*Sw)
        exergyLoss=exergDist+exergBott+exergReboilout+exergCondout-exergFeed-ExergReboilin-exergCondin
        totalEL=Eloss+exergyLoss
        ELPP=totalEL/FDist/XDist
        write (2, '(12E15.4)') xf, FDist, XDist,FSiderate,xf1, xf2, feed1, feed2, Eloss, Exergyloss,ELPP, RefluxR
        End Do
        CLOSE (11,status='keep')
        CLOSE (2,status='keep')
end

subroutine HWater(T, Tref,Tbw, Hw,flag)          !evaluate enthalpy of water
        double precision, intent(in):: T, Tref
        double precision, intent(out):: Hw
        double precision Awv, Bwv, Cwv, Dwv
        double precision Awl, Bwl, Cwl
        double precision delHv, Tbw, R
        integer, intent(in):: flag
        delHv=40656 !J/mol
        R=8.314
        !parameters for water Cp in vapor (Smith, 2005)
        Awv=3.47
        Bwv=0.00145
        Cwv=0
        Dwv=12100
        !parameters for water Cp in liquid (Smith, 2005)
        Awl=8.712
        Bwl=0.00125
        Cwl=0.00000018
        if (flag .EQ. 0) then
                Hw=R*((Awv*T+0.5*Bwv*T**2+1.0/3.0*Cwv*T**3-Dwv/T)-
(Awv*Tbw+0.5*Bwv*Tbw**2+1.0/3.0*Cwv*Tbw**3-Dwv/Tbw)+delHv/R+(Awl*Tbw+0.5*Bwl*Tbw**2+1.0/3.0*Cwl*Tbw**3)-
(Awl*Tref+0.5*Bwl*Tref**2+1.0/3.0*Cwl*Tref**3))
        else
                Hw=R*((Awl*T+0.5*Bwl*T**2+1.0/3.0*Cwl*T**3)-(Awl*Tref+0.5*Bwl*Tref**2+1.0/3.0*Cwl*Tref**3))
        end if
end subroutine HWater

subroutine HEthanol(T, Tref, Tbe, He, flag)          !evaluate enthalpy of ethanol
        double precision, intent(in):: T, Tref
        double precision, intent(out):: He
        integer, intent(in):: flag
        double precision Aev, Bev, Cev, Dev
        double precision Ael, Bel, Cel
        double precision Tbe, R ! delHv
        delHv=38489 !J/mol
        R=8.314
        Aev=3.518
        Bev=0.020001
        Cev=-0.000006002
        Dev=0
        !parameters for ethanol Cp in liquid (Smith, 2005)
        Ael=33.866
        Bel=-0.1726
        Cel=0.00034917
        if (flag .Eq. 0) then
                He=R*((Aev*T+0.5*Bev*T**2+1.0/3.0*Cev*T**3-Dev/T)-
(Aev*Tbe+0.5*Bev*Tbe**2+1.0/3.0*Cev*Tbe**3-Dev/Tbe)+delHv/R+(Ael*Tbe+0.5*Bel*Tbe**2+1.0/3.0*Cel*Tbe**3)-
(Ael*Tref+0.5*Bel*Tref**2+1.0/3.0*Cel*Tref**3))
        else
                He=R*((Ael*T+0.5*Bel*T**2+(1.0/3.0)*Cel*T**3)-(Ael*Tref+0.5*Bel*Tref**2+(1.0/3.0)*Cel*Tref**3))
        end if
end subroutine HEthanol

subroutine SWater(T, Tref, Tbw, P, Pref, Sw, flag)          !evaluate entropy of water
```

```
        double precision, intent(in):: T, Tref, P, Pref
        double precision, intent(out):: Sw
        integer, intent(in):: flag
        double precision Awv, Bwv, Cwv, Dwv
        double precision Awl, Bwl, Cwl
        double precision delHv, Tbw, R
        delHv=40656 !J/mol
        R=8.314
        Awv=3.47
        Bwv=0.00145
        Cwv=0
        Dwv=12100
        !parameters for water Cp in liquid (Smith, 2005)
        Awl=8.712
        Bwl=0.00125
        Cwl=0.00000018
        if (flag .EQ. 0) then
                Sw=R*((Awv*log(T)+Bwv*T+0.5*Cwv*T**2-0.5*Dwv/T**2-log(P/pref))-
(Awv*log(Tbw)+Bwv*Tbw+0.5*Cwv*Tbw**2-0.5*Dwv/Tbw**2-
log(P/Pref))+delHv/Tbw/R+(Awl*log(Tbw)+Bwl*Tbw+0.5*Cwl*Tbw**2-log(P/Pref))-
(Awl*log(Tref)+Bwl*Tref+0.5*Cwl*Tref**2-log(P/pref)))
        else
                Sw=R*((Awl*log(T)+Bwl*T+0.5*Cwl*T**2-log(P/Pref))-(Awl*log(Tref)+Bwl*Tref+0.5*Cwl*Tref**2-
log(P/Pref)))
        end if
end subroutine SWater

subroutine SEthanol(T, Tref, Tbe, P, Pref, Se, flag)        !evalute entropy of ethanol
        double precision, intent(in):: T, Tref, P, Pref
        double precision, intent(out):: Se
        integer, intent(in):: flag
        double precision Aev, Bev, Cev, Dev
        double precision Ael, Bel, Cel
        double precision Tbe, R ! delHv
        delHv=38489 !J/mol
        R=8.314             !J/molK
        !parameters for ethanol Cp in vapor (Smith, 2005)
        Aev=3.518
        Bev=0.020001
        Cev=-0.000006002
        Dev=0
        !parameters for ethanol Cp in liquid (Smith, 2005)
        Ael=33.866
        Bel=-0.1726
        Cel=0.00034917
        if (flag .EQ. 0) then
                Se=R*((Aev*log(T)+Bev*T+0.5*Cev*T**2-0.5*Dev/T**2-log(P/Pref))-
(Aev*log(Tbe)+Bev*Tbe+0.5*Cev*Tbe**2-0.5*Dev/Tbe**2-
log(P/Pref))+delHv/Tbe/R+(Ael*log(Tbe)+Bel*Tbe+0.5*Cel*Tbe**2-log(P/Pref))-(Ael*log(Tref)+Bel*Tref+0.5*Cel*Tref**2-
log(P/Pref)))
        else
                Se=R*((Ael*log(T)+Bel*T+0.5*Cel*T**2-log(P/Pref))-(Ael*log(Tref)+Bel*Tref+0.5*Cel*Tref**2-
log(P/Pref)))
        end if
end subroutine SEthanol


subroutine MolToKg(Fmol, Xmol, Fkg, Xkg)        !convert mole mass and mole concentration into mass
!Convert unit from mol/s and mol% to kg/hr and w%
        double precision Fetmol, Fetkg, Fwatermol, Fwaterkg
        double precision, intent(in):: Fmol, Xmol
        double precision, intent(out):: Fkg, Xkg
        Fetmol = Fmol * Xmol
        Fwatermol = Fmol * (1-Xmol)
        Fetkg = Fetmol * 46.068 * 3600 / 1000
        Fwaterkg = Fwatermol * 18.015 * 3600 / 1000
        Fkg = Fetkg + Fwaterkg
        Xkg = Fetkg / Fkg
end subroutine MolToKg
```

```
subroutine KgToMol(Fkg, Xkg, Fmol, Xmol)        !convert mass into mole
!Convert unit from mol/s and mol% to kg/hr and w%
        double precision Fetmol, Fetkg, Fwatermol, Fwaterkg
        double precision, intent(in):: Fkg, Xkg
        double precision, intent(out):: Fmol, Xmol
        Fetkg = Fkg * Xkg
        Fwaterkg = Fkg * (1-Xkg)
        Fetmol = Fetkg / 46.068 * 1000 /3600
        Fwatermol = Fwaterkg / 18.015 * 1000 / 3600
        Fmol = Fetmol + Fwatermol
        Xmol = Fetmol / Fmol
end subroutine KgToMol

subroutine pervap(NumOfStages,Tf,Pp,F,Xef,Xer,Pm,maxarea,totarea,totrec,totstages,totenergy, Xeo, Fo, Tout,
best_xep,CCapM, COpM, ELoss)
        double precision Xep,Xwp,Psatet,Psatw,Gamaet,Gamaw,Xei,Xepcal, Tbw_r, Tbe_r, Tbw_p, Tbe_p, Pref,Tef
        double precision Xwo,vapener, T, xe, ye, Fp, He, Hw, Se, Sw,Qc, Tcin, Tcout,Tbin, Tbout,QB
        double precision Xwi,Fi,Ti,Net,Nw,fXep,dif,dA,F1,x1, T1, SFi, SFo, Paral_N, Tube_N
        double precision Tout,dHvapmix,Cpmix,energy
        double precision best_Xep
        double precision Aet,Bet,Cet,Aw,Bw,Cw,Tref,dHvapet,dHvapw,NumOfStage
        double precision Cpet,Cpw,Eet,Ew,Qet,Qw,R_gas
        double precision exergyFeed, exergyReten, exergyPerm, exergyCond, exergcondin, exergcondout,
exergReboilin, exergReboilout, exergyHeat, exergytot, exergyretu
        double precision energyFeed, energyReten, energyPerm, energyCond, energycondin, energycondout,
energyReboilin, energyReboilout, energyHeat, energytot, exergyLRVP
        integer j, i
        double precision uxep,lxep, Tol, QE, CCapM, COpM, CCap, COp,EFi,EPerm,ERet,EHeatin,EHeatout,Flps, Fcw,
Pvp, Fcl, Fcv
        double precision,intent(in):: NumOfStages,Tf,Pm,Pp,maxarea,F,Xef,Xer
        double precision,intent(out):: totarea,totrec,totstages,totenergy,Xeo, Fo,ELoss
        COMMON /C1/Aet,Bet,Cet,Aw,Bw,Cw,Tref,R_gas
        COMMON /C2/Cpet,Cpw,Eet,Ew,Qet,Qw,dHvapet,dHvapw,dA
                R_gas = 8.3145D0            !ideal gas constant
                Aet = 8.1122D0              !Antoine equation parameters for ethanol
                Bet = 1592.864D0
                Cet = 226.184D0
                Aw = 7.96681D0              !Antoine equation parameters for water
                Bw = 1668.21D0
                Cw = 228.0D0
                Tref = 353.15D0             !reference temperature for permeate flux calculation
                Tef=298.15                  !surrounding temperature
                Pref=1.013 !bar
                dHvapet = 896000.0D0        !latent heat of water
                dHvapw = 2326000.0D0        !latent heat of ethanol
                Cpet = 2400D0               !heat capacity of ethanol at standard conditions
                Cpw = 4180D0                !heat capacity of water at standard conditions
                Eet = 25700.0D0             !energy parameter of ethanol for permeate flux calculation
                Ew = 17000.0D0              !energy parameter of water for permeate flux calculation
                Qet = 0.007 !0.000159D0     flux parameter of ethanol for permeate flux calculation
                Qw = 11.31 !0.62833D0       flux parameter of water for permeate flux calculation
                dA = 0.001                  !membrane slice area
                call TrayTemperature(Pm,0.0D0,T)
                Tbw_r=T+273.15
                call TrayTemperature(Pm,1.0D0,T)
                Tbe_r=T+273.15
                call TrayTemperature(Pp,0.0D0,T)
                Tbw_p=T+273.15
                call TrayTemperature(Pp,1.0D0,T)
                Tbe_p=T+273.15
                Xei = Xef
                Xwi = 1 - Xei
                Xeo = Xef
                Fi = F
                Ti = Tf
                Tl = Ti - 10.0D0
                totstages = 1.0D0
                totarea = 0.0D0
                totenergy = 0.0D0
                CCapM = 0
```

```
COpM =0
ELoss=0.
exergytot=0.
Tube_N=100
if (NumOfStages .EQ. 0) then
        NumOfStage = NumOfStages
else
        NumOfStage = NumOfStages
end if
Paral_N=Floor(Fi/(2.2*maxarea/xwi)/100.0)
SFi=Fi/(Paral_N*100.0)

do while ((totstages .LT. NumOfStage) .AND. (Xeo .LE. Xer))
        Psatet=(10**(Aet-Bet/((Ti-10.-273.15D0)+ Cet)))*(1.01325D0/760.0D0)
        Psatw =(10**(Aw-Bw/((Ti-10.-273.15D0)+ Cw)))*(1.01325D0/ 760.0D0)
        Gamaet = DExp((1.1477D0 - 0.7209D0 * Xei) * Xwi**2)
        Gamaw = DExp((1.0574D0 + 0.7209D0 * Xwi) * Xei**2)
        Xepcal=1-gamaw*Psatw/Pp*(1-Xei)! calculate xep
        IF (Xepcal .LT. 0) THEN
                lxep=0.D0
        Else
                lxep=Xepcal
        END IF
        uxep=Xei
        Tol=1.0d-3
        Call GoldenSearch(Pm,Pp,maxarea,lxep,uxep,Tol,SFi,Ti,Xei,best_Xep,SFo,Xeo,Tout)
        If ((Ti-Tout .LT. 10.0) .and. (Xeo .LE. Xer))Then
                Paral_N=Paral_N+1
                SFi=Fi/(paral_N*Tube_N)
        else
                Call Flux(Pm,Pp,maxarea,best_Xep,SFi,Ti,Xei,totstages)
                Fo=SFo*Paral_N*Tube_N
                totarea= totarea + maxarea*Paral_N*Tube_N
                totstages = totstages + 1.0D0
                call KgToMol(Fo, Xeo, F1, X1)
                call KgToMol(Fi, xei, F1, X1)
                call TrayTemperature(pm, xei,T1)
                T1=T1+273.15        !exergy loss and energy consumption evaluation
                call HWater(T1, Tef, Tbw_r, Hw,1)
                call HEthanol(T1, Tef, Tbe_r, He,1)
                call SWater(T1, Tef, Tbw_r, Pm, Pref, Sw,1)
                call SEthanol(T1, Tef, Tbe_r, Pm, Pref, Se,1)
                exergFeed=F1*x1*(He-Tef*Se)+F1*(1-x1)*(Hw-Tef*Sw)
                energyFeed=F1*x1*He+F1*(1-x1)*Hw
                call KgToMol(Fo,Xeo,F1,X1)
                call Hwater(Tout,Tef, Tbw_r, Hw,1)
                call Hethanol(Tout, Tef,Tbe_r,He,1)
                call SWater(Tout, Tef, Tbw_r, Pm, Pref, Sw,1)
                call SEthanol(Tout, Tef, Tbe_r, Pm, Pref, Se,1)
                exergyReten=F1*x1*(He-Tef*Se)+F1*(1-x1)*(Hw-Tef*Sw)
                energyReten=F1*x1*He+F1*(1-x1)*Hw
                Fp=Fi-Fo
                call KgToMol(Fp, best_Xep, F1,X1)
                call Hwater(Tout,Tef, Tbw_p, Hw,0)
                call Hethanol(Tout, Tef,Tbe_p,He,0)
                call SWater(Tout, Tef, Tbw_p, Pp, Pref, Sw,0)
                call SEthanol(Tout, Tef, Tbe_p, Pp, Pref, Se,0)
                exergyPerm=F1*x1*(He-Tef*Se)+F1*(1-x1)*(Hw-Tef*Sw)
                energyPerm=F1*x1*He+F1*(1-x1)*Hw
                Tbin=393.15D0       !K
                Tbout=368.15D0      !K
                Call TrayTemperature(pm,Xeo,Ti) !calculate saturate temperature
                Ti=Ti+273.15
                call Hwater(Ti,Tout, Ti, Hw,1)
                call Hethanol(Ti, Tout,Ti,He,1)
                QB=Hw+He
                call HWater(Tbin, Tbout, Tbw_r, Hw,0)
                Flps=QB/Hw
                call KgToMol(Fo,Xeo,F1,X1)
                call Hwater(Ti,Tef, Ti, Hw,1)
```

```
                                    call Hethanol(Ti, Tef,Ti,He,1)
                                    call SWater(Ti, Tef, Ti, Pm, Pref, Sw,1)
                                    call SEthanol(Ti, Tef, Ti, Pm, Pref, Se,1)
                                    exergyHeat=F1*x1*(He-Tef*Se)+F1*(1-x1)*(Hw-Tef*Sw)
                                    energyHeat=F1*x1*He+F1*(1-x1)*Hw
                                    call HWater(Tbin, Tef, Tbw_r, Hw,0)
                                    call Swater(Tbin, Tef, Tbw_r, Pm, Pref, Sw,0)
                                    exergReboilin=Flps*(Hw-Tef*Sw)
                                    energyReboilin=Flps*Hw
                                    call HWater(Tbout, Tef, Tbw_r, Hw,1)
                                    call Swater(Tbout, Tef, Tbw_r, Pm, Pref, Sw,1)
                                    exergReboilout=Flps*(Hw-Tef*Sw)
                                    energyReboilout=Flps*Hw
                                    call KgToMol(Fp,best_Xep,F1,x1)
                                    call condenserM(Tout-273.15,Pp*100.,x1, T, xe, ye)
                                    T=T+273.15
                                    call Hwater(T,Tef, Tbw_p, Hw,0)
                                    call Hethanol(T, Tef,Tbe_p,He,0)
                                    call SWater(T, Tef, Tbw_p, Pp, Pref, Sw,0)
                                    call SEthanol(T, Tef, Tbe_p, Pp, Pref, Se,0)
                                    exergyCond=0.1*(ye*(He-Tef*Se)+(1-ye)*(Hw-Tef*Sw))
                                    energyCond=0.1*(ye*He+(1-ye)*Hw)
                                    call Hwater(T, Tef, T, Hw,1)
                                    call Hethanol(T, Tef, T, He,1)
                                    call SWater(T, Tef, T, Pp, Pref, Sw,1)
                                    call SEthanol(T, Tef, T, Pp, pref, Se,1)
                                    exergyCond=F1*(0.9*(xe*(He-Tef*Se)+(1-xe)*(Hw-Tef*Sw))+exergyCond)
                                    energyCond=F1*(0.9*(xe*He+(1-xe)*Hw)+energyCond)
                                    Tcin=293.15D0       !K
                                    Tcout=308.15D0      !K
                                    call Hwater(Tout,T, Tbw_r, Hw,1)
                                    call Hethanol(Tout,T, Tbe_r, He,1)
                                    Qc=Hw+He
                                    call HWater(Tcout, Tcin, Tbw_r, Hw,1)
                                    Fcw=Qc/Hw
                                    call HWater(Tcin, Tef, Tbw_r, Hw,1)
                                    call Swater(Tcin, Tef, Tbw_r, Pm, Pref, Sw,1)
                                    exergcondin=Fcw*(Hw-Tef*Sw)
                                    energycondin=Fcw*Hw
                                    call HWater(Tcout, Tef, Tbw_r, Hw,1)
                                    call Swater(Tcout, Tef, Tbw_r, Pm, Pref, Sw,1)
                                    exergcondout=Fcw*(Hw-Tef*Sw)
                                    energycondout=Fcw*Hw
                                    call LRVP(Pp, 1.20D0, 123.5D0, Fp, best_xep,T, Tcin, Pvp, Fcw)
                                    xe=Fp*best_xep/(Fp+Fcw)
                                    Fp=Fp+Fcw
                                    call KgToMol(Fp,Xe,F1,X1)
                                    call HWater(T, Tef, Tbw_r, Hw,1)
                                    call Hethanol(T, Tef, Tbe_r, He,1)
                                    call SWater(T, Tef, Tbw_r, 120.0D0, Pref, Sw,1)
                                    call Sethanol(T, Tef, Tbe_r, 120.0D0, Pref, Se,1)
                                    exergyretu=F1*x1*(He-Tef*Se)+F1*(1-x1)*(Hw-Tef*Sw)
                                    energyLRVP=F1*x1*He+F1*(1-x1)*Hw
                                    exergytot=exergReboilout-exergReboilin+exergCondout-exergCondin
                                    energytot=energyReboilout-energyReboilin+energyHeat+energyCondout-
energyCondin-energyFeed-Pvp*1000+energycond+energyLRVP
                                    Eloss=Eloss+exergytot
                                    totenergy=totenergy+energytot
                                    WRITE (22,'(9E15.4) ') Ti, Xeo, Fo, Tout, best_Xep, totenergy, totstages,
Paral_N, totarea
! Initializes the variables for the next stage
                                    Xei = Xeo
                                    Xwi = 1 - Xeo
                                    Fi = Fo
                                    energy = 0.0D0
                                    QE=Fo*(1-Xeo)*(Ti-Tout)*4.18+Fo*Xeo*(Ti-Tout)*2.44 !kJ/h
                                    CCap=0
                                    Cop=0
                                    call HeatExchanger(1, QE/3600, 2, CCap, COp)
                                    print*,    ELoss
```

```
                                        CCapM=CCapM+CCap
                                        COpM=COpM+Cop
                                        Paral_N=Floor(Fi/(2.2*maxarea/xwi)/100.0)
                                        SFi=Fi/(paral_N*100.0)
                                       WRITE (3,'(11E15.4)') exergReboilout, exergReboilin, exergyHeat, exergCondout,
exergCondin,exergyCond,exergFeed,Pvp*1000,exergyretu,exergytot, energytot
                                end if
                        end do
                                        totrec = Fo*Xeo/(Xef*F)
                                        Eloss=Eloss-Pvp*1000
END subroutine pervap

subroutine condenserM(T0, P, zet,T,xe,ye)          !evaluate concentrations on liquid and vapor phase after condenser
        double precision:: T0, T,P, Psatet, Psatw,xe,xw,ye,yw,zet,zw,Fkg, xeg, xwg,gamaet, gamaw, alpha,error
        double precision:: Vfrct, Lfract
        double precision:: conv, Aet, Bet, Cet, Aw, Bw, Cw
        Aet=16.8958
        Bet=3795.17
        Cet=230.918
        Aw=16.3872
        Bw=3885.7
        Cw=230.17
        zw=1-zet
        Vfrct=0.1
        Lfrct=1-Vfrct
        conv=0.000001
        error=1.
        gamaet=1.
        gamaw=1.
        Do While (error .GT. conv)
                Psatet=exp(Aet-Bet/(T+Cet))
                Psatw=exp(Aw-Bw/(T+Cw))
                alpha=Psatet/Psatw
                xe=zet*P/((1-Vfrct)*gamaet*Psatet+Vfrct*P)
                xw=1-xe
                call MolToKg(1.0D0,xe,Fkg,xeg)
                xwg=1-xeg
                Gamaet = Exp((1.4177 - 0.7209 * Xeg) * Xwg**2)
                Gamaw = Exp((1.0574 + 0.7209 * Xwg) * Xeg**2)
                yw=xw*gamaw*Psatw/P
                ye=xe*gamaet*Psatet/P
                if (yw .LE. 1.0) then
                        ye=1-yw
                end if
                if (ye .LE. 1.0) then
                        yw=1-ye
                end if
                Psatet=P*(ye/gamaet+yw*alpha/gamaw)
                T=Bet/(Aet-log(Psatet))-Cet
                error=abs(T-T0)
                T0=T
        end do
end subroutine condenserM

subroutine LRVP(Ps,Pc,Sc,Fp,xep,Tin, Tcin, Pvp,Fcw)        !evaluate the conditions after liquid ring vacuum pump
        double precision:: Ps, Pc, Sc, Fp, Tin, Tcin, Pvp, Fcw, xep
        double precision:: Pis, effis, Qc, Qk, cp, rolph, deltT,vapH, Qt
        effis=0.4  !Bannwarth, Helmut 2005 P192
        vapHw=2263          !kJ/kg
        vapHe=896           !kJ/kg
        cp=4.2              !kJ/kgK
        rolph=1000          !kg/m3
        deltT=85.5+273.15-Tin
        Pis=0.001/27.0*Ps/1.013*760.0*Sc*log(Pc/Ps)
        Pvp=Pis/effis
        Bannwarth, Helmut 2005 P192
        Qc=0.9*Pvp*3600
        Bannwarth, Helmut 2005 P177
        Qk=Fp*0.1*(vapHw*(1.-xep)+vapHe*xep)*0.9
        Qt=Qc+Qk
```

```
        Fcw=Qt/cp/deltT-Fp
end subroutine LRVP

Subroutine F(Pm,Pp,maxarea,X,Fi,Ti,Xei,Fo,Xeo,dif,Tout)    !function F used in Golden search method
                COMMON /C1/Aet,Bet,Cet,Aw,Bw,Cw,Tref,R_gas
                COMMON /C2/Cpet,Cpw,Eet,Ew,Qet,Qw,dHvapet,dHvapw,dA
                double precision Aet,Bet,Cet,Aw,Bw,Cw,Tref,R_gas
                double precision Cpet,Cpw,Eet,Ew,Qet,Qw,dA,dHvapet,dHvapw
                double precision, intent(in):: Pm,Pp,maxarea,X, Fi, Ti, Xei
                double precision, intent(out):: Fo,Xeo, dif, Tout
                double precision Slice_Xei, Slice_Ti, Slice_Fi, Slice_Xwi
                double precision Slice_Fo, Slice_Tout, Slice_Xeo, Slice_Xwo
                double precision area, Xep, Xwp
                double precision Psatet, Psatw,Gamaet,Gamaw,Net,Nw,dHvapmix,Cpmix,vapener
                integer flag
                Slice_Xei=Xei
                Slice_Xwi=1-Slice_Xei
                Xep=X
                Xwp=1-Xep
                Slice_Ti=Ti
                Slice_Fi=Fi
                area=dA
                flag=0
                do while (area .LE. maxarea)
                        Psatet=(10**(Aet-Bet/((Slice_Ti-273.150)+ Cet)))*(1.01325/760.00)
                        Psatw =(10**(Aw-Bw/((Slice_Ti-273.150)+ Cw)))*(1.01325/ 760.00)
                        Gamaet = DExp((1.4177D0 - 0.7209D0 * Slice_Xei) * Slice_Xwi**2)
                        Gamaw = DExp((1.0574D0 + 0.7209D0 * Slice_Xwi) * Slice_Xei**2)
                        Net= Qet*Exp((Eet/R_gas)*(1/Tref-1/Slice_Ti))*(Slice_Xei*Gamaet*Psatet-Xep*Pp)*dA
                        Nw = Qw*Exp((Ew/R_gas)*(1/Tref-1/Slice_Ti))*(Slice_Xwi*Gamaw*Psatw-Xwp*Pp)*dA
                        if (Nw .LT. 0.0) then
                                flag=1
                                area=maxarea+1.0
                        else
                                Slice_Fo = Slice_Fi - (Net + Nw)
                                Slice_Xeo = (Slice_Fi * Slice_Xei- Net) / Slice_Fo
                                Slice_Xwo = 1 - Slice_Xeo
                                dHvapmix = Xep * dHvapet + Xwp * dHvapw
                                Cpmix = Slice_Xeo * Cpet + Slice_Xwo * Cpw
                                vapener = (Net + Nw) * dHvapmix
                                Slice_Tout = Slice_Ti - vapener / (Cpmix * Slice_Fo)
                                area=area+dA
                                Slice_Xei=Slice_Xeo
                                Slice_Xwi=Slice_Xwo
                                Slice_Fi=Slice_Fo
                                Slice_Ti=Slice_Tout
                        end if
                end do
                if (flag .EQ. 0) then
                        Fo=Slice_Fo
                        Xeo=Slice_Xeo
                        fXep = (Fi * Xei - Fo * Xeo)/(Fi - Fo)
                        dif = (X - fXep)**2
                        Tout = Slice_Tout
                else
                        dif=1000.0
                        Fo=0.0
                        Xeo=0.0
                        fXep=1-Slice_Xwi*Gamaw*Psatw/Pp
                        Tout =0.0
                end if
END  Subroutine F

Subroutine GoldenSearch(Pm,Pp,maxarea,AX,BX,TOL,Fi,Ti,Xei,XMIN,Fo,Xeo,Tout)        !golden search method
                COMMON /C1/Aet,Bet,Cet,Aw,Bw,Cw,Tref,R_gas
                COMMON /C2/Cpet,Cpw,Eet,Ew,Qet,Qw,dHvapet,dHvapw,dA
                double precision Aet,Bet,Cet,Aw,Bw,Cw,Tref,R_gas
                double precision Cpet,Cpw,Eet,Ew,Qet,Qw,dA,dHvapet,dHvapw
                double precision, intent(in):: Pm,Pp,maxarea,AX,BX,TOL,Fi,Ti,Xei
                double precision, intent(out):: XMIN,Xeo,Fo,Tout
```

```
                double precision X0,X1, X2,X3, F1,F2,Fo1,Fo2,Xeo1,Xeo2,Tout1,Tout2
                double precision R,C
                R=.61803399
                C=1.-R  !Golden ratios
                X0 = AX
                X3 = BX
                do while (ABS(X3-X0).GT.TOL)
                        X1 = X3 - R * ( X3 - X0 )
                        X2 = X1 + R * ( X1 - X0 )
                        Call F(Pm,Pp,maxarea,X1,Fi,Ti,Xei,Fo1,Xeo1,F1,Tout1)
                        Call F(Pm,Pp,maxarea,X2,Fi,Ti,Xei,Fo2,Xeo2,F2,Tout2)
                        IF (F1 .EQ. 1000.0) THEN
                                X0=X1
                        End IF
                        IF (F2 .EQ. 1000.0) Then
                                X0=X2
                        else
                                IF(F2.LT.F1) THEN
                                        X0=X1
                                ELSE
                                        X3=X2
                                ENDIF
                        end if
                end do
        IF(F1.LT.F2) THEN
                XMIN=X1
                Fo=Fo1
                Xeo=Xeo1
                Tout = Tout1
        ELSE
                XMIN=X2
                Fo=Fo2
                Xeo=Xeo2
                Tout = Tout2
        ENDIF
end Subroutine GoldenSearch

Subroutine Flux(Pm,Pp,maxarea,X,Fi,Ti,Xei,N)      !calculate permeate flux
                COMMON /C1/Aet,Bet,Cet,Aw,Bw,Cw,Tref,R_gas
                COMMON /C2/Cpet,Cpw,Eet,Ew,Qet,Qw,dHvapet,dHvapw,dA
                double precision Aet,Bet,Cet,Aw,Bw,Cw,Tref,R_gas
                double precision Cpet,Cpw,Eet,Ew,Qet,Qw,dA,dHvapet,dHvapw
                double precision, intent(in):: Pm,Pp,maxarea,X, Fi, Ti, Xei, N
                double precision Slice_Xei, Slice_Ti, Slice_Fi, Slice_Xwi
                double precision Slice_Fo, Slice_Tout, Slice_Xeo, Slice_Xwo
                double precision area, Xep, Xwp
                double precision Psatet, Psatw,Gamaet,Gamaw,Net,Nw,dHvapmix,Cpmix,vapener
                Slice_Xei=Xei
                Slice_Xwi=1-Slice_Xei
                Xep=X
                Xwp=1-Xep
                Slice_Ti=Ti
                Slice_Fi=Fi
                area=dA
                energy=0.0
                do while (area .LE. maxarea)
                        Psatet=(10**(Aet-Bet/((Slice_Ti-273.15D0)+ Cet)))*(1.01325D0/760.0D0)
                        Psatw =(10**(Aw-Bw/((Slice_Ti-273.15D0)+ Cw)))*(1.01325D0/ 760.0D0)
                        Gamaet = DExp((1.4177D0 - 0.7209D0 * Slice_Xei) * Slice_Xwi**2)
                        Gamaw = DExp((1.0574D0 + 0.7209D0 * Slice_Xwi) * Slice_Xei**2)
                        Net= Qet*Exp((Eet/R_gas)*(1/Tref-1/Slice_Ti))*(Slice_Xei*Gamaet*Psatet-Xep*Pp)*dA
                        Nw = Qw*Exp((Ew/R_gas)*(1/Tref-1/Slice_Ti))*(Slice_Xwi*Gamaw*Psatw-Xwp*Pp)*dA
                        Slice_Fo = Slice_Fi - (Net + Nw)
                        Slice_Xeo = (Slice_Fi * Slice_Xei- Net) / Slice_Fo
                        Slice_Xwo = 1 - Slice_Xeo
                        dHvapmix = Xep * dHvapet + Xwp * dHvapw
                        Cpmix = Slice_Xeo * Cpet + Slice_Xwo * Cpw
                        vapener = (Net + Nw) * dHvapmix
                        Slice_Tout = Slice_Ti - vapener / (Cpmix * Slice_Fo)
                        area=area+dA
```

```
                    energy=energy+vapener
                    Slice_Xei=Slice_Xeo
                    Slice_Xwi=Slice_Xwo
                    Slice_Fi=Slice_Fo
                    Slice_Ti=Slice_Tout
                    WRITE (4,'(10E15.4)') N, Net, Nw, Slice_Fo, Slice_Xeo, Xep, Slice_Tout
                end do
END  Subroutine Flux

subroutine  GetInitialConditions(mF,xf,NTRAY,NFeed,  D,  Fdraw,  Ndraw,  Feed1,xf1,NFEED1,Feed2,xf2,NFEED2,Fout,
Yout,x,y, QB, QC,T,L,CostCol, totrec,RefluxR)
        Integer::i,j,Counter
        Real(8)::zf,B,DeltaT,Time,SumT,SumL,SumV,xx,yy,yf, Rmin,Dt
        Real(8)::Tf,hf,hf1,Tf1,hf2,Tf2, RefluxR
        Real(8),Dimension(100)::Hv,PD,hdow,M0,L0,V0,T0,h0,z,Qloss, Diat
        Real(8),Dimension(100)::M,P,V,hl
        Real(8),Dimension(2,100)::x0
        Real(8),Dimension(2,100),intent(out)::y,x
        Real(8),Dimension(100),intent(out)::T,L
  CHARACTER*50 FICHIER
  INTEGER F1(3,10),NODE(3)
        INTEGER, intent(in):: NFEED1,NFEED2, Ndraw
  DOUBLE PRECISION SORNEU(10,3),POIDS(10,10,2),MINMAX(10,2,2)
        DOUBLE PRECISION, intent(in):: Feed1,xf1,Feed2,xf2, mF, xf, D, Fdraw
        DOUBLE PRECISION, intent(out):: QB,QC,Fout, Yout,totrec, Costcol
  FICHIER="POID056.DAT"
  CALL POIDINITIAL(NODE,POIDS,FICHIER,MINMAX,F1)
        P(1)=101.3
        P(2)=101.3
        Do j=3,NTRAY
                P(j)=P(j-1)+0.        !kPa
        End do
         xx=xf*46.068/(xf*46.068+(1-xf)*18.015)
         CALL GETY(xx,yy,NODE,SORNEU,POIDS,MINMAX,F1)
  yf=18.015*yy/(yy*18.015+(1-yy)*46.068)
        Rmin=(0.8182-yf)/(yf-xf)
        RefluxR=Rmin
        x(1,1)=0.0
        Dt=1.5
        Do while ((ABS(x(1,1)-0.8182) .GT. 1.0E-3) .And. (RefluxR .GE. Rmin))
                L(1)=D*RefluxR
                M(1)=2.0
                M(NTRAY)=2.3
                zf=(xf*mF+xf1*Feed1+xf2*Feed2)/(mF+Feed1+Feed2)
                xx=xf*46.068/(xf*46.068+(1-xf)*18.015)
                Call TrayTemperature1(xx,Tf)
                Call LiquidMEnthalpy(xx,hf)
                xx=xf1*46.068/(xf1*46.068+(1-xf1)*18.015)
                Call TrayTemperature1(xx,Tf1)
                Call LiquidMEnthalpy(xx,hf1)
                xx=xf2*46.068/(xf2*46.068+(1-xf2)*18.015)
                Call TrayTemperature1(xx,Tf2)
                Call LiquidMEnthalpy(xx,hf2)
                Do j=1,NTRAY
                xx=zf*46.068/(zf*46.068+(1-zf)*18.015)
                Call TrayTemperature1(xx,T0(j))
                x0(1,j)=xf
                x0(2,j)=1.0-x0(1,j)
                PD=0.6
                Qloss=0
                xx=x0(1,j)*46.068/(x0(1,j)*46.068+(1-x0(1,j))*18.015)
                Call LiquidMEnthalpy(xx,h0(j))
                End do
                Do j=1,NFEED1-1
                L0(j)=L(1)
                End do
                Do j=NFEED1,Ndraw-1
                L0(j)=L(1)+Feed1
                End do
                Do j=Ndraw, NFeed-1
```

```
                L0(J)=L(1)+Feed1-Fdraw
                End do
                Do j=NFEED,NFEED2-1
                L0(j)=L(1)+Feed1+mF-Fdraw
                End do
                Do j=NFEED2,NTRAY
                L0(j)=mF+L0(NFEED-1)+Feed2
                End do
                Do j=2,NTRAY
                        V0(j)=L(1)+D
                End do
                Call TransientColumnProfileLoad(NTRAY,M,P,T,V0,L0,y,x0)
                Call PhysicalPropertiesCalculation(NTRAY)
                call initialM0(NTRAY, x0, M0)
                Counter=0
                DeltaT=0.0002
100             SumL=0.0
                SumV=0.0
                SumT=0.0
                Do j=2,NTRAY
                Do i=1,2
                 xx=x0(1,j)*46.068/(x0(1,j)*46.068+(1-x0(1,j))*18.015)
                 CALL GETY(xx,yy,NODE,SORNEU,POIDS,MINMAX,F1)
          y(i,j)=18.015*yy/(yy*18.015+(1-yy)*46.068)
                End do
                End do
                V(2)=L(1)+D
                x(1,1)=(M(1)*x0(1,1)+(V0(2)*y(1,2)-(L0(1)+D)*x0(1,1))*DeltaT)/M(1)
        !above feed stage
                Do j=2,NFEED1-1
                        M(j)=M0(j)+(V0(j+1)-V0(j)+L0(j-1)-L0(j))*DeltaT
                        x(1,j)=(M0(j)*x0(1,j)+(V0(j+1)*y(1,j+1)-V0(j)*y(1,j)+L0(j-1)*&
                        x0(1,j-1)-L0(j)*x0(1,j))*DeltaT)/M(j)
                End do
                M(NFEED1)=M0(NFEED1)+(V0(NFEED1+1)-V0(NFEED1)+L0(NFEED1-1)-
L0(NFEED1)+Feed1)*DeltaT
        x(1,NFEED1)=(M0(NFEED1)*x0(1,NFEED1)+(V0(NFEED1+1)*y(1,NFEED1+1)-
V0(NFEED1)*y(1,NFEED1)+L0(NFEED1-1)*&
                        x0(1,NFEED1-1)-L0(NFEED1)*x0(1,NFEED1)+Feed1*xf1)*DeltaT)/M(NFEED1)
                if (Ndraw .EQ. NFeed) then
                Do j=NFeed1+1,NFeed-1
                        M(j)=M0(j)+(V0(j+1)-V0(j)+L0(j-1)-L0(j))*DeltaT
                        x(1,j)=(M0(j)*x0(1,j)+(V0(j+1)*y(1,j+1)-V0(j)*y(1,j)+L0(j-1)*&
                        x0(1,j-1)-L0(j)*x0(1,j))*DeltaT)/M(j)
                End do
                M(NFeed)=M0(NFeed)+(V0(NFeed+1)-V0(NFeed)+L0(NFeed-1)-L0(NFeed)+mf-Fdraw)*DeltaT
                x(1,NFeed)=(M0(NFeed)*x0(1,NFeed)+(V0(NFeed+1)*y(1,NFeed+1)-
V0(NFeed)*y(1,NFeed)+L0(NFeed-1)*&
                        x0(1,NFeed-1)-L0(NFeed)*x0(1,NFeed)-Fdraw*x0(1,NFeed)+mf*xf)*DeltaT)/M(NFeed)
                else
                Do j=NFeed1,Ndraw-1
                        M(j)=M0(j)+(V0(j+1)-V0(j)+L0(j-1)-L0(j))*DeltaT
                        x(1,j)=(M0(j)*x0(1,j)+(V0(j+1)*y(1,j+1)-V0(j)*y(1,j)+L0(j-1)*&
                        x0(1,j-1)-L0(j)*x0(1,j))*DeltaT)/M(j)
                End do
                M(Ndraw)=M0(Ndraw)+(V0(Ndraw+1)-V0(Ndraw)+L0(Ndraw-1)-L0(Ndraw)-Fdraw)*DeltaT
                x(1,Ndraw)=(M0(Ndraw)*x0(1,Ndraw)+(V0(Ndraw+1)*y(1,Ndraw+1)-
V0(Ndraw)*y(1,Ndraw)+L0(Ndraw-1)*&
                        x0(1,Ndraw-1)-L0(Ndraw)*x0(1,Ndraw)-Fdraw*x0(1,Ndraw))*DeltaT)/M(Ndraw)
                Do j=Ndraw+1,NFEED-1
                        M(j)=M0(j)+(V0(j+1)-V0(j)+L0(j-1)-L0(j))*DeltaT
                        x(1,j)=(M0(j)*x0(1,j)+(V0(j+1)*y(1,j+1)-V0(j)*y(1,j)+L0(j-1)*&
                        x0(1,j-1)-L0(j)*x0(1,j))*DeltaT)/M(j)
                End do
        !feed stage
                M(NFEED)=M0(NFEED)+(V0(NFEED+1)-V0(NFEED)+L0(NFEED-1)-L0(NFEED)+mF)*DeltaT
                x(1,NFEED)=(M0(NFEED)*x0(1,NFEED)+(V0(NFEED+1)*y(1,NFEED+1)-
V0(NFEED)*y(1,NFEED)+L0(NFEED-1)*&
                        x0(1,NFEED-1)-L0(NFEED)*x0(1,NFEED)+mF*xf)*DeltaT)/M(NFEED)
                end if
```

```
        !stripping section
                Do j=NFEED+1,NFEED2-1
                        M(j)=M0(j)+(V0(j+1)-V0(j)+L0(j-1)-L0(j))*DeltaT
                        x(1,j)=(M0(j)*x0(1,j)+(V0(j+1)*y(1,j+1)-V0(j)*y(1,j)+L0(j-1)*&
                        x0(1,j-1)-L0(j)*x0(1,j))*DeltaT)/M(j)
                End do
                M(NFEED2)=M0(NFEED2)+(V0(NFEED2+1)-V0(NFEED2)+L0(NFEED2-1)-
L0(NFEED2)+Feed2)*DeltaT
                x(1,NFEED2)=(M0(NFEED2)*x0(1,NFEED2)+(V0(NFEED2+1)*y(1,NFEED2+1)-
V0(NFEED2)*y(1,NFEED2)+L0(NFEED2-1)*&
                        x0(1,NFEED2-1)-L0(NFEED2)*x0(1,NFEED2)+Feed2*xf2)*DeltaT)/M(NFEED2)
                if ((NFEED2+1) .LT. NTRAY) then
                Do j=NFEED2+1,NTRAY-1
                        M(j)=M0(j)+(V0(j+1)-V0(j)+L0(j-1)-L0(j))*DeltaT
                        x(1,j)=(M0(j)*x0(1,j)+(V0(j+1)*y(1,j+1)-V0(j)*y(1,j)+L0(j-1)*&
                                x0(1,j-1)-L0(j)*x0(1,j))*DeltaT)/M(j)
                End do
                end if
        !reboiler
                L(NTRAY)=L0(NTRAY-1)-V0(NTRAY)
                x(1,NTRAY)=(M(NTRAY)*x0(1,NTRAY)+(L0(NTRAY-1)*x0(1,NTRAY-1)-V0(NTRAY)*y(1,NTRAY)-
L0(NTRAY)*x0(1,NTRAY))*DeltaT)/M(NTRAY)
                do j=1,NTRAY
                        xx=x(1,j)*46.068/(x(1,j)*46.068+(1-x(1,j))*18.015)
                        CALL GETY(xx,yy,NODE,SORNEU,POIDS,MINMAX,F1)
                  y(1,j)=18.015*yy/(yy*18.015+(1-yy)*46.068)
                end do
                Do j=1,NTRAY
                        x(2,j)=1.0-x(1,j)
                        y(2,j)=1.0-y(1,j)
                End do
                Do j=1,NTRAY
                        xx=x(1,j)*46.068/(x(1,j)*46.068+(1-x(1,j))*18.015)
                        Call TrayTemperature1(xx,yy)
                        T(j) = yy
                End do
                Do j=1,NTRAY
                        xx=x(1,j)*46.068/(x(1,j)*46.068+(1-x(1,j))*18.015)          !convert mole% into mass%
                        yy=y(1,j)*46.068/(y(1,j)*46.068+(1-y(1,j))*18.015)          !convert mole% into mass%
                        Call VaporMEnthalpy(yy,Hv(j))
                        Call LiquidMEnthalpy(xx,hl(j))
                End do
                QC=V0(2)*Hv(2)-(L0(1)+D)*hl(1)-M(1)*(hl(1)-h0(1))/DeltaT    !the unit for QC:kJ/s
                Do j=2,NFEED1-1
                V(j+1)=((M(j)*hl(j)-M0(j)*h0(j))/DeltaT+V(j)*Hv(j)-L0(j-1)*hl(j-1)+L0(j)*hl(j)-Qloss(j+1))/Hv(j+1)
                End do
                V(NFEED1+1)=((M(NFEED1)*hl(NFEED1)-
M0(NFEED1)*h0(NFEED1))/DeltaT+V(NFEED1)*Hv(NFEED1)-L0(NFEED1-1)*hl(NFEED1-1)+L0(NFEED1)*hl(NFEED1)-
Feed1*hf1-Qloss(NFEED1+1))/Hv(NFEED1+1)
                if (Ndraw .EQ. NFeed) then
                Do j=NFEED1+1,NFEED-1
                        V(j+1)=((M(j)*hl(j)-M0(j)*h0(j))/DeltaT+V(j)*Hv(j)-L0(j-1)*hl(j-1)+L0(j)*hl(j)-Qloss(j+1))/Hv(j+1)
                End do
                V(NFEED+1)=((M(NFEED)*hl(NFEED)-M0(NFEED)*h0(NFEED))/DeltaT+V(NFEED)*Hv(NFEED)-
L0(NFEED-1)*hl(NFEED-1)+L0(NFEED)*hl(NFEED)+Fdraw*hl(NFeed)-mF*hf-Qloss(NFEED+1))/Hv(NFEED+1)
                else
                Do j=NFEED1+1,Ndraw-1
                        V(j+1)=((M(j)*hl(j)-M0(j)*h0(j))/DeltaT+V(j)*Hv(j)-L0(j-1)*hl(j-1)+L0(j)*hl(j)-Qloss(j+1))/Hv(j+1)
                End do
                V(Ndraw+1)=((M(Ndraw)*hl(Ndraw)-M0(Ndraw)*h0(Ndraw))/DeltaT+V(Ndraw)*Hv(Ndraw)-L0(Ndraw-
1)*hl(Ndraw-1)+L0(Ndraw)*hl(Ndraw)+Fdraw*hl(Ndraw)-Qloss(Ndraw+1))/Hv(Ndraw+1)
                Do j=Ndraw+1,NFEED-1
                        V(j+1)=((M(j)*hl(j)-M0(j)*h0(j))/DeltaT+V(j)*Hv(j)-L0(j-1)*hl(j-1)+L0(j)*hl(j)-Qloss(j+1))/Hv(j+1)
                End do
                V(NFEED+1)=((M(NFEED)*hl(NFEED)-M0(NFEED)*h0(NFEED))/DeltaT+V(NFEED)*Hv(NFEED)-
L0(NFEED-1)*hl(NFEED-1)+L0(NFEED)*hl(NFEED)-mF*hf-Qloss(NFEED+1))/Hv(NFEED+1)
                end if
                Do j=NFEED+1,NFeed2-1
                        V(j+1)=((M(j)*hl(j)-M0(j)*h0(j))/DeltaT+V(j)*Hv(j)-L0(j-1)*hl(j-1)+L0(j)*hl(j)-Qloss(j+1))/Hv(j+1)
                End do
```

```
                V(NFEED2+1)=((M(NFEED2)*hl(NFEED2)-
M0(NFEED2)*h0(NFEED2))/DeltaT+V(NFEED2)*Hv(NFEED2)-L0(NFEED2-1)*hl(NFEED2-1)+L0(NFEED2)*hl(NFEED2)-
Feed2*hf2-Qloss(NFEED2+1))/Hv(NFEED2+1)
                if ((NFEED2+1) .LT. NTRAY) then
                Do j=NFEED2+1,NTRAY-1
                        V(j+1)=((M(j)*hl(j)-M0(j)*h0(j))/DeltaT+V(j)*Hv(j)-L0(j-1)*hl(j-1)+L0(j)*hl(j)-Qloss(j+1))/Hv(j+1)
                End do
                end if
                QB=(M(NTRAY)*(hl(NTRAY)-h0(NTRAY)))/DeltaT-L0(NTRAY-1)*hl(NTRAY-
1)+V(NTRAY)*Hv(NTRAY)+L0(NTRAY)*hl(NTRAY)
                Call TransientColumnProfileLoad(NTRAY,M,P,T,V,L0,y,x)
                Call PhysicalPropertiesCalculation(NTRAY)
                call loadcolumnsize(Dt)
                Call LiquidFlow(NTRAY,NFEED,L)
                Call TransientColumnProfileLoad(NTRAY,M,P,T,V,L,y,x)
                Do j=1,NTRAY
                        SumL=SumL+abs((L(j)-L0(j))/L0(j))
                        SumT=SumT+abs((T(j)-T0(j))/T0(j))
                End do
                Do j=2,NTRAY
                SumV=SumV+abs((V(j)-V0(j))/V0(j))
                End do
                If                              ((SumL.LT.FLOAT(NTRAY)*1.0E-6).and.(SumT.LT.FLOAT(NTRAY)*1.0E-
6).and.(SumV.LT.FLOAT(NTRAY)*1.0E-6)&
                .and.(abs(D+L(NTRAY)+Fdraw-mF-Feed1-Feed2)/(mF+Feed1+Feed2).LT.1.0E-5))          Then
        !convergence?
                        OPEN(1,FILE='RES-001.DAT')
                        CLOSE (1)
                        if (x(1,1) .GT. 0.8182) then
                                RefluxR=RefluxR-0.01
                        else
                                RefluxR=RefluxR+0.01
                        end if
                Else
                Do j=1,NTRAY
                        T0(j)=T(j)
                        M0(j)=M(j)
                        h0(j)=hl(j)
                        L0(j)=L(j)
                        V0(j)=V(j)
                        Do i=1,2
                                x0(i,j)=x(i,j)
                        End do
                End do
                        Counter=Counter+1
                        goto 100
                end if
        end do
200 FORMAT(15E14.4)
201 FORMAT(97HM(j)    T(j)    P(j)    L(j)    V(j)    hl(j)   x(1,j)   x(2,j)    y(1,j)   y(2,j))
        Do j=1, NTray
                WRITE (100,'(9E15.4) '), j,    T(j),    P(j),    L(j),    V(j),    hl(j),   x(1,j),   y(1,j)
        end do
        Fout = D
        Yout = x(1,1)
        CLOSE (100,status='keep')
        totrec=Fout*yout/mf/xf
        call ColumnCost(RefluxR, Fout, Yout, NTRAY, CostCol)
End subroutine GetInitialConditions

Module PhysicalProperties
        implicit None
        Real(8)::R,Mw1,Mw2
        Real(8),Dimension(100)::DensityV,DensityL,ViscoV,ViscoL,SurTen
End Module PhysicalProperties

Module TransientColumnProfile
        Implicit None
        Real(8),Dimension(100)::M,P,T,V,L
        Real(8),Dimension(2,100)::y,x
```

```
End Module TransientColumnProfile

Module ColumnSize
        Implicit None
        Real(8)::Dt,S,At,An,Ab,Ad,Lw,Wdc,Dh,Af,hw,hcl,TrayThick,Pitch,D_reflux
End Module ColumnSize

Subroutine PhysicalPropertiesCalculation(NTRAY)
        Use TransientColumnProfile
        Use PhysicalProperties
        Implicit None
        Integer::j
        integer,intent(in)::NTRAY
        Real(8),Dimension(100)::ViscoVP1,ViscoVP2,ViscoLP1,ViscoLP2,Fi12,Fi21
        R=8314.3
        Mw1=46.068
        Mw2=18.015
        Do j=1,NTRAY
        DensityV(j)=(P(j)*1000.0/(R*(273.15+T(j))))*(Mw1*y(1,j)+Mw2*y(2,j))     !kg/m3
        DensityL(j)=x(1,j)*(1.648/0.27627**(1+(1-(273.15+T(j))/513.92)**0.2331))*46.069+&
                        x(2,j)*(5.459/0.30542**(1+(1-(273.15+T(j))/647.13)**0.081))*18.015
        ViscoVP1(j)=1.499+3.0741e-1*(273.15+T(j))-4.4479E-5*(273.15+T(j))**2
        ViscoVP2(j)=-36.826+4.29e-1*(273.15+T(j))-1.62E-5*(273.15+T(j))**2
        Fi12(j)=((1.0+(sqrt(ViscoVP1(j)/ViscoVP2(j))))*((Mw2/Mw1)**0.25))**2)/(sqrt(8.0)*sqrt(1.0+Mw1/Mw2))
        Fi21(j)=((1.0+(sqrt(ViscoVP2(j)/ViscoVP1(j))))*((Mw1/Mw2)**0.25))**2)/(sqrt(8.0)*sqrt(1.0+Mw2/Mw1))
        ViscoV(j)=ViscoVP1(j)/(1.0+(y(2,j)/y(1,j))*Fi12(j))+ViscoVP2(j)/(1.0+(y(1,j)/y(2,j))*Fi21(j))      !uPa.s
        ViscoLP1(j)=10.0**(-6.4406+1.1176E3/(273.15+T(j))+1.3721E-2*(273.15+T(j))-1.5465E-5*(273.15+T(j))**2)
        ViscoLP2(j)=10.0**(-10.2158+1.7925E3/(273.15+T(j))+1.7730E-2*(273.15+T(j))-1.2631E-5*(273.15+T(j))**2)
        ViscoL(j)=(x(1,j)*sqrt(ViscoLP1(j))+x(2,j)*sqrt(ViscoLP2(j)))**2
        SurTen(j)=x(1,j)*(71.3681*(1.0-((273.15+T(j))/562.05))**1.2291)+&
                        x(2,j)*(70.9158*(1.0-((273.15+T(j))/591.75))**1.3220)          !mN/m=Dyn/cm
        End do
        ViscoV(1)=0.0
End subroutine PhysicalPropertiesCalculation

Subroutine ColumnDesign(NTRAY,NFEED,L,V,y,x,DiaT)
        Use PhysicalProperties
        Implicit none
        Integer::j
        Real(8),Dimension(100)::Qv,Ql,Flv,Csb,Cs,Unf,NetArea,DonArea,TotalArea,DiaT
        Real(8),Dimension(100),intent(in)::L,V
        Real(8),Dimension(2,100),intent(in)::y,x
        integer,intent(in)::NTRAY,NFEED
        Do j=1,NTRAY
        Qv(j)=V(j)*(Mw1*y(1,j)+Mw2*y(2,j))/(3600.0*DensityV(j))       !m3/s
        Ql(j)=L(j)*(Mw1*x(1,j)+Mw2*x(2,j))/(3600.0*DensityL(j))       !m3/s
        End do
        Do j=2,NTRAY-1
        Flv(j)=((L(j)*(Mw1*x(1,j)+Mw2*x(2,j)))/(V(j)*(Mw1*y(1,j)+Mw2*y(2,j))))*(DensityV(j)/DensityL(j))**0.5
        Csb(j)=10.0**(-0.6855-0.1005*log10(Flv(j)))
        Unf(j)=(Csb(j)*((SurTen(j)/20.0)**0.2)*Sqrt((DensityL(j)-DensityV(j))/DensityV(j)))*0.3048
        NetArea(j)=Qv(j)/(0.8*Unf(j))
        DonArea(j)=Ql(j)/0.09144
        TotalArea(j)=DonArea(j)+NetArea(j)
        DiaT(j)=Sqrt(4.0*TotalArea(j)/3.141593)
        !Print *, j,An(j),Ad(j),At(j),DiaT(j)
        End do
End subroutine ColumnDesign

Subroutine LoadColumnSize(Dts)
        Use ColumnSize
        Implicit None
        real(8):: Dts
        !Column geometry
        Dt=dts/0.3048*12.
        S=18.0
        At=(3.141593*0.25*Dt**2)/12.0**2
        An=0.92*At
        Ab=0.84*At
        Ad=0.08*At
```

```
        Lw=0.67*Dt
        Wdc=0.13*Dt
        Dh=3.0/16.0
        Af=0.1
        hw=2.0
        hcl=1.5
        TrayThick=0.135
        Pitch=0.951*Dh/sqrt(Af)
        D_reflux=40.0
End Subroutine LoadColumnSize

subroutine initialM0(NTRAY, x, M0)
                Use PhysicalProperties
                Implicit None
                Real(8):: Dt, hw, At, An, Vol, Mwave
                integer j
                integer, intent(in):: NTRAY
                Real(8),Dimension(2,100),intent(in)::x
                Real(8), Dimension(100), intent(out):: M0
                Dt=1.5
                hw=2.0/12.0*0.3048 !m
                At=3.141593*0.25*Dt**2 !m2
                An=0.84*At          !m2
                Vol=An*hw           !m3
                Do j=1, NTRAY
                        Mwave=Mw1*x(1,j)+Mw2*x(2,j)
                        M0(j)=Vol*DensityL(j)/Mwave
                end do
end subroutine initialM0

Subroutine DowncomerLiquidHeight(NTRAY,NFEED,hdow)
        Use TransientColumnProfile
        Use PhysicalProperties
        Use ColumnSize
        Implicit None
        Integer j
        Real(8)::FaiFroth
        Real(8),Dimension(100)::Qv,Ql,Fga,AeraFactor,hd,how,Rh,Ufc,NRe,FrictionF,hg,hda
        integer,intent(in)::NTRAY,NFEED
        Real(8),Dimension(100),intent(out)::hdow
        Data FaiFroth/0.6/
        Do j=2,NTRAY-1
        Qv(j+1)=(V(j+1)*(Mw1*y(1,j+1)+Mw2*y(2,j+1))/(60.0*DensityV(j+1)))*264.2
        Ql(j)=(L(j)*(Mw1*x(1,j)+Mw2*x(2,j))/(60.0*DensityL(j)))*264.2 !gal/min
        hd(j)=(0.186/0.77**2)*(DensityV(j+1)/DensityL(j))*((Qv(j)*0.1337/60.0)/(Af*Ab))**2 !height of liquid,in
        Fga(j)=((Qv(j)*0.1337/60.0)/Ab)*sqrt(DensityV(j+1)*0.06243)
        AeraFactor(j)=0.69-0.06*Fga(j)
        how(j)=0.48*(0.9815+0.0955*log10(Ql(j)/((Lw/12.0)**2.5)))*((Ql(j)/Lw)**0.667)
        Rh(j)=((0.6*(hw+how(j)))/0.22)*2.78/(2.0*((0.6*(hw+how(j)))/0.22)+12.0*2.78)
        Ufc(j)=(1.0/37.4)*((Ql(j)/Lw)/(0.6*(hw+how(j))))*(Lw/(2.78)) !ft/s
        NRe(j)=Rh(j)*Ufc(j)*(DensityL(j)*0.06243)/(ViscoL(j)*0.672E-3)
        FrictionF(j)=10.0**(3.3816-1.0003*log10(NRe(j)))
        hg(j)=(12.0*FrictionF(j)*(Ufc(j)**2)*2.47)/(32.2*Rh(j)) ! height of liquid,in
        hda(j)=0.03*(Ql(j)/(100.0*Ad))**2          !friction loss for liquid through downcomer
        End do
        Do j=2,NTRAY-2
        hdow(j)=(hd(j+1)+AeraFactor(j+1)*(hw+how(j+1)+0.5*hg(j+1))+hda(j)+&
                        hd(j)+AeraFactor(j)*(hw+how(j)+0.5*hg(j)))/FaiFroth          !height of liquid,in
        If (hdow(j).GT.S) Then
                Print*,""
                Print *, 'Waring: Downcomer',j,' is in flooding'
        End if
        End do
        hdow(NTRAY-1)=(hda(NTRAY-1)+hd(NTRAY-1)+AeraFactor(NTRAY-1)*(hw+how(NTRAY-1)+0.5*hg(NTRAY-
1)))/FaiFroth        !height of liquid,in
        If (hdow(NTRAY).GT.S) Then
                print*,""
                Print *, 'Waring: Downcomer',NTRAY,' is in flooding'
        End if
End subroutine DowncomerLiquidHeight
```

```
Subroutine LiquidFlow(NTRAY,NFEED,Lflow)
        Use TransientColumnProfile
        Use PhysicalProperties
        Use Columnsize
        Implicit None
        Integer::j
        Real(8),Dimension(100)::L0,Ql,Qv,Fga,AeraFactor,how,hd,Rh,Ufc,NRe,FrictionF,hg,hda,Mholdup,hdowc,Fw
        integer,intent(in)::NTRAY,NFEED
        Real(8),Dimension(100),intent(out)::Lflow
        Do j=1,NTRAY
        L0(j)=L(j)
        End do
        Ql(1)=(L0(1)*(Mw1*x(1,1)+Mw2*x(2,1))/(60.0*DensityL(1)))*264.2
        Do j=2,NTRAY-1
        Qv(j+1)=(V(j+1)*(Mw1*y(1,j+1)+Mw2*y(2,j+1))/(60.0*DensityV(j+1)))*264.2
        Ql(j)=(L0(j)*(Mw1*x(1,j)+Mw2*x(2,j))/(60.0*DensityL(j)))*264.2

        hd(j+1)=(0.186/0.77**2)*(DensityV(j+1)/DensityL(j))*(((Qv(j+1)*0.06243)*0.1337/60.0)/(Af*Ab))**2
        Fga(j)=((Qv(j+1)*0.1337/60.0)/Ab)*sqrt(DensityV(j+1)*0.06243)
        AeraFactor(j)=0.69-0.06*Fga(j)
        how(j)=0.48*(0.9815+0.0955*log10(Ql(j)/((Lw/12.0)**2.5)))*((Ql(j)/Lw)**0.667)      !height of liquid,in
        Rh(j)=((0.6*(hw+how(j)))/0.22)*2.78/(2.0*((0.6*(hw+how(j)))/0.22)+12.0*2.78)      !in ft
        Ufc(j)=(1.0/37.4)*((Ql(j)/Lw)/(0.6*(hw+how(j))))*(Lw/(2.78)) !ft/s
        NRe(j)=Rh(j)*Ufc(j)*(DensityL(j)*0.06243)/(ViscoL(j)*0.672E-3)
        FrictionF(j)=10.0**(3.3816-1.0003*log10(NRe(j)))
        hg(j)=(12.0*FrictionF(j)*(Ufc(j)**2)*2.47)/(32.2*Rh(j)) ! height of liquid
        hda(j)=0.03*(Ql(j)/(100.0*Ad))**2          !friction loss for liquid through downcomer
        MHoldup(j)=(M(j)*(Mw1*x(1,j)+Mw2*x(2,j)))*2.2046 !lb
        Fw(j)=0.9815+0.0955*log10(Ql(j)/(Lw/12.0)**2.5)
0.0002*((Ql(j)/Lw/12.0)**2.5)**2.0+0.000006*((Ql(j)/Lw/12.0)**2.5)**3.0
        End do

        Do j=2,NTRAY-2
        hdowc(j)=hd(j+1)+AeraFactor(j+1)*(hw+how(j+1)+0.5*hg(j+1))+hda(j)+&
                        hd(j)+AeraFactor(j)*(hw+how(j)+0.5*hg(j))          !height of liquid,in
        End do
        hdowc(NTRAY-1)=hda(NTRAY-1)+hd(NTRAY-1)+AeraFactor(NTRAY-1)*(hw+how(NTRAY-1)+0.5*hg(NTRAY-
1))      !height of liquid,in

        Do j=2,NTRAY-1
        Ql(j)=((((12.0*MHoldup(j)/(DensityL(j)*0.06243)-Ad*hdowc(j))/(Ab*AeraFactor(j))-hw-0.5*hg(j))/&
                (0.48*Fw(j)))**1.5)*Lw
        Lflow(j)=((Ql(j)*0.1337*(DensityL(j)*0.06243)*0.4536)/(Mw1*x(1,j)+Mw2*x(2,j)))*60.0
        if (Lflow(j).LT.0) then
                print*, "Liquid flow smaller than 0!!!"
        end if
        End do
End subroutine LiquidFlow

Subroutine LiquidLevel(NTRAY,M1,M23,Drum_H,Base_H)
        Use TransientColumnProfile
        Use PhysicalProperties
        Use ColumnSize
        Implicit none
        Real(8),intent(in)::M1,M23
        integer,intent(in)::NTRAY
        Real(8),intent(out)::Drum_H,Base_H
        Real(8)::Pi
        Pi=3.1415926
        Drum_H=(M1*(Mw1*x(1,1)+Mw2*x(2,1))/DensityL(1))/(Pi*((D_reflux*0.0254)**2)/4.0)        !m
        Base_H=(M23*(Mw1*x(1,NTRAY)+Mw2*x(2,NTRAY))/DensityL(NTRAY))/(Pi*((Dt*0.0254)**2)/4.0)    !m
End subroutine LiquidLevel

Subroutine LiquidMEnthalpy(x1,LMEnthalpy)
        Implicit None
        Real(8),intent(in)::x1
        Real(8),intent(out)::LMEnthalpy
        Real(8)::MolarMass
        LMEnthalpy=-336.9*x1**3+619.8*x1**2-495.8*x1+417.3      !kJ/kg
```

```
        MolarMass = x1*46.068 + (1-x1)*18.015  !g/mol
        LMEnthalpy = LMEnthalpy / 1000 * MolarMass !kJ/mol
End subroutine LiquidMEnthalpy

   SUBROUTINE GETY(X,Y,NODE,SORNEU,POIDS,MINMAX,F)
    INTEGER NODE(3),F(3,10)
    DOUBLE PRECISION POIDS(10,10,2),MINMAX(10,2,2)
    DOUBLE PRECISION SORNEU(10,3),SOMME(10,2)
    Real(8),intent(in)::X
        Real(8),intent(out)::Y
    SORNEU(1,1)=(X-MINMAX(1,1,1))/(MINMAX(1,1,2)-MINMAX(1,1,1))
    SORNEU(NODE(1),1)=1.
    SORNEU(NODE(2),2)=1.
    CALL SOMMATION(NODE,SORNEU,SOMME,POIDS,F)
    Y=SORNEU(1,3)*(MINMAX(1,2,2)-MINMAX(1,2,1))+MINMAX(1,2,1)
    RETURN
    END

    SUBROUTINE SOMMATION(NODE,SORNEU,SOMME,POIDS,F)
    INTEGER NODE(3),F(3,10)
    DOUBLE PRECISION SORNEU(10,3),SOMME(10,2),POIDS(10,10,2)
    DO 10 J=1,NODE(2)-F(1,2)
      SOMME(J,1)=0.
      DO 20 I=1,NODE(1)
        SOMME(J,1)=SOMME(J,1)+POIDS(I,J,1)*SORNEU(I,1)
  20 CONTINUE
      SORNEU(J,2)=1./(1.+EXP(-SOMME(J,1)))
  10 CONTINUE
    DO 30 K=1,NODE(3)
      SOMME(K,2)=0.
      DO 40 J=1,NODE(2)
        SOMME(K,2)=SOMME(K,2)+POIDS(J,K,2)*SORNEU(J,2)
  40   CONTINUE
      SORNEU(K,3)=1./(1.+EXP(-SOMME(K,2)))
  30 CONTINUE
    RETURN
    END

    SUBROUTINE POIDINITIAL(NODE,POIDS,FICHIER,MINMAX,F)
        CHARACTER*50 FICHIER
    INTEGER NODE(3),F(3,10)
    DOUBLE PRECISION POIDS(10,10,2),MINMAX(10,2,2)
     OPEN(3,FILE=FICHIER,STATUS='OLD')
    READ(3,*) (NODE(I),I=1,3)
    READ(3,*) (F(1,I),I=1,5)
    READ(3,*) (F(2,J),J=1,NODE(2)-F(1,2))
    READ(3,*) (F(3,K),K=1,NODE(3))
    READ(3,*) (MINMAX(I,1,1),I=1,NODE(1)-F(1,1))
    READ(3,*) (MINMAX(I,1,2),I=1,NODE(1)-F(1,1))
    READ(3,*) (MINMAX(K,2,1),K=1,NODE(3))
    READ(3,*) (MINMAX(K,2,2),K=1,NODE(3))
    DO 10 I=1,NODE(1)
  10 READ (3,*) (POIDS(I,J,1),J=1,NODE(2)-F(1,2))
    DO 11 J=1,NODE(2)
  11 READ (3,*) (POIDS(J,K,2),K=1,NODE(3))
    CLOSE(3)
    RETURN
    END

Subroutine TransientColumnProfileLoad(NTRAY,Ms,Ps,Ts,Vs,Ls,ys,xs)
        Use TransientColumnProfile
        Implicit None
        Integer::i,j
        integer,intent(in)::NTRAY
        Real(8),Dimension(100),Intent(in)::Ms,Ps,Ts,Vs,Ls
        Real(8),Dimension(2,100),Intent(in)::ys,xs
        Do j=1,NTRAY
        M(j)=Ms(j)
        P(j)=Ps(j)
        T(j)=Ts(j)
```

```
        V(j)=Vs(j)
        L(j)=Ls(j)
        Do i=1,2
        y(i,j)=ys(i,j)
        x(i,j)=xs(i,j)
        End do
        End do
End subroutine TransientColumnProfileLoad

Subroutine TrayTemperature1 (xx,yy)
        implicit None
        Real(8),intent(in)::xx
        Real(8),intent(out)::yy
        yy=-50.07*xx**3+104.2*xx**2-75.81*xx+99.37
End subroutine TrayTemperature1

Subroutine TrayTemperature (P, xx,T)
        double precision:: T0, Psatet, Psatw,xe,xw,ye,yw,zet,zw,Fkg, xeg, xwg,gamaet, gamaw, alpha,error,Tsatet,
Tsatw, Pg
        double precision:: conv, Aet, Bet, Cet, Aw, Bw, Cw
        double precision:: xet,F
        double precision, intent(in):: P, xx
        double precision, intent(out):: T
        Aet=16.8958
        Bet=3795.17
        Cet=230.918
        Aw=16.3872
        Bw=3885.7
        Cw=230.17
        conv=0.000001
        error=1.
        gamaet=1.
        gamaw=1.
        Pg=P*100.          !tranfer to kPa
        call KgToMol(1.D0, xx, F, xet)
        Tsatet=Bet/(Aet-log(Pg))-Cet
        Tsatw=Bw/(Aw-log(Pg))-Cw
        if (xet .EQ. 0.0) then
                T=Tsatw
        else
                if (xet .EQ. 1.0) then
                        T=Tsatet
                else
                        T=xet*Tsatet+Tsatw*(1-xet)
                        Do While (error .GT. conv)
                                Psatet=exp(Aet-Bet/(T+Cet))
                                Psatw=exp(Aw-Bw/(T+Cw))
                                alpha=Psatet/Psatw
                                Gamaet = Exp((1.1477 - 0.7209 * Xx) * (1-xx)**2)
                                Gamaw = Exp((1.0574 + 0.7209 * (1-xx)) * xx**2)
                                Psatet=Pg*(xet*gamaet+(1-xet)*gamaw/alpha)
                                T=Bet/(Aet-log(Psatet))-Cet
                                error=abs(T-T0)
                                T0=T
                        end do
                end if
        end if
end subroutine Traytemperature

Subroutine VaporMEnthalpy(y1,VMEnthalpy)
        Implicit None
        Real(8),intent(in)::y1
        Real(8),intent(out)::VMEnthalpy
        Real(8)::MolarMass
        VMEnthalpy=-1614*y1+2676  !kJ/kg
        MolarMass = y1*46.068 + (1-y1)*18.015  !g/mol
        VMEnthalpy = VMEnthalpy / 1000 * MolarMass !kJ/mol
End subroutine VaporMEnthalpy
```